NASA Tech Briefs

Official Publication of the
National Aeronautics and
Space Administration
April 1993 Vol. 17 No. 4

Transferring Engineering
Technology to Over 200,000
Qualified Readers Throughout
Industry and Government

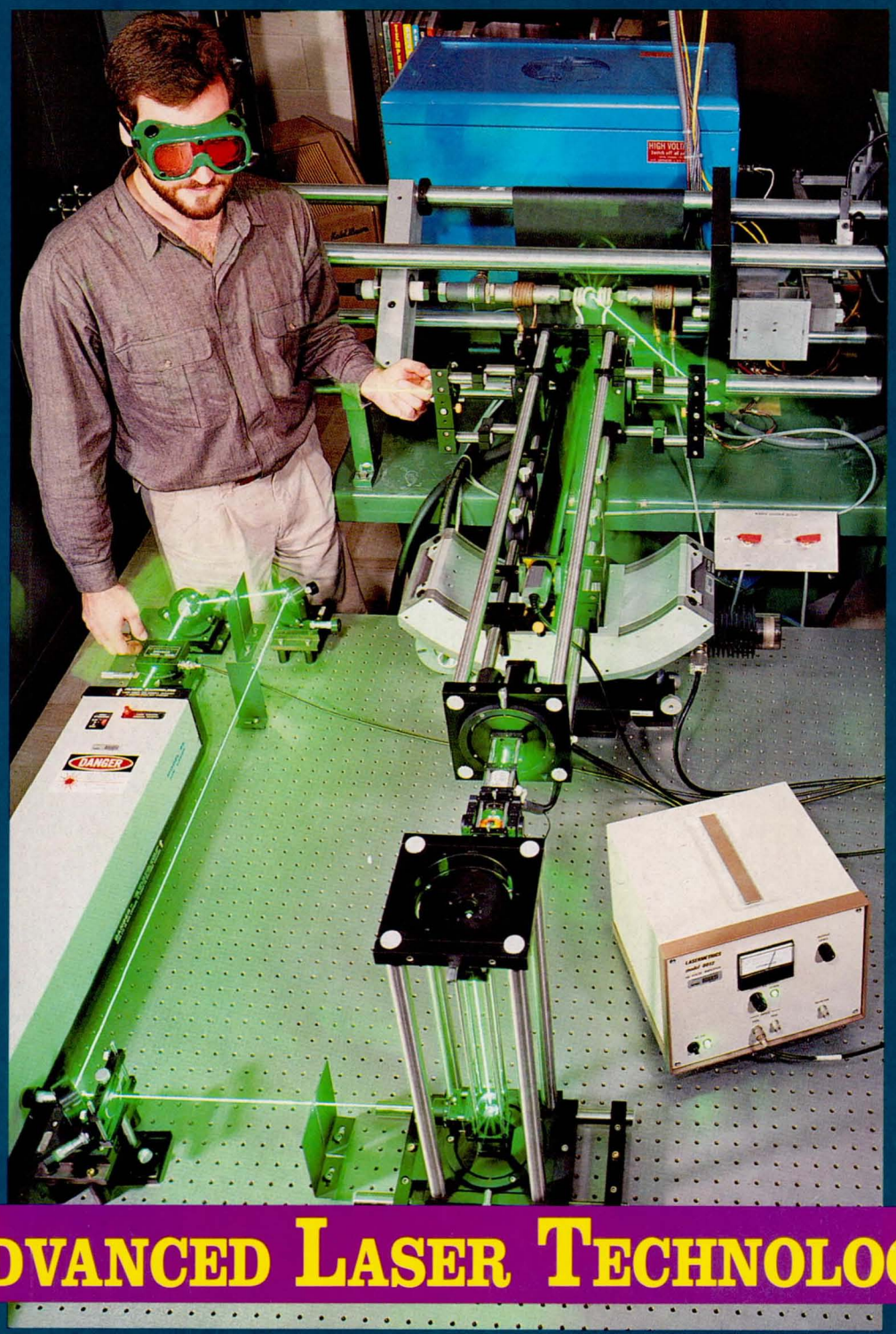

ADVANCED LASER TECHNOLOGY

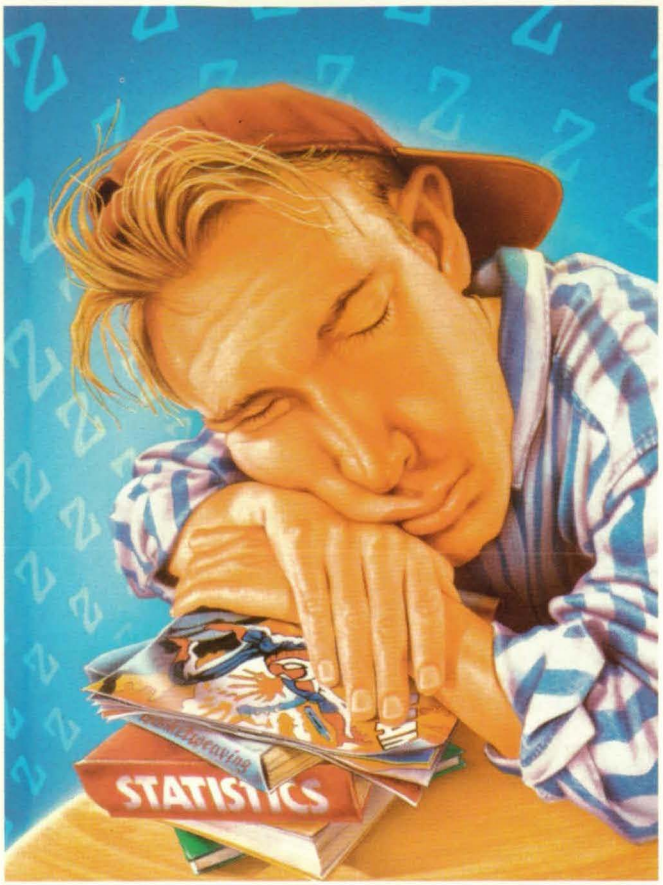

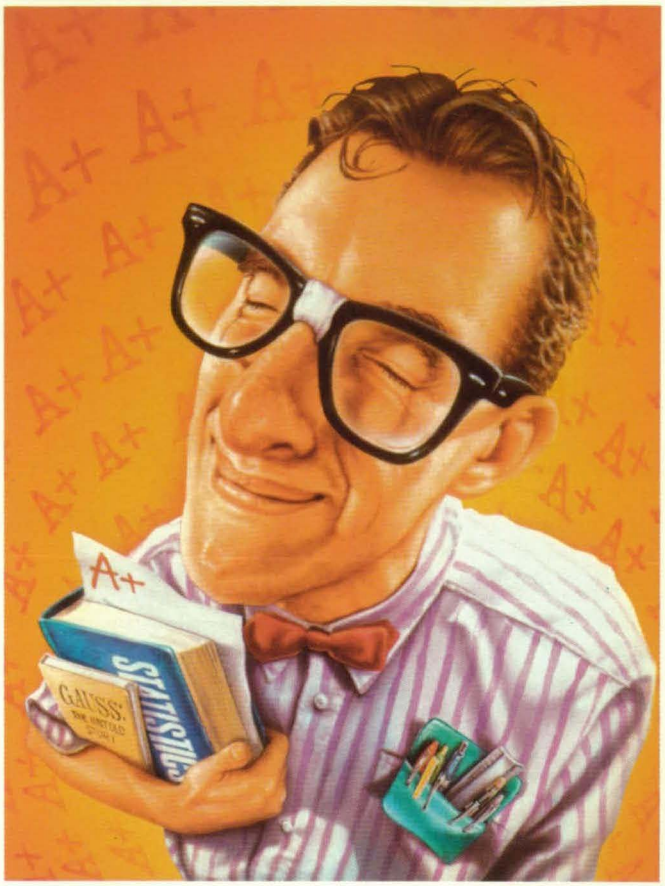

STATGRAPHICS *Plus*. For People Who Made It Through Statistics With Their Eyes Closed.

Whether you aced statistics in your sleep, or just plain slept, you'll find STATGRAPHICS *Plus* is a software dream come true: more than 250 menu-driven procedures, eye-popping graphics, and full support for the power and capacity of your 386/486 PC. No wonder *Software Digest* rated us number one for ease of use and learning.

How easy? This easy.

No matter how much–or how little–you know about statistics, STATGRAPHICS *Plus* does the work for you. Calculating precisely the solutions you need, from sales forecasts to assembly-line analyses to cancer research studies. And then displaying the results in stunning graphics that let you *see* the answer. With simple, point-and-click menus and a powerful graphics editor that makes generating presentation-quality results a cinch.

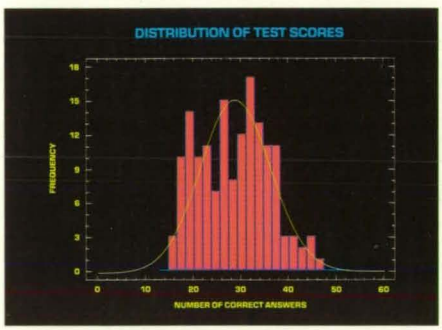

What you don't know, STATGRAPHICS *Plus* does.

Even if you've forgotten some–or all–of your statistics, STATGRAPHICS *Plus* remembers: Regression analysis. ANOVA. Quality control. Experimental design. Multivariate and time series procedures. Lifetime data analysis. And compatibility with your existing database, spreadsheet, and ASCII files. There's much, much more, too, including award-winning documentation, on-line help and telephone support.

But seeing is believing: call us today for more information. And witness the power of STATGRAPHICS *Plus* with your own eyes. It's the perfect tool for people that know their statistics. And for people who don't.

STATGRAPHICS® *Plus*

In Maryland, 301-984-5123.
Outside the U.S., 301-984-5412.

(800) 592-0050, Ext.450

Manugistics, Inc., 2115 East Jefferson St., Rockville, MD 20852. STATGRAPHICS is a registered trademark of Statistical Graphics Corporation. Evaluation © Software Digest Ratings Report, Vol. 8, No. 5 issue covering statistics programs. STATGRAPHICS *Plus* runs on 386, 386SX, and 486 computers with at least 4 MB of RAM and a graphics card. Version for 286/640K machines also available. © 1993 Manugistics, Inc. Authorized international dealers: Australia (03) 866 1766, United Kingdom (0753) 831 451, France (01) 45-27-20-61, Germany (069) 80053-0/(0212) 339099, Italy (02) 29404830, Spain (01) 341.535.0125, Sweden (0) 31 776 01 21, Netherlands (03402) 66336.

For More Information Circle No. 399

The right tool for the job.

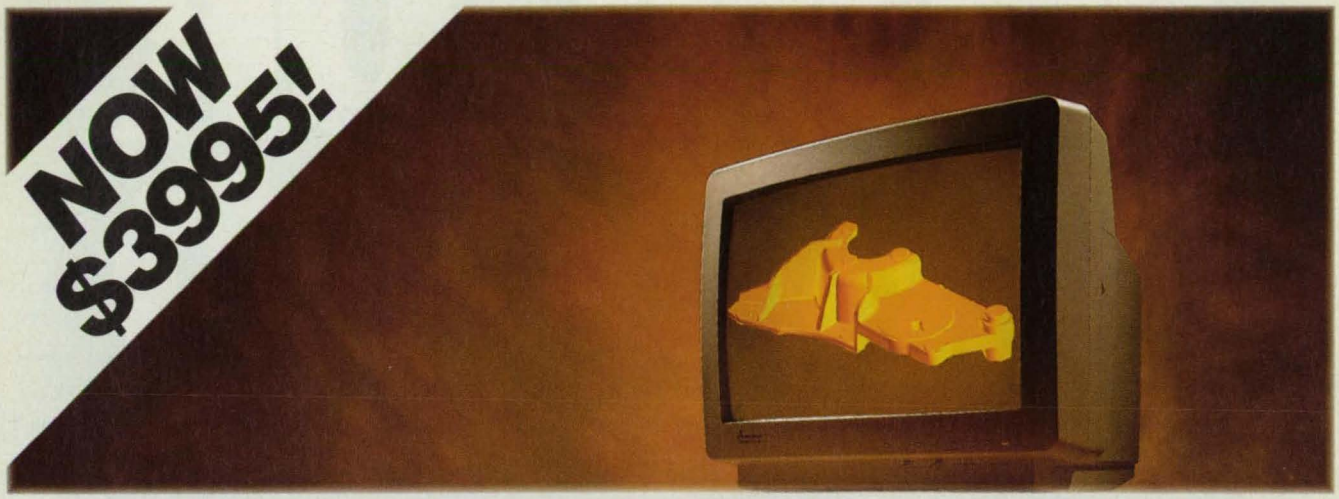

Having the right tool, like brake spring pliers or an oil filter wrench, can turn a potentially frustrating job . . . into one that is manageable and enjoyable. If your job is mechanical design, then the right tool for the job is Personal Designer® software. It provides the right combination of CAD capabilities including: ■ Comprehensive 2-D Drafting/Detailing ■ True 3-D Modeling ■ Hidden Line Removal ■ Bezier and NURB Surfaces ■ Faceted and Smooth Shaded Pictures.

With Personal Designer software, you're equipped to tackle challenging mechanical design problems. Build sizeable models (up to 64,000 entities) with complete associativity. Change the part, and all drawings, dimensions, crosshatching, and multiple views update automatically. Create drawings to ANSI, ISO, and JIS standards. Customize the user interface. And exchange data with other CAD packages via IGES or DXF.™

There's a lot more. You can fillet, sweep, and intersect complex surface geometry, and take advantage of software options for project management (PDex) and integrated 2½- and 3-axis NC programming (Personal Machinist®). To further expand your horizons, utilize the hundreds of available third party offerings. And draw on the expertise of Computervision's worldwide network of VARs.

There's a direct translator available, too. So, should you ever need Computervision's top-of-the-line CADDS® software, you can take Personal Designer data bases with you.

The bottom line: Personal Designer software is a smart buy in today's crowded marketplace. It's available for 386/486 PCs as well as the SPARCstation® workstation. And prices for 2D start at $1,995.

Get the right tool for the job, from the company that pioneered CAD/CAM.

Computervision Corporation
Personal CAD/CAM Business Unit
100 Crosby Drive, Bedford, MA 01730
Telephone (800) 248-7728 (U.S. except MA)
(617) 275-1800, ext. 4594 FAX (617) 271-0015

COMPUTERVISION

PERSONAL cad cam PRODUCTS

For More Information Circle No. 554

Personal Designer® 5.0

Part database courtesy of American Tool and Mold, Inc., St. Joseph, MI.

THE ALL NEW ASTRO-MED

MONITOR & RECORD

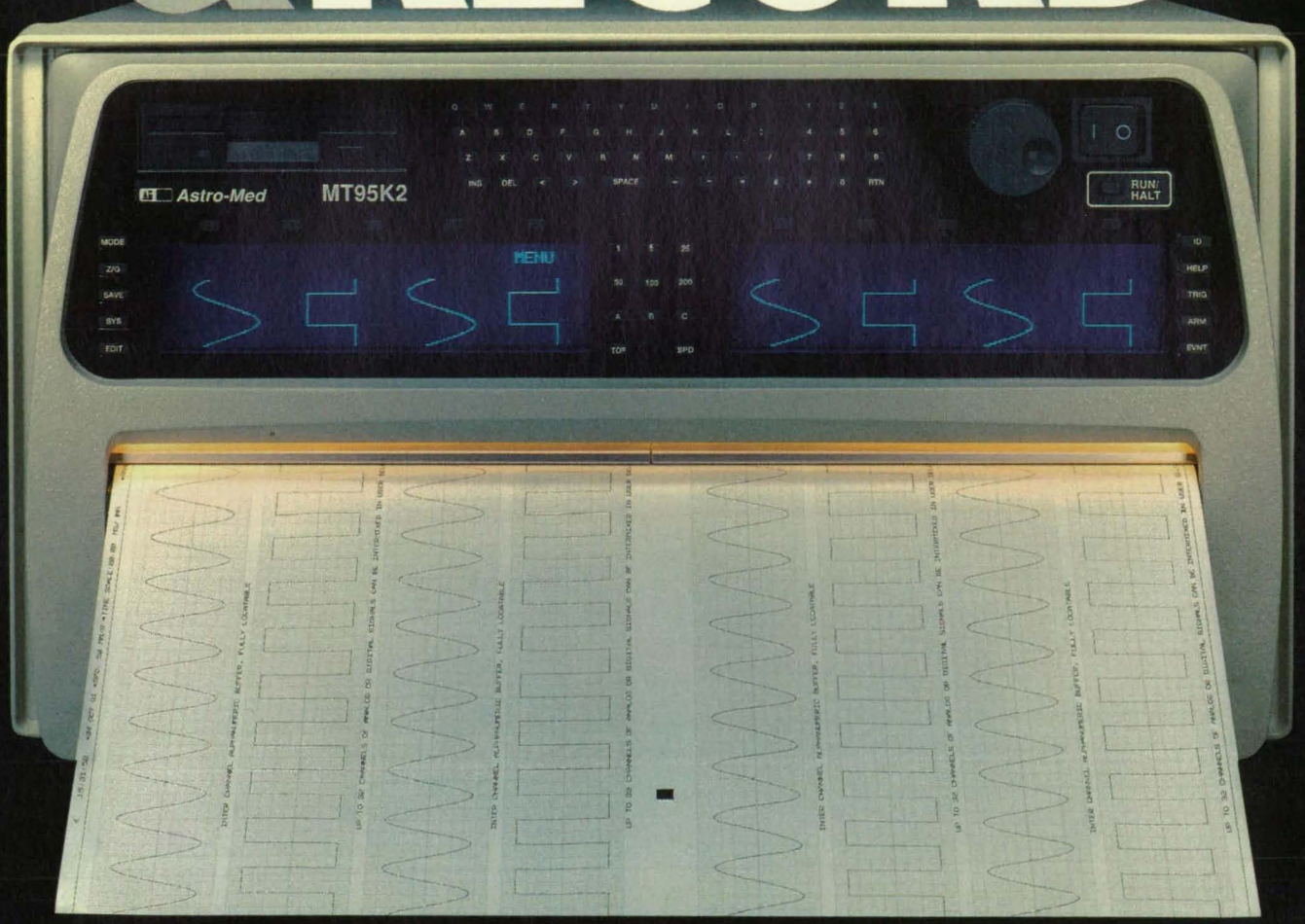

- **No Delay...see full traces on monitor while recording!**
- **Personal Chart Setups with on-board floppy drive**
- **Data Capture...up to 32 megabytes in RAM; 120 megabyte internal hard drive; stream to external drive via SCSI**
- **8 to 32 Waveform Channels...plus 64 events; DC to 20 kHz; chart speeds to 500 mm/sec**
- **Laser Printer Chart Resolution...300 dpi; clear, crisp traces**

Put simply, the MT95K2 is another major Astro-Med innovation in "chart recording": you can preview your data, record it, store it, play it back, send it to disk for analysis, record it again, and more! Whether you need basic 8 channel recorder or a sophisticated 32 channe recording system, the MT95K2 is the perfect platform for you today.

Call, Fax, or write for details!

Astro-Med, Inc.

Astro-Med Industrial Park, West Warwick, Rhode Island 02893
Phone: (401) 828-4000 • Toll Free (800) 343-4039
Fax (401) 822-2430 • Telex 710-382-6409

Sales and Service Centers in London, Paris, Frankfurt and Milan

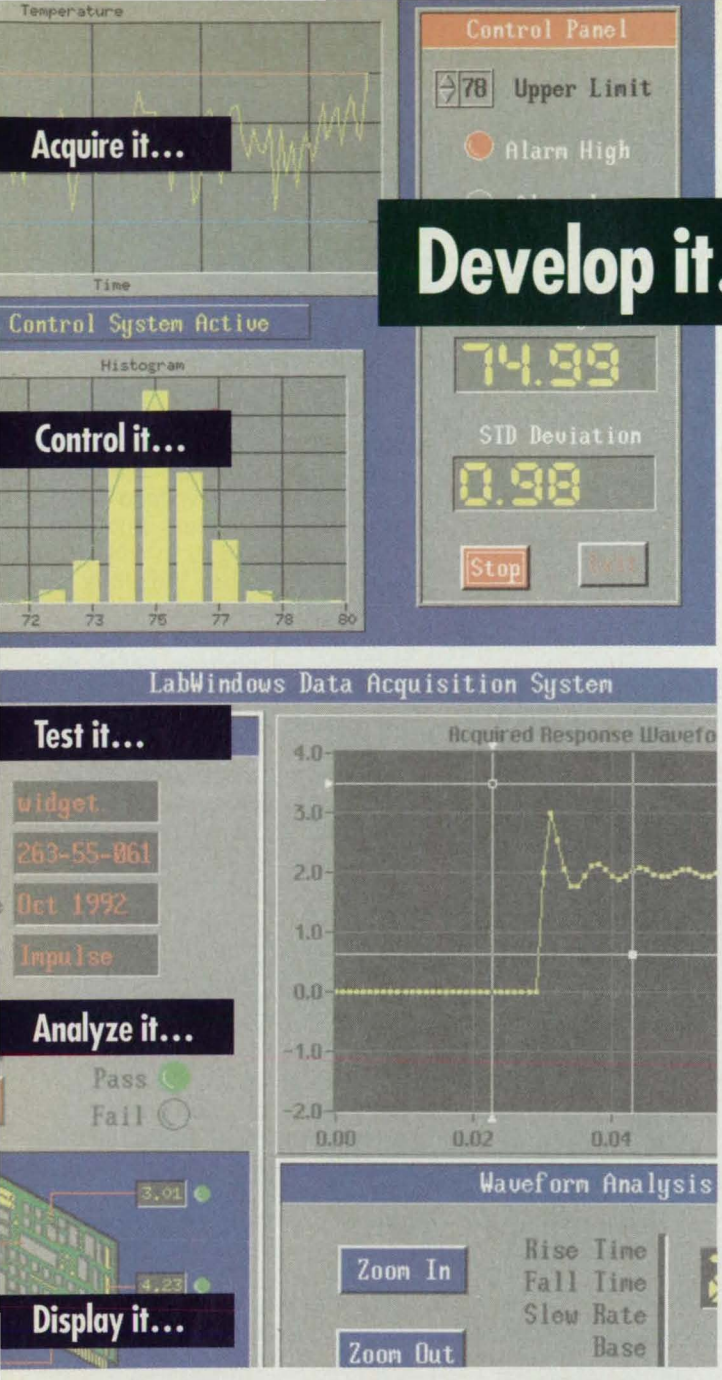

Develop it...with LabWindows®!

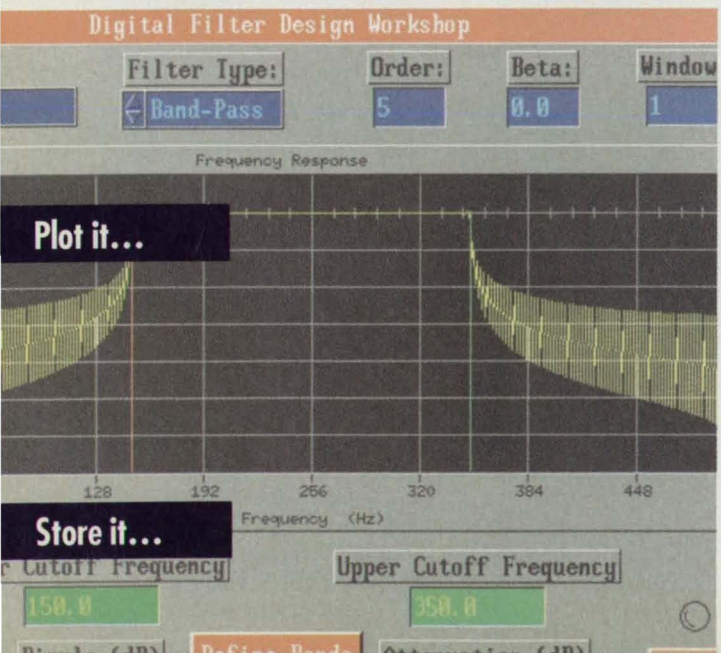

LabWindows for DOS accelerates the development of your data acquisition, instrument control, and data analysis programs with software tools based on proven industry standards.

Flexibility

With LabWindows, you can design and control custom graphical user interfaces (GUIs) with graphs, strip charts, push-buttons, menu bars, and more. And, to acquire your data, you can select from over 290 instrument drivers for IEEE 488, RS-232, and VXIbus instruments, or from a wide range of analog and digital plug-in data acquisition boards. Add in over 150 functions from the LabWindows Advanced Analysis Library for all of your signal processing.

Standard Programming Languages

LabWindows libraries are compatible with Microsoft C, BASIC, Professional BASIC, Visual Basic for DOS, Borland C++, and Turbo C++ compilers. With LabWindows, you can acquire, analyze, and present your data while maintaining the flexibility of standard C and BASIC programming languages.

Call for FREE Demo Disk
(800) 433-3488
(U.S. and Canada)

NATIONAL INSTRUMENTS®
The Software is the Instrument®
6504 Bridge Point Parkway
Austin, TX 78730-5039
Tel: (512) 794-0100
95 (800) 010 0793 (Mexico)
Fax: (512) 794-8411

For More Information Circle No. 681

Branch Offices
Australia 03 879 9422 • Belgium 02 757 00 20 • Canada 519 622 9310 • Denmark 45 76 26 00
Finland 90 527 2321 • France 1 48 65 33 70 • Germany 089 7 14 50 93 • Italy 02 48301892
Japan 03 3788 1921 • Netherlands 01720 45761 • Norway 03 846866 • Spain 91 896 0675
Sweden 08 984970 • Switzerland 056 27 00 20 • U.K. 0635 523545

See us at Electro booth #1401

LABORATORY HV SUPPLIES...
to 60 kV and 45 W

High performance and low cost DC high voltage are now available for the lab bench with the EL Series of tightly regulated, low ripple, and highly stable power supplies. Voltage ranges are 0 to 3 kV through 0 to 60 kV. Operating features include low stored energy for safety and an automatic crossover from constant-voltage to constant-current regulation for protection from overloads, arcs, and shorts.
Glassman High Voltage

100 W POWER SUPPLY TO 60 kV
3.5 in. and only 13 lbs.

The EH Series offer 100 W high voltage power supplies of superior quality in a compact and low weight package and at an affordable price. Rack panel height is only 3.5 inches and weight 13 lbs. Standard features include local and remote control and monitoring, tight regulation, low ripple, and fast response. Voltage ranges are 0 to 1 kV through 0 to 60 kV. Positive, negative, or reversible polarity models are available.
Glassman High Voltage

TWO UNBEATABLE HV MODULES...15 W/75 W

The 15 W Series MJ, with outputs from 0 to 3 kV through 0 to 30 kV, and the 75 W Series MK, 0 to 1 kV through 0 to 60 kV, both provide premium regulated and low-ripple power supply performance in a line-operated, compact, and lightweight package. Air insulation allows for easy serviceability, in contrast to wasteful "throw-away" modules.

- Constant voltage/constant current operation
- Low stored energy for safety
- Local and remote control
- Remote TTL enable/disable
- External interlock terminals
- Available with positive or negative polarity

Call for full information on the MJ and MK Series, or other Glassman supplies, 1 kV to 500 kV, 15 W to 15 kW.

Innovations in high voltage power supply technology.

GLASSMAN HIGH VOLTAGE INC.

Glassman High Voltage, PO Box 551, Whitehouse Station, NJ 08889, telephone (908) 534-9007. Also Glassman Europe, in the UK call (0256) 810808 and in Asia, Glassman Japan (044) 877-4546.

2 kW HV SUPPLIES TO 125 kV...
only 8.75 in. and 47 lbs.

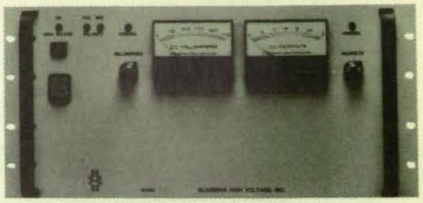

No longer does the combination of high DC voltage and high power mean a big, clumsy supply. The new LT Series from Glassman provides up to 2 kW of power with voltage ranges, depending on the model, from 0 to 1 kV through 0 to 125 kV in only a 8.75 inch high rack panel. Weight is less than 47 pounds. Line voltage is 220/240 V single-phase.

Voltage regulation is better than 0.005% for both load and line variations. Ripple is less than 0.03%. Automatic crossover from constant-voltage to constant-current regulation protects both the supply and load against shorts, arcs, or overloads. Current regulation is 0.05% from short circuit to rated voltage. The LT Series can be ordered with an optional current "trip" circuit that can be switch-selected to provide either current limiting or trip operation in the event of an overload.

All LT Series supplies feature full remote control capabilities including voltage/current program and monitoring terminals, TTL high voltage enable/disable, safety interlock terminals, and a +10 V reference source. Positive, negative, or reversible polarity models are available. Choice of dual analog or digital meters or a blank panel.
Glassman High Voltage

HV TO 75 kV AND 1000 W
Rack panel height only 5.25 in.

The WX Series of 1000 W regulated power supplies are available with DC outputs from 0 to 1 kV through 0 to 75 kV. Rack panel height is only 5.25 inches and weight less than 30 lbs. The Series WX is offered with a choice of dual analog voltage and current meters, dual digital meters, or with a blank panel for OEM/system applications. Positive, negative, or reversible polarity models are available.
Glassman High Voltage

Stanford Graphics 2.1. Power Graphing!

In the "real world," communicating your analysis requires more than a pretty picture. Consider Stanford Graphics for Windows for your serious presentations. It delivers the best of both worlds: presentation *and* analysis. Now you can have everything you need to create high-impact presentations without sacrificing number-crunching muscle. And, you won't need a Master's degree to use it either! Stanford Graphics' Quick Start options will have you up and running in minutes. So you'll be able to concentrate on your message, and not the method. Even data analysis and tinkering are a breeze. Just click on a point to change its value; pull a lever to adjust a formula. So don't wait another nano-second. Call right now for a free Demo Disk that will unleash the power of Stanford Graphics.

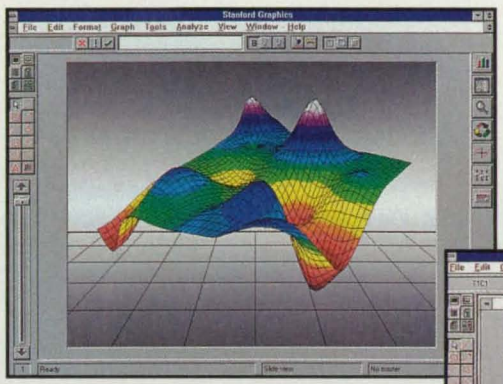

Tap into powerful auto-processing graphs to transform raw data into stunning presentations.

*"Stanford is a breakthrough product that combines technical charting, data analysis, and presentation tools. Basically, it's fabulous." **

– PC Magazine
March, 1992

"When it comes to charting power, data analysis and sheer brute strength, nothing comes close to Stanford Graphics."

– Windows Magazine
November, 1992

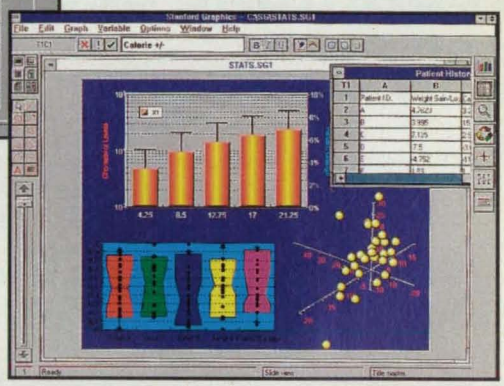

Find the meaning behind your data with advanced statistical graphs and functions, including Student t-tests & multiple regression analysis.

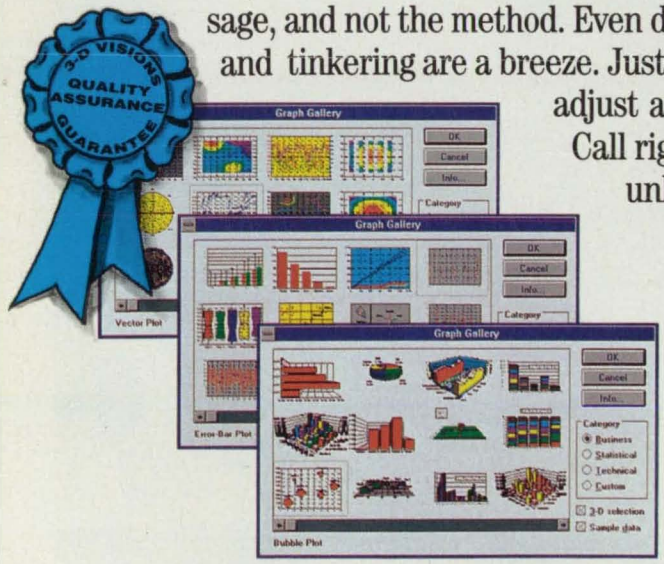

See your data in ways you've never dreamed possible with the Gallery of over 165 business, statistical & technical graphs.

Free Demo!

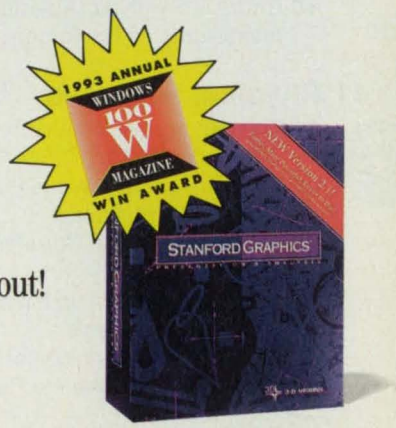

Form *and* Substance. Presentation simplicity *and* technical sophistication. Finally...presentation graphics with numerical clout!

3D 3-D VISIONS
2780 Skypark Drive • Torrance, CA 90505
Tel: 310-325-1339 • Fax: 310-325-1505

Call Toll Free Today.
1-800-729-4723

The development, maintenance, and implementation of this product have no connection with Stanford University. * Reprinted with permission, March 17, 1992, © 1992 Ziff Communications Co.

For More Information Circle No. 398

April 1993
Volume 17 Number 4

Contents

NASA Tech Briefs

Transferring Engineering Technology to
Over 200,000 Qualified Readers
Throughout Industry and Government

FEATURES

TECHNICAL SECTION

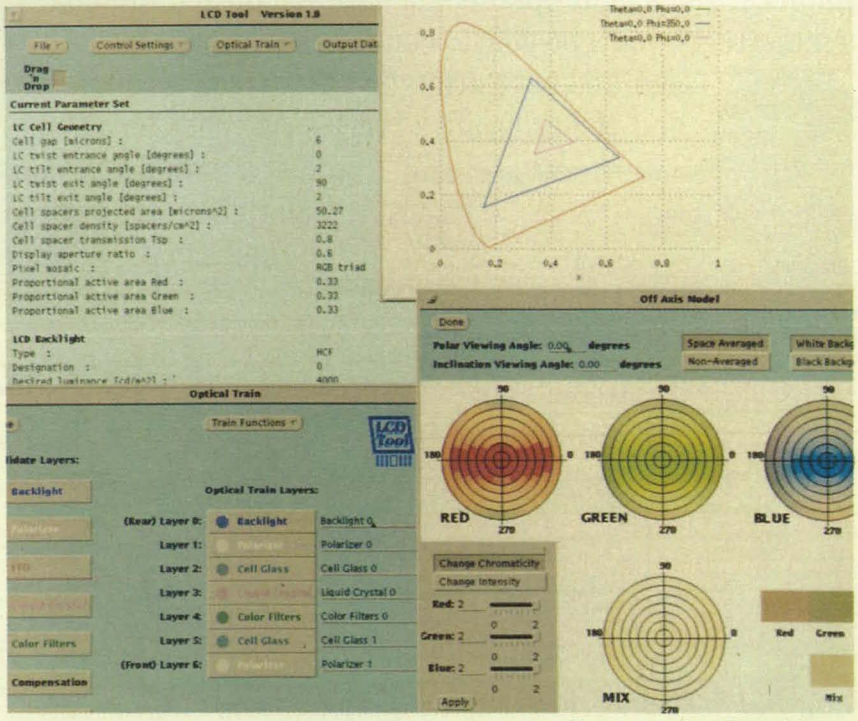

Photo courtesy Ames Research Center

ViDEOS, a computer-aided design tool for developing high-resolution visual displays such as active matrix liquid crystal displays, enables engineers to evaluate display designs in a virtual environment. The program's graphical user interface (above) permits easy manipulation of design parameters. For more on the ViDEOS project, turn to NASA's Innovators, page 14.

(Continued on page 8)

GOULD
Electronics

Honey, I shrunk the recorder.

Gould shrinks the best of recording systems into a space not much bigger than this page. Introducing the TA11 Recording-System Portable. The first system that brings 4, 8 or 16 channels of conditioning, monitoring, capturing, storing, recording and communicating down to a portable size. At a very economical price.

Measuring just 14″W x 16″D x 7⅜″H and weighing approximately 28 lbs., the rugged TA11 features built-in, programmable signal conditioning suitable for most of your industrial applications, plus a unique 11″ chart.

For More Information Circle No. 418

For easy operation, we've included traditional, push-button recorder controls for basic functions. A flip-up LCD panel with proven touchscreen technology provides straightforward setup and control of advanced functions. It also minimizes paper waste by allowing you to set up and monitor traces without running the chart. And because it displays in real time, you can work more efficiently, viewing slow-changing signals as they occur.

The TA11 takes flexibility even further with multi-channel, logical OR triggering for capturing transients. It also offers two levels of waveform capture memory for up to 8MS of total memory. Allocate it to all 16 channels, and you can have up to 512kS per channel. And for storing data and setups, there's a built-in RAM card.

Once again, Gould puts its expertise to work for you, condensing high-performance recording system capabilities to create a whole new class of instruments. Starting at under $10,000. Call Gould at (216) 328-7000 for details, or for immediate response, complete the FAST ACTION FAX and send it today.

NTB 4/93

FAST ACTION FAX (216) 328-7400

Yes!

- ☐ Have a Gould Representative call me to arrange a demonstration
- ☐ Rush me a free TA11 technical brochure
- ☐ **I'm interested in Gould's convenient rent-to-own plan**

(Please print)

Name: _____

Title: _____

Company: _____

Street: _____

City: _____ State: _____ Zip: _____

Telephone: (_____)_____

FAX or mail coupon/photocopy (you may affix business card) to Gould Inc., Test and Measurement Group, 8333 Rockside Road, Valley View, OH 44125.

Contents *(continued)*

DEPARTMENTS

on the cover:

A laser system developed by Sverdrup Technology for NASA's Lewis Research Center measures strain on high-temperature specimens such as rocket engines and aircraft turbines. Using a laser speckle technique, the system can deduce two-dimensional strain without contacting the specimen. See the tech brief on page 25, part of this month's special focus on optoelectronics.

Photo courtesy Lewis Research Center

NASA Tech Briefs, ISSN 0145-319X, USPS 750-070, copyright © 1993 in U.S., is published monthly by Associated Business Publications Co., Ltd., 41 E. 42nd St., New York, NY 10017-5391. The copyrighted information does not include the (U. S. rights to) individual tech briefs which are supplied by NASA. Editorial, sales, production and circulation offices at 41 East 42nd Street, New York, NY 10017-5391. Subscription for non-qualified subscribers in the U.S. , Panama Canal Zone, and Puerto Rico, $75.00 for 1 year; $125.00 for 2 years; $200.00 for 3 years. Single copies $10.00. Foreign subscriptions one-year U.S. Funds $150.00. Remit by check, draft, postal, express orders or VISA, MasterCard, and American Express. Other remittances at sender's risk. Address all communications for subscriptions or circulation to NASA Tech Briefs, 41 East 42nd Street, New York, NY 10017-5391. Second-class postage paid at New York, NY and additional mailing offices.

POSTMASTER: please send address changes to NASA Tech Briefs, 41 E. 42nd Street, Suite 921, New York, NY 10017-5391.

A landmark satellite network for the U.S. Army is providing training to National Guard and Army Reserve troops via satellite. The program is being run by Oklahoma State University using Hughes Aircraft Company's InTELEconference very small aperture terminals (VSATs). The InTELEconference system offers an unprecedented range of meeting options, including two-way audiovisual conferencing, multi-site video interaction, and conventional lecture-style broadcasting. It uses state-of-the-art digital compression and VSAT technology to achieve high-quality, multi-site audio and video transmission at far lower costs than previously available.

Global vegetation, snow and ice, radiative balance and environmental effects will be surveyed as part of NASA's Mission to Planet Earth, through use of a new electro-optical sensor now being developed by Hughes. This Moderate Resolution Imaging Spectrometer-Nadir, or MODIS-N, scheduled to fly aboard NASA's first Earth Observing System (EOS) platform in 1998, will also provide supporting data on climate and the oceans. The instrument is part of the multi-year Global Change Research Program to study and understand the earth as a total system in order to provide the scientific basis for environmental policy into the next century.

Air travelers of the future will benefit from the integration of a wide range of airport operations into a single, shared-data, computer network. This means, for example, that flight arrival time information from air traffic control will automatically be fed to gate management, baggage-handling, customs, security and other administrative and passenger-service functions. As a result, more planes can be accommodated, passenger convenience and safety improved, and airport revenues increased. Hong Kong's new Chap Lap Kok Airport, currently in the early stages of construction, will have such a network, and Hughes has been selected to serve as program management consultant for the integration of air traffic control systems into the overall airport operations.

Automobile drivers will soon enjoy more and more benefits of technology once reserved for defense. Already working on near obstacle detection systems for cars, Hughes is increasing its efforts to apply sensor technology to commercial vehicles. These "smart cameras" would help identify other vehicles in fog, rain, and snow, giving drivers vital information that could help reduce accidents and casualties. As part of increasing its diversification into commercial markets, Hughes is also studying additional sensor applications for traffic management and airport systems.

A new wiring analyzer will help Boeing test all the wiring in its 747, 767, and 777 wide-bodied jets. The high-speed, high-voltage FACT tester is the newest of three distinct generations of FACT systems developed by Hughes. The new model is the easiest to operate because it is run by a PC with a graphical user interface program. The FACT system is especially useful to commercial airlines, since an airplane has 65,000 to 70,000 wires to test. Tests performed by the FACT system include continuity and high voltage insulation, with continuity tests run at up to 6,000 per minute and leakage tests up to 3,000 per minute.

For more information write to: P.O. Box 80032, Los Angeles, CA 90080-0032

HUGHES

Subsidiary of GM Hughes Electronics

NASA Tech Briefs

Official Publication of National Aeronautics and Space Administration

ABP BPA

NASA Tech Briefs

THE ASPIRIN PEOPLE LEARNED A LONG TIME AGO THAT BUFFERED WAS BETTER.

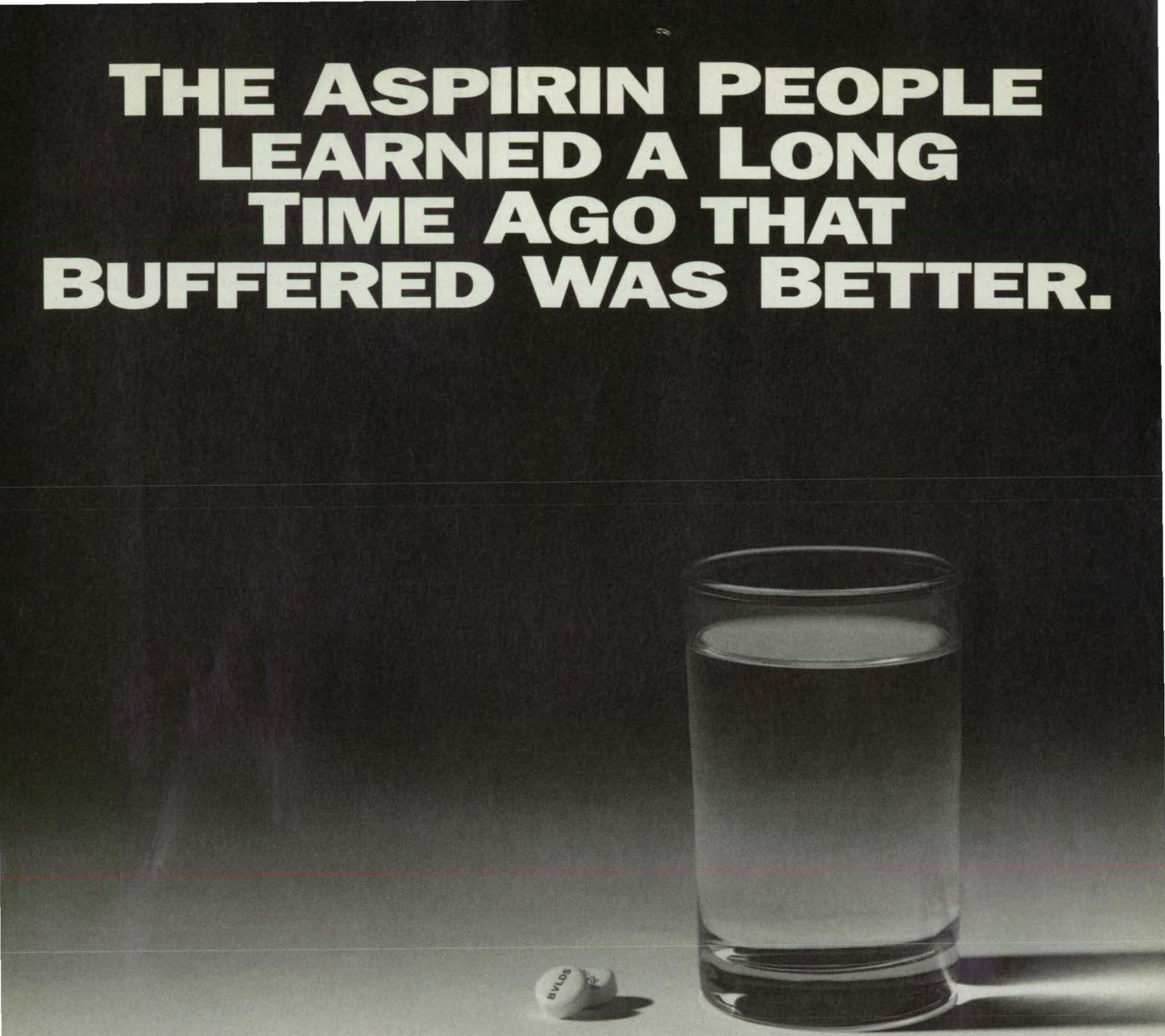

The Metrum BVLDS uses a 16 MB buffer to give you the kind of speed and flexibility you need to relieve painful data acquisition and playback headaches.

It's just what the doctor ordered. Not only can the VLDS instrumentation recorder store an amazing 10.4 gigabytes of information on a single ST-120 cassette, it can also do it at a burst rate of up to 20 megabytes per second.

And now, Metrum's Buffered VLDS makes it possible to set variable rates for acquisition and playback. Anywhere from 0 to 32 Mbits per second streaming. Not to mention, the BVLDS has a simple remedy for interfacing problems, with parallel TTL, differential, bit serial and ANSI standard SCSI interfaces.

Plus, you'll get it all at a price you'll find very easy to stomach.

So call and order a BVLDS now. And you won't need to call anyone in the morning.

METRUM

FOR MORE INFORMATION ON WHY BUFFERED IS BETTER, JUST CALL 1-800-METRUM-2.

For literature circle 684

For a product demo circle 610

NASA PATENTS

Over the past three decades, NASA has granted more than 1000 patent licenses in virtually every area of technology. The agency has a portfolio of 3000 patents and pending applications available now for license by businesses and individuals, including these recently patented inventions:

Multiperiod-Grating Surface-Emitting Lasers

(US Patent No. 5,164,956)

Inventor: **Robert J. Lang**, Jet Propulsion Laboratory

Hybrid gratings are used to lower threshold currents, increase quantum efficiencies, and improve the beamwidth of grating-coupled, surface-emitting distributed feedback (DFB) lasers. A first-order grating at one or both ends of the laser's active region provides retroflection of light back into the active region. A second-order grating at the opposite end couples light out perpendicular to the laser's surface or in a selected direction. The gratings may be curved to focus coupled light for use as part of a monolithic read head for a laser recorded disk.

For More Information Circle No. 750

Multi-Heat Addition Turbine Engine

(US Patent No. 5,184,460)

Inventors: **Leo C. Franciscus** and **Theodore A. Brabbs**, Lewis Research Center

A novel gas turbine engine utilizes heat addition devices to transfer energy to air. The devices are positioned between multiple turbines, which extract energy from air and convert it to work. The engine provides dry power and lower fuel consumption or lower combustor exit temperatures than conventional gas turbine engines.

For More Information Circle No. 753

Regenerable Biocide Delivery Unit

(US Patent No. 5,176,836)

Inventors: **Richard L. Sauer**, **Gerald V. Colombo**, and **Clifford D. Jolly**, Johnson Space Center

A new apparatus enables continuous, long-term microbial control in potable, hygiene, and experimental water supplies for both space and terrestrial use. Water is purified by passing it through an iodinated anion exchange resin bed to impart an iodine residual. A bed of iodine crystals is connected with the iodinated resin bed and activated periodically—such as by timer, measured flow of water, or iodine residual level—to recharge the bed with bound iodine.

For More Information Circle No. 754

Near-Real-Time Stereo Vision System

(US Patent No. 5,179,441)

Inventors: **Charles H. Anderson** and **Larry H. Matthies**, Jet Propulsion Lab

A vision system developed at JPL has enabled the first autonomous, cross-country robotic traverses (of up to 100 meters) with all computing done aboard the vehicle. The near-real-time stereo vision system comprises two cameras mounted on three-axis rotation platforms, image-processing boards, and a CPU programmed with specialized stereo vision algorithms. Bandpass-filtered image pyramids are computed, stereo matching is performed by least-squares correlation, and confidence ranges are estimated by means of Bayes' theorem to yield range images from 60 x 64 stereo pairs at rates up to two seconds per frame.

For More Information Circle No. 755

Compliant Walker

(US Patent No. 5,174,590)

Inventors: **James J. Kerley**, **Wayne D. Eklund**, and **J. Allen A. Crane**, Goddard Space Flight Center

An innovative walker employs robotics technology to permit people with limited use of their legs to become ambulatory under their own power. It can be applied in the treatment of injured or post-operative patients and as an aid to the permanently disabled. The walker incorporates an upright wheeled frame that at least partially surrounds an upright user wearing a partial body harness. The harness is attached to the frame by a cable-compliant apparatus that provides shock and vibration protection and corrects for misalignments.

For More Information Circle No. 752

Spectroscopic Wear Detector

(US Patent No. 5,187,542)

Inventor: **George C. Madzsar**, Lewis Research Center

Mr. Madzsar has developed a nonintrusive, noncontacting technique to monitor and measure component wear that requires no disassembly or use of radioactive isotopes. First, the elemental composition of the structure to be monitored is determined. Then, atoms of an elemental species not appearing in the material are implanted beneath the surface at a depth based on the maximum allowable wear. As the component wears, the implanted species eventually surfaces and can be detected by spectroscopic monitoring of exhaust gasses.

For More Information Circle No. 751

All you need for complete multichannel waveform acquisition and analysis is the Nicolet MultiPro. It's the transient analyzer that gives you all the inputs you need to handle 2 or 200 channel applications. And with no multiplexing, data is never lost. MultiPro also offers 8 or 12-bit digitizers, 1-200 MS/s, waveforms of over 3 million points, and Microsoft® Windows™ control software to give you complete solutions quickly and accurately. All in a turnkey system that's up and running in minutes. The Nicolet MultiPro Multichannel Transient Analyzer. Nothing else comes close. Call 1-800-356-8088 today.

Nicolet

INSTRUMENTS OF DISCOVERY

Nicolet Measurement Instruments
Madison, Wisconsin, USA 53711-4495
608/271-3333, FAX 608/273-5061
For More Information Circle No. 526

NASA's
INNOVATORS

DESIGNING TOMORROW'S DISPLAYS

From home to office and everywhere in between, electronic displays provide the windows to information conveyed by computers, car dashboards, televisions, and a widening array of other consumer products. As display applications have proliferated, so too have the technologies for creating them, each offering a range of attributes. A new software tool called the Video Display Engineering and Optimization System (ViDEOS) offers engineers an efficient way to evaluate display designs to identify the one best-suited to a particular application.

ViDEOS is a computer-aided design (CAD) tool for engineering, performance optimization, and systems integration of high-resolution visual displays. A comprehensive development tool, ViDEOS combines representations of display characteristics—including optical, electrical, and signal processing—with a model of human vision. ViDEOS permits evaluation of design concepts in a virtual environment, thereby reducing the number of physical prototypes needed, shortening development times and cutting costs.

"ViDEOS provides end-to-end simulations, modeling everything from the light source to the image as it would be seen by the display user," said Dr. James Larimer, co-principle investigator at NASA's Ames Research Center, which is coordinating the project. "It can take months to build a display from scratch. Using our CAD program can rule out designs with major flaws very quickly."

The project thus far has focused on liquid crystal displays (LCDs), compact, lightweight flat panels that consume moderate amounts of power compared to conventional cathode ray tubes (CRTs), making them ideal for such applications as laptop computers. ViDEOS also can be applied to alternate flat panel technologies such as cold cathode and electroluminescent displays, as well as CRTs.

ViDEOS incorporates technology conceived during NASA's Cockpit Visibility Modeling System project, under-

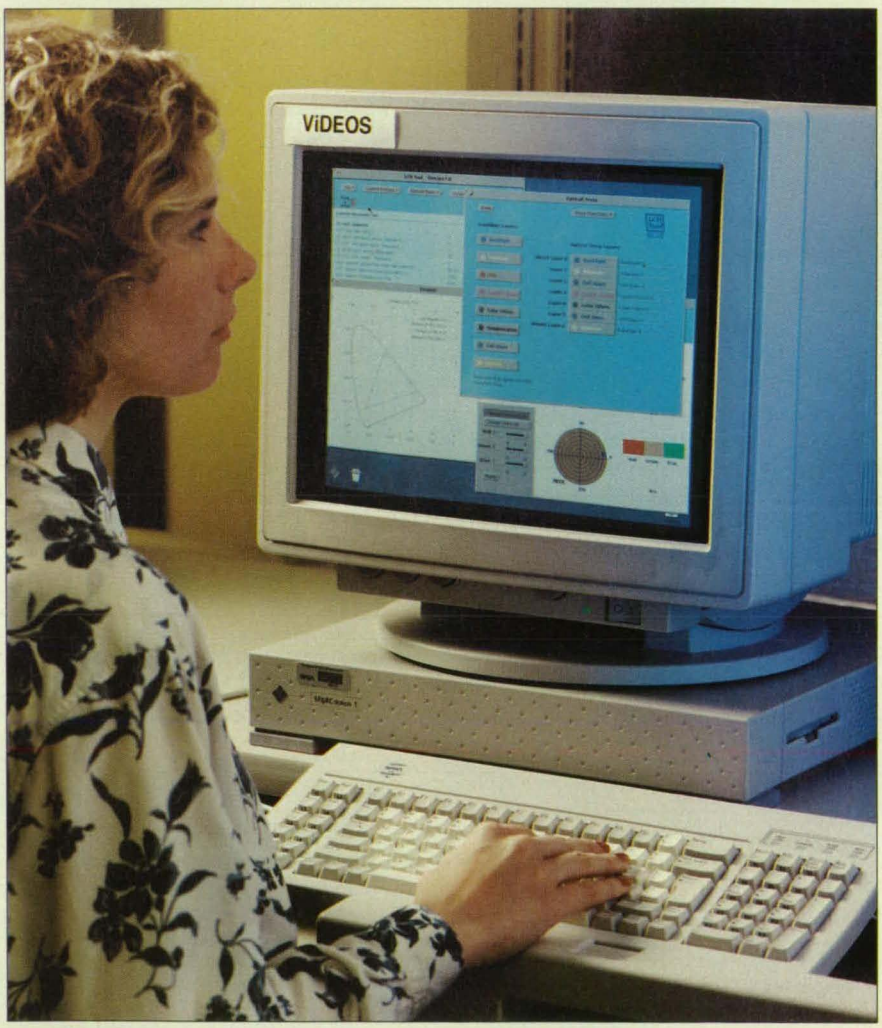

ViDEOS, a computer-aided design tool for developing high-resolution visual displays, provides a graphical user interface for easy manipulation of design parameters.

BACKUP 50 GB IN HALF THE TIME.

Two 8mm tape drives, each capable of storing up to 25 GB, can be combined in a single desktop cabinet. This dual configuration lets you take full advantage of our Advanced SCSI Processor.

Now, two drives can work together simultaneously to maximize backup speed and capacity with a variety of recording modes.

STRIPING MODE. In striping mode, you can write data to two tapes at once, in alternate blocks–doubling speed and capacity. In fact, you can back up 50 GB overnight this way.

MIRRORING MODE. In mirroring mode, you write the same data to two tapes at the same time. This is ideal for users who want to keep a backup off-site, for extra security, or for users who need to exchange data with other sites.

OFF-LINE COPY. An off-line copy function lets you copy the contents of one tape to another–without tying up the host. Off-line verify ensures that the tapes are identical.

CASCADE MODE. In cascade mode, data spills over to the second tape when the first tape is full.

FLEXIBILITY IS ONLY HALF THE STORY. Our data compression option is the fastest available. And it's switch-selectable, so you can still read and write standard 8mm tapes. Bright backlit status displays give you complete drive status information: recording mode, transfer rate, compression ratio,tape remaining and more.

Best of all, you get the advantages of 8mm helical scan technology–reliable, unattended operation and the best price-performance on the market.

Plug compatible with virtually every computer system, the drives are fully backed by our 12-month warranty that includes support from our in-house engineering staff.

For information, call today at

(804) 873-9000

CONTEMPORARY CYBERNETICS

TRUE PLUG COMPATIBILITY

Alliant	Convergent	DEC Unibus	ICL	Novell	Plexus	Sun
Alpha Micro	Data General	Gould/Encore	Intergraph	OS/2	Prime	Texas Instruments
Altos	DEC 3100/5000	HP	Macintosh	PS/2	Pyramid	Unisys
Apollo	DEC BI-Bus	IBM AS/400	McDonnell Douglas	Parallel Port	Sequent	Wang
Arix	DEC DSSI	IBM Mainframe	Motorola	PC 386/ix	Silicon Graphics	*and more*
AT&T	DEC HSC	IBM RISC/6000	NCR	PC MS-DOS	STC	
Basic-4	DEC Q-Bus	IBM RT	NeXT	PC Xenix/Unix	Stratus	
Concurrent	DEC TU/TA81	IBM S/38	Pertec			

Rock Landing Corporate Center • 11846 Rock Landing • Newport News, Virginia 23606 • Fax (804)873-8836

For More Information Circle No. 422

ViDEOS predicts the effects on image quality of reducing the resolution of particular color pixels. Reducing the resolution of the blue pixels (above) has little effect on the image, whereas reducing green pixel resolution (below) introduces significant spatial error.

taken to develop CAD tools for modeling cockpit displays. The resulting system enhanced the engineer's appreciation of design factors influencing the pilot's visual perception of displays such as an air speed indicator. In 1991, the NASA project came to the attention of the Defense Advanced Research Projects Agency's (DARPA's) High Resolution Systems Program, which was looking for technology to support the US flat panel display industry.

DARPA has assembled an extremely diverse project team, according to Larimer, to ensure that ViDEOS will cover all aspects of display development. Participants, which cumulatively have received over $1.5 million in funding from DARPA to support the project's second year, include the David Sarnoff Research Center, Optical Imaging Systems Inc., VCD Sciences Inc., the Liquid Crystal Institute at Kent State University, the University of Virginia, the University of Wisconsin, and Stanford University.

The ViDEOS development team has focused on a highly promising type of flat panel display known as active matrix LCDs (AMLCDs), capable of the video rate imagery critical to many defense applications. AMLCDs, which resemble dynamic random-access memory (DRAM) chips in complexity, employ an array of thin-film-transistors, (TFTs), each of which activates a single pixel in the display. This eliminates the crosstalk voltage that plagues passive LCDs, reducing image distortions and permitting larger screens with rapid refresh rates.

Software modules in the current ViDEOS' format include a liquid crystal optics modeler, a tool to help with circuit layout, a display tool, and a human vision model. Variable parameters in the LCD layer include the cell thickness, the orientation of the rubbing layers, the birefringence of the liquid crystal material, and its elasticity and viscosity. Properties of the other layers also may vary, including filter thickness, the electrical properties of the circuit, and composition of the light source.

Varying these parameters has a direct impact on image properties such as resolution, contrast, and chromaticity. As ViDEOS can predict, certain tradeoffs—such as decreasing the resolution while increasing the grayscale or altering the pixel pitch of individual colors (see images above)—can lower the cost of manufacturing the display without causing an unacceptable degree of image degradation.

The display model also reveals whether the image will flicker or jitter. "We can generate a bit map of the screen you would actually see if you built the display a particular way," said Larimer. "We've confirmed the accuracy of our predicted images by modeling existing displays."

Currently built to run on standard UNIX workstations, ViDEOS is being adapted to port easily to a variety of standard engineering workstations and to accommodate integration of software from outside sources. Providing a graphical user interface for ease of use (see sample screen on page 14), the program is targeted to both display manufacturers and those who integrate displays into laptop computers, car dashboards, control interfaces, telecommunications equipment, video games, and other systems. Further, it provides a precise means for the two types of users to communicate.

The software is in use at a number of US companies through technology exchange agreements with the program directors. A company thereby can obtain the software in return for providing feedback regarding, for example, the accuracy of its predictions and its ease of use. Current users include Kopin, Planar Systems, Silicon Video, and Xerox PARC, as well as various avionics display manufacturers. ❑

For more information about the technology described in this article contact Dr. James Larimer, Ames Research Center, Mail Code 269-6, Moffett Field, CA 94035.

DESKTOP MANUFACTURING...

We are the leading supplier of sealed CO_2 lasers to manufacturers of "desktop" or fully automatic laser processing equipment, covering a power range from 7 to 200 Watts. We manufacture more CO_2 lasers than any other company in the world.

The parts shown above are all manufactured or marked in seconds to minutes with a sealed 25 Watt CO_2 laser on the same workstation. A PC generated CAD file addresses the laser beam in intensity and x-y motion.

Laser and machine operating costs are about half a penny per Watt-hour, while creating parts worth $5 per Watt-hour; all without hard tooling. Laser acquisition cost is $100–$150 per Watt, while a gas life of 10,000 "on" hours assures years of reliable service.

Our sealed CO_2 lasers help make it possible

If you are interested in putting the extreme productivity of sealed CO_2 lasers to work in your applications, talk to us—we will help you. Our patented "All Metal" technology is simple, reliable and proven world wide in thousands of installations:

COLOR MARKING OF ALUMINUM • CUTTING • DRILLING • ENGRAVING • ELECTRONIC COMPONENT MARKING • GASKET MANUFACTURING • GLASS PROCESSING • HEAT SEALING • MODEL MAKING • MOLD TRIMMING • PERFORATING • PLASTIC PARTS • POLYMERIZING • RESISTOR TRIMMING • SCRIBING • SIGN MAKING • SAIL CUTTING • SOLDERING • TEXTILE CUTTING • WATERMARK SENSING • WELDING • WIRE STRIPPING • 3D LITHOGRAPHY

Our representatives:

ustralia: Spectra-Physics PTY Ltd, Croydon, Phone 61-3-723-6600
hina: Global Technology, Beijing, Phone 86-1-83-13388
gland: Optilas, Milton Keynes, Phone 44-908-221123
ance: Optilas, Evry Cedex, phone 33-1-60-79-59-00
ermany: Optilas, Puchheim, Phone 49-89-801035
rael: Applied Technologic Services, Herzelia, Phone 972-52-574111
apan: Kantum Electronics, Tokyo, Phone 81-3-3-758-1113
letherlands: Optilas, Alphen Aan Den Rijn, Phone 31-1720-31234
ingapore: Plasim Corp., Singapore, Phone 65-294-6600
Spain: Optilas Iberica, s.a., Madrid, phone 34-1-519-01-65
weden: Latronix AB, Taby, Phone 46-8-7569190

SYNRAD INC.

11816 North Creek Parkway North
Bothell, WA 98011-8205

(206) 483-6100
FAX: (206) 485-4882

For More Information Circle No. 397

New Product Ideas

New Product Ideas are just a few of the many innovations described in this issue of *NASA Tech Briefs* and having promising commercial applications. Each is discussed further on the referenced page in the appropriate section in this issue. If you are interested in developing a product from these or other NASA innovations, you can receive further technical information by requesting the TSP referenced at the end of the full-length article or by writing the Technology Utilization Office of the sponsoring NASA center (see page 20). NASA's patent-licensing program to encourage commercial development is described on page 20.

GaAs Optoelectronic Integrated-Circuit Neurons

New monolithic integrated circuits are being developed for use as artificial neurons. Optical switching energy and power consumed by these circuits are only 38 pJ and 1.8 mW, respectively.
(See page 25.)

Ball Lenses Collimate and Focus Diode-Laser-Array Beams

Ball lenses perform as well as or better than the multiple element lenses in collimating and focusing pump light from an array of diode lasers onto the input face of a solid-state laser. Low cost, low loss, and simplicity outweigh spherical aberration.
(See page 26.)

Thinner, More-Efficient Oxygen-Separation Cells

A new oxygen-separation cell is more efficient, smaller, lighter, and easier to manufacture than earlier designs. Potential applications include use as gas separators, filters, and fuel cells.
(See page 41.)

Surface-Acoustic-Wave Piezoelectric Microbalance

A prototype microbalance is expected to provide about 400 times the mass sensitivity per unit area of prior microbalances. The device can be used to analyze airborne particles in environments as diverse as clean rooms or the upper atmosphere.
(See page 42.)

Roller Locking Brake

This electromagnetically releasable brake provides high locking torque. The unit is useful in robots and other machinery requiring automatic braking after disengagement of electrical power.
(See page 71.)

Bag for Formulating and Dispensing Intravenous Solution

A large-volume parenteral bag can be used to formulate and dispense a sterile intravenous solution in a non-sterile environment. The bag can be used in field and facilities that lack proper sterilization. Accompanying innovations include a solute-filled syringe and a unit-dose bag for formulating intravenous solutions.
(See page 83)

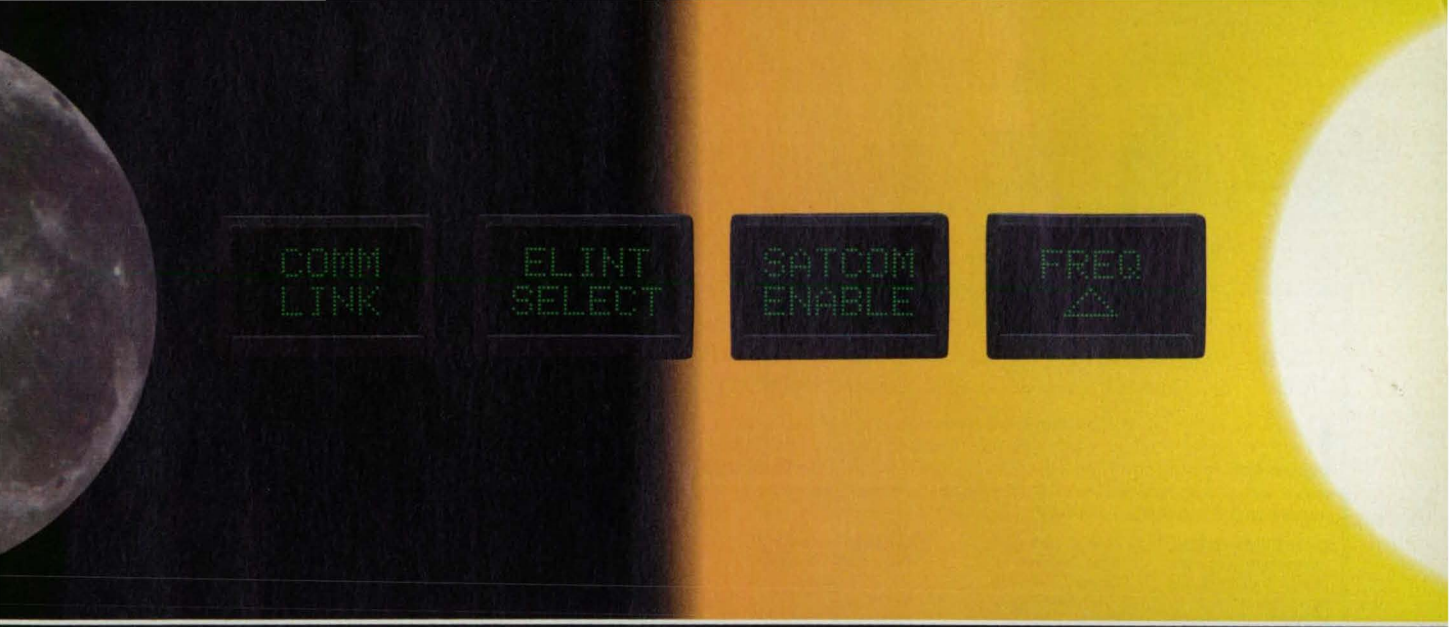

The NVIS-Sunlight Readable Electro-Optical Display System.

The VIVISUN 5000 electro-optical display system incorporates LED lighting that is both NVIS compatible and sunlight readable per MIL-L-85762A. This interactive system also provides rugged reliability and meets the environmental extremes that military programs demand.

The VIVISUN 5000 LED dot-matrix electro-optical display has a 1000:1 dimming ratio which achieves NVIS compatibility and sunlight readability (10,000 foot-candles). System features include: Total Legend Flexibility • Serial Data Line via RS-232C or RS-422 • Interactive Tactile Response.

The VIVISUN 5000 electro-optical display system is the solution for your ruggedized military design requirements.

Contact us today.

AEROSPACE OPTICS INC.
3201 Sandy Lane, Fort Worth, Texas 76112
Phone (817) 451-1141 • Fax (817) 654-3405

VIVISUN 5000 electro-optical display system. The day-night all weather lighting solution.

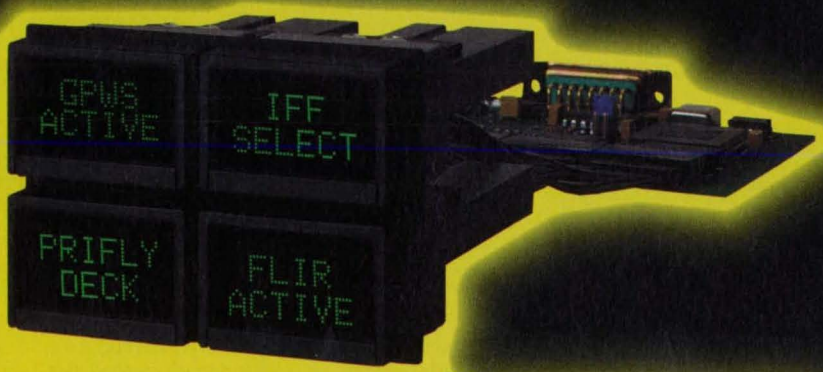

SERIES

VIVISUN 5000™

HOW YOU CAN BENEFIT FROM NASA's TECHNOLOGY UTILIZATION SERVICES

If you're a regular reader of TECH BRIEFS, then you're already making use of one of the low-and no-cost services provided by NASA's Technology Transfer Program. But a TECH BRIEFS subscription represents only a fraction of the technical information and applications/engineering services offered by this Program. In fact, when all of the components of NASA's Technology Transfer Network are considered, TECH BRIEFS represents the proverbial tip of the iceberg.

We've outlined below NASA's Technology Transfer Network—named the participants, described their services, and listed the individuals you can contact for more information relating to your specific needs. We encourage you to make use of the information, access, and applications services offered.

How You Can Access Technology Transfer Services At NASA Field Centers:

Technology Utilization Officers & Patent Counsels—Each NASA Field Center has a Technology Utilization Officer (TUO) and a Patent Counsel to facilitate technology transfer between NASA and the private sector.

If you need further information about new technologies presented in *NASA Tech Briefs*, request the Technical Support Package (TSP). If a TSP is not available, you can contact the Technology Utilization Officer at the NASA Field Center that sponsored the research. He can arrange for assistance in applying the technology by putting you in touch with the people who developed it. If you want information about the patent status of a technology or are interested in licensing a NASA invention, contact the Patent Counsel at the NASA Field Center that sponsored the research. Refer to the NASA reference number at the end of the Tech Brief.

Ames Research Ctr.
Technology Utilization Officer:Geoffrey S. Lee
Mail Code 223-3
Moffett Field, CA 94035
(415) 604-4044
Patent Counsel:
Darrell G. Brekke
Mail Code 200-11
Moffett Field, CA 94035
(415) 604-5104

Lewis Research Center
Technology Utilization Officer: Anthony F. Ratajczak
Mail Stop 7-3
21000 Brookpark Road
Cleveland, OH 44135
(216) 433-5568
Patent Counsel:
Gene E. Shook
Mail Code LE-LAW
21000 Brookpark Road
Cleveland, OH 44135
(216) 433-5753

John C. Stennis Space Center
Acting Technology Utilization Officer:
Charles Hill
Code HA-30
Stennis Space Center, MS 39529
(601) 688-1929

John F. Kennedy Space Center
Technology Utilization Officer: James A. Aliberti
Mail Stop PT-PAT-A
Kennedy Space Center, FL 32899
(407) 867-3017
Patent Counsel:
Bill Sheehan
Mail Code PT-PAT
Kennedy Space Center, FL 32899
(407) 867-2544

Langley Research Ctr.
Technology Utilization Officer: Joseph J. Mathis, Jr.
Head, TU & AO Office
Mail Stop 200
Hampton, VA 23681-0001
(804) 864-2484
Patent Counsel:
Dr. George F. Helfrich
Mail Stop 143
Hampton, VA 23681-0001
(804) 864-3221

Goddard Space Flight Center
Technology Utilization Officer: Dr. George Alcorn
Mail Code 702
Greenbelt, MD 20771
(301) 286-5810
Patent Counsel:
R. Dennis Marchant
Mail Code 204
Greenbelt, MD 20771
(301) 286-7351

Jet Propulsion Lab.
NASA Resident Office
Technology Utilization Officer: Arif Husain
Mail Stop 180-801D
4800 Oak Grove Drive
Pasadena, CA 91109
(818) 354-4862
Patent Counsel:
Thomas H. Jones
Mail Code 180-801G
4800 Oak Grove Drive
Pasadena, CA 91109
(818) 354-5179

Technology Utilization Mgr. for JPL: Dr. Norman L. Chalfin
Mail Stop 156-211
4800 Oak Grove Drive
Pasadena, CA 91109
(818) 354-2240

George C. Marshall Space Flight Center
Technology Utilization Officer: Ismail Akbay
Code AT01
Marshall Space Flight Center,
AL 35812
(205) 544-2223
Patent Counsel:
Robert L. Broad, Jr.
Mail Code CC01
Marshall Space Flight Center,
AL 35812
(205) 544-0021

Lyndon B. Johnson Space Center
Technology Utilization Officer: Richard B. Ramsell
Mail Code IC-4
Building 4 South
Houston, TX 77058
(713) 483-3809
Patent Counsel:
Edward K. Fein
Mail Code AL3
Houston, TX 77058
(713) 483-4871

NASA Headquarters
Technology Utilization Officer: Leonard A. Ault
Code CU
Washington, DC 20546
(202) 358-0721
Associate General Counsel for Intellectual Property: Jack Mannix
Code GP
Washington, DC 20546
(202) 453-2424

How You Can Utilize **NASA's Regional Technology Transfer Centers (RTTCs)**— A nationwide network offering a broad range of technology transfer and commercialization services.

You can contact NASA's network of RTTCs for assistance in solving a specific technical problem or locating technology or markets that match your interests. The RTTCs are experienced in working with industry to define technology needs and acquire and commercialize applicable technology. User fees are charged for most services. **For more information, call 1-800-472-6785** and you will be connected to the RTTC in your geographical region (or you may call or write directly to the RTTC in your region).

REGIONAL TECHNOLOGY TRANSFER CENTERS (RTTCs)

RTTC Directors

NORTHEAST
Dr. William Gasko
Center tor Technology Commercialization
Massachusetts Technology Park
100 North Drive
Westborough, MA 01581
(508) 870-0042

MID-ATLANTIC
Ms. Lani S. Hummel
University of Pittsburgh
823 William Pitt Union
Pittsburgh, PA 15260
(412) 648-7000
(800) 257-2725 (toll-free US)

SOUTHEAST
Mr. J. Ronald Thornton
Southern Technology Application Center
University of Florida
College of Eng.
Box 24
One Progress Boulevard
Alachua, FL 32615
(904) 462-3913
(800) 225-0308 (outside FL)

MID-CONTINENT
Mr. Gary Sera
Texas Engineering Experiment Station
Texas A&M University System
237 WERC Collge Station,
Texas 77843-3401
409-845-8762

MID-WEST
Dr. Joseph W. Ray
Great Lakes Industrial Technology Center
25000 Great Northern Corporate Center
Suite 450
Cleveland, OH 44070-5310
(216) 734-0094

FAR-WEST
Mr. Robert Stark
Technology Transfer Center
University of Southern California
3716 South Hope Street,
Suite 200
Los Angeles, CA 90007-4344
(213) 743-6132
(800) 642-2872 (CA only)
(800) 872-7477 (toll-free US)

If you are interested in information, applications, research, training, and services relating to satellite and aerial data for Earth resources, contact NASA's transfer point for earth observing technology: **Technology Application Center, University of New Mexico, 2500 Yale Blvd. S.E., Suite 100, Albuquerque, NM 87131-6031; Dr. Stan Morain, Director (505) 277-3622.**

If you represent a public sector organization with a particular need, you can contact NASA's Application Team for technology matching and problem solving assistance. Staffed by professional engineers from a variety of disciplines, the Application Team works with public sector organizations to identify and solve critical problems with existing NASA technology. **Technology Application Team, Research Triangle Institute, P.O. Box 12194, Research Triangle Park, NC 27709; *Dr. Doris Rouse, Director,* (919) 541-6980**

A Shortcut To Software: **COSMIC®**—For software developed with NASA funding, contact COSMIC, NASA's Computer Software Management and Information Center. New and updated programs are announced in the Computer Programs section. COSMIC publishes an annual software catalog. For more information call or write: **COSMIC®**, 382 East Broad Street, Athens, GA 30602 *John A. Gibson, Director,* (706) 542-3265; FAX (706) 542-4807.

If You Have a Question..**NASA Center For AeroSpace Information** can answer questions about NASA's Technology Transfer Network and its services and documents. The CASI staff supplies documents and provides referrals. Call, write or use the feedback card in this issue to contact: **NASA Center For AeroSpace Information,** Technology Transfer Office, P.O. Box 8757, Baltimore, MD 21240-0757. *Walter M. Heiland, Manager,* (410) 859-5300, Ext. 245.

Faster design cycles with MATRIX$_X$

There's no faster, better way to design control systems than with the MATRIX$_X$® design automation family. Whatever your application or industry – automotive, aerospace, process control, servo design or other – MATRIX$_X$ pulls your team together, accelerating the design cycle from concept to prototype.

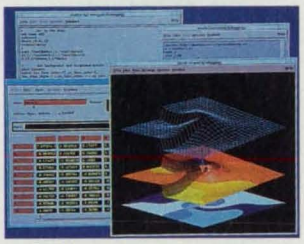

Xmath provides powerful analysis and visualization with a programmable GUI.

One integrated line.

With our integrated suite of tools, you design; we manage the details. You prototype the same model you simulate. So accuracy and integrity are assured. There's no time wasted or information lost, translating your design from one tool to the next. Now, design tradeoff studies take minutes instead of weeks, giving you more time to optimize designs. What's more, our in-house expert applications engineering group is standing by to work with you on your toughest problems.

Leadership through innovation.

Integrated Systems continues to be the innovator. *Xmath*™ is the first object-oriented analysis and visualization package with a user-programmable GUI. Since its introduction in 1985, *SystemBuild*,™ our graphical dynamic simulation package, has been consistently upgraded. *AutoCode*™ is the first and only automatic code generator. And only Integrated Systems gives you the power to take your design from concept to implementation – with the high-performance *AC-100*™ system, now based on the super-charged Intel i860. *Version 3.0*, offering interactive graphical debugging, was introduced in September 1992 to rave reviews.

On-going quality.

Over the last twelve months we've dramatically improved the quality of our products. But that's just the beginning. You can count on us to meet and exceed your expectations, today and tomorrow.

Driven worldwide.

Leading automotive manufacturers in the U.S., Japan and Europe routinely use MATRIX$_X$. Both in the lab and on the test track. We're a standard for computer peripherals and process control applications. And Space Station Freedom is currently being designed with our integrated approach.

Take us for a spin.

Call **800-932-6284** and we'll send you our informative handbook, "Accelerating Systems Design." Or ask for a comprehensive evaluation to see how MATRIX$_X$ can cost-effectively address your design needs.

AC-100 reduces testing from months to days.

integrated systems

CORPORATE HEADQUARTERS
3260 JAY STREET, SANTA CLARA, CA 95054
TEL: (408) 980-1500 FAX: (408) 980-0400
email: info@isi.com

UNITED KINGDOM HEADQUARTERS
FIRST FLOOR, GATEHOUSE, FRETHERNE ROAD, WELWYN GARDEN CITY
HERTS AL8 6NS, ENGLAND
TEL: 0707 331199 FAX: 0707 391108

For More Information Circle No. 567

Far-Infrared Imaging Radiometer

A 128×128 array of $Al_xGa_{1-x}As$ quantum-well photodetectors provides thermal resolution of 0.1 K.

Goddard Space Flight Center, Greenbelt, Maryland

A relatively inexpensive far-infrared imaging radiometer (see figure) contains a 128×128-picture-element array of $Al_xGa_{1-x}As$ quantum-well detectors. The array is bonded via indium bumps to a high-capacity, silicon-based, integrated-circuit multiplexer. The response of the array is nearly uniform from one picture element to another to such a high degree that a thermal resolution of 0.1 K or finer can be attained by a simple, two-point absolute calibration.

The new imaging radiometer puts far-infrared imaging technology within reach of small scientific laboratories. The radiometer is potentially useful in remote sensing from airborne platforms — for example, detection of actual and latent forest fires, thermal measurements of forest canopies to detect stress, counting large animals, assessment of thermal pollution in rivers, and quantitative imaging radiometry of terrain to obtain data for use in mathematical modeling of energy balances in the biosphere. Industrial applications may include rapid thermal imaging of heat-sensitive components. Astronomical applications would include imaging of planets and of the Sun.

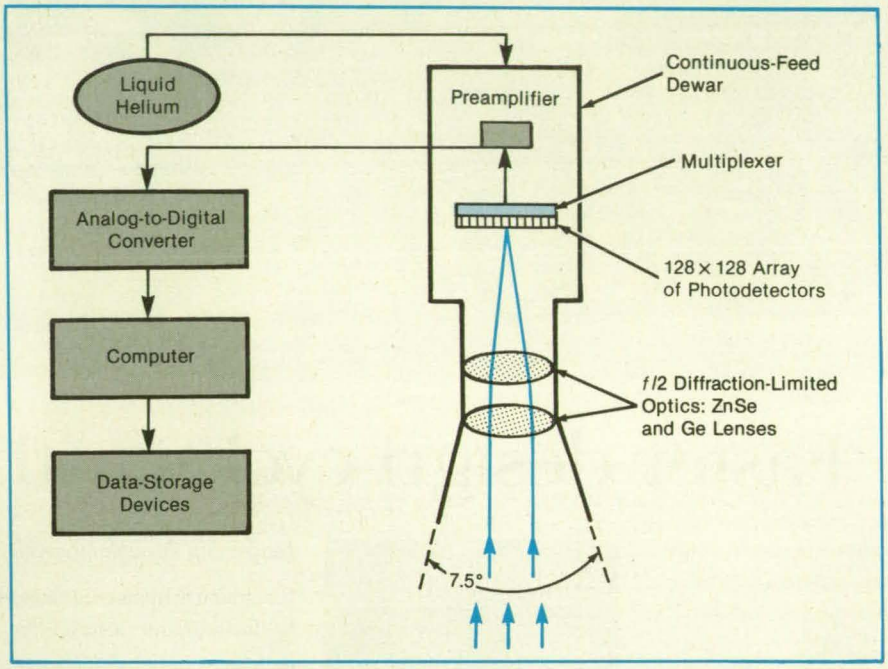

This **Thermal Imaging Radiometer** includes diffraction-limited *f*/2 optics, a 128×128 array of $Al_xGa_{1-x}As$ quantum-well detectors, and a high-capacity integrated-circuit multiplexer.

Unlike some other imaging infrared radiometers, this one includes no moving parts and operates in the staring mode; that is, the photodetector in each picture element continuously integrates the incident radiation. Thus, its detection efficiency is inherently greater than that of radiometers in which scenes are scanned by mechanically steered mirrors across single elements or linear arrays of HgCdTe detectors. Furthermore, the cost of manufacture of $Al_xGa_{1-x}As$ quantum-well arrays is far less than that of comparably sized HgCdTe arrays.

The radiometer includes diffraction-limited *f*/2 imaging optics with a 7.5° instantaneous field of view and transmission > 90 percent at 9 μm, the wavelength of peak response of the detectors. The detectors and the multiplexer circuit are cooled to 60 K with liquid helium to achieve best sensitivity. Although the detectors can be operated at the temperature of liquid nitrogen (77 K), lower temperature is preferable because the dark current of the detectors increases exponentially with temperature. The multiplexer can operate at temperatures down to about 35 K.

This work was done by Kathrine Forrest and Murzy Jhabvala of **Goddard Space Flight Center** *and Ravi Kaipa of STX. For further information, Circle 45 on the TSP Request Card. GSC-13467*

Laser System Measures Two-Dimensional Strain

Noncontact measurements yield principal components of strain, even at high temperatures.

Lewis Research Center, Cleveland, Ohio

Principal strains on the surface of a hot specimen have been determined at temperatures up to 750 °C by use of a noncontact optical method based on the work of I. Yamaguchi. In this method, strains are deduced from measured shifts in laser speckle patterns reflected from the specimen. Unlike in optical methods that involve gratings or fiducial marks, no preparation of the surface is required.

Laser speckle is an interference effect that occurs when spatially coherent light is diffracted by a rough surface. A camera that contains a linear array of photodiodes detects a component of the speckle pattern produced when a laser beam illuminates the diffusely reflecting surface of the specimen. As strain is induced in the specimen, the speckle pattern shifts by an amount directly proportional to the surface strain. The shifts in the speckle pattern are calculated by cross-correlating one-dimensional speckle patterns recorded with and without strain. By measuring the shifts in the speckle pattern with each of two laser beams, spurious shifts due to rigid-body motion of the specimen can be mathematically canceled. The residual differential speckle shift is due to only the surface strain component parallel to the linear photodiode array.

Actually, only one laser beam is used, but it is made to impinge on the specimen alternately at equal and opposite angles (see figure). Both the axis of the photodiode array and the sensed strain component on the surface of the specimen lie

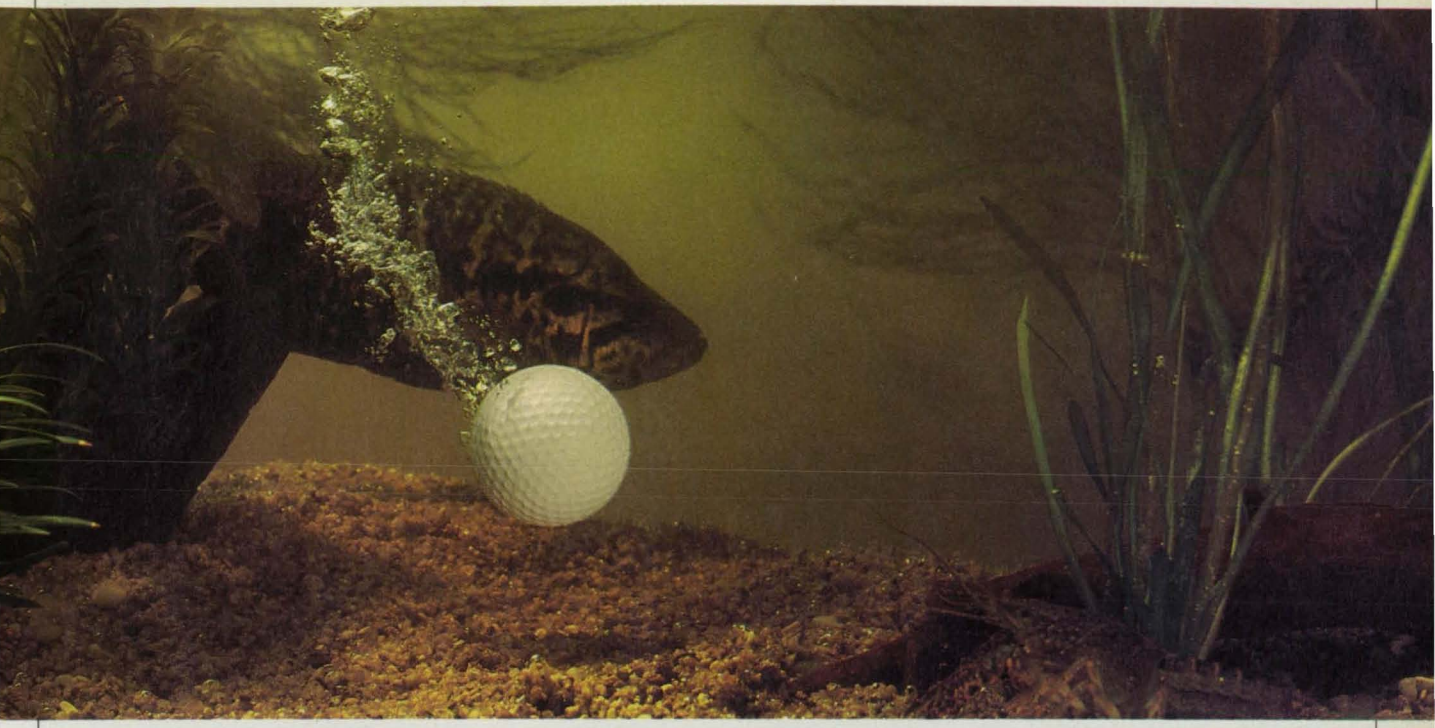

Too bad everything in your life isn't as accurate as our frame grabber.

THE DT3851

- No Compromise™ Analog Design for sharp images
- Digital Clock Sync™ yields low pixel jitter for accurate digitization
- Precision Input™ maximizes grayscale resolution in difficult low-light conditions
- Sync Sentinel™ for digitizing from VCRs in pause mode
- Fully programmable acquisition digitizes video from standard, non-standard and high resolution devices
- Single or dual monitor operation up to 1024 x 768 resolution

In this frustratingly imperfect world, it's comforting to have one thing that's always on the mark. Such as the DT3851 frame grabber, from Data Translation. The DT3851 digitizes images with unsurpassed accuracy, from almost any input device. And when you digitize with greater accuracy and precision, you'll get better data and more accurate measurements.

Of course, we also designed this board to take full advantage of Windows.™ So all of the DT3851's sophisticated features are easy to use.

To learn more about the amazingly accurate DT3851, call us today. We'll send you a brochure and our free 3-Book Set full of product and application information. And you'll see what you've been missing.

DATA TRANSLATION®

For More Information Circle No. 549

FOR MORE PRODUCT INFORMATION OR OUR FREE 3-BOOK SET CALL **800-525-8528**, EXT. **312**.

in the plane determined by the two beam directions. The axis of the photodiode array must also be parallel to the surface of the specimen. By rotating the optical assembly that directs the beams, the sensitive axis of the strain-measuring system can be aligned in any desired direction on the surface of the specimen.

The laser wave front at the surface of the specimen should be made planar to minimize sensitivity to rigid-body motion of the specimen. In general, wave fronts are planar at the waists of laser beams. Accordingly, lenses are used to position the waist of the laser beam at the surface of the specimen. The application of an appropriate bias voltage to a Pockels cell rotates the polarization vector of the laser beam by 90°, thereby switching the laser beam from one path to the other at a polarization beam-splitting cube.

A set of three strain-component measurements in different directions through a point on the surface provides sufficient information to determine the magnitudes and orientations of the two principal strain axes at that point by means of a purely geometric coordinate transformation. The state of the specimen must be stable within the resolution limit during the time required to perform the three measurements.

The resolution of the system is 15 microstrain; the one-dimensional strain-measurement error is ±15 microstrain ±0.9 percent of the strain reading. Two-dimensional measurements have a maximum theoretical error of three times the one-dimensional error.

Future work is expected to reduce the sensitivity of the system to decorrelation caused by translation of speckle patterns perpendicular to the direction along which strain is being measured. The resulting transverse shift in the speckle pattern will be tracked by recording and analyzing two-dimensional speckle fields. A fast correlating processor is expected to keep computation time within acceptable limits.

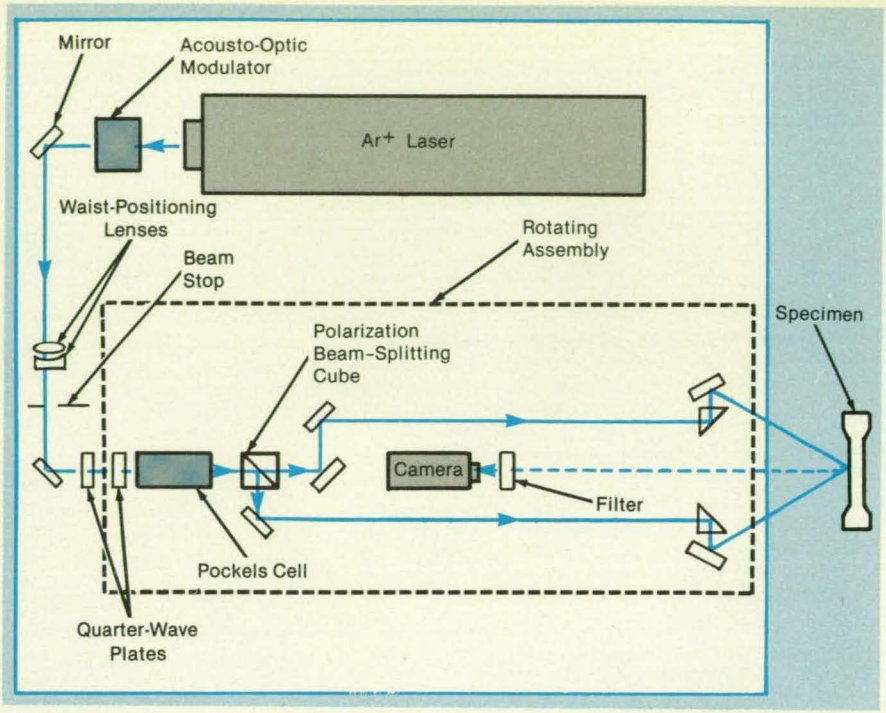

The **Optical Strain-Measuring System** includes a rotatable assembly to enable the measurement of strain in any desired direction along the surface of the specimen.

This work was done by Christian T. Lant of Sverdrup Technology, Inc., for **Lewis Research Center**. *Further information may be found in NASA CR-185116 [N89-26218], "Two-Dimensional High Temperature Optical Strain Measurement System — Phase II."*

Copies may be purchased [prepayment required] from the National Technical Information Service, Springfield, Virginia 22161, Telephone No. (703) 487-4650. Rush orders may be placed for an extra fee by calling (800) 336-4700. LEW-15046

Hydrazine Detectors Based on Raman Scattering

Raman spectra of gases adsorbed on substrates are excited by lasers and measured.

John F. Kennedy Space Center, Florida

Optoelectronic sensors for the safety-oriented monitoring of hydrazine and monomethyl hydrazine in the air are being developed. Hydrazine and its derivatives are hypergolic liquid rocket fuels that also have some industrial uses. They are toxic, tumorigenic, and explosive; consequently, the goal of the sensor-development program is to measure concentrations as low as a few parts per billion in continuous monitoring as well as peak concentrations up to hundreds of parts per million, such as might be encountered near leaks.

The developmental sensors are based on Raman scattering from the hydrazine or monomethyl hydrazine adsorbed on roughened metal or metal oxide substrates. A substrate is placed in the flow of air to be monitored. The surface of the substrate is illuminated with visible laser light, causing the emission of a spectrum that includes peaks that correspond to vibrations of the adsorbate molecules.

The intensity of these peaks depends on the degree of coverage of the surface by the adsorbate, and this, in turn, depends on the concentration of the adsorbate vapor in the air. Consequently, the intensity of the spectrum or of selected peaks serves as a measure of the concentration of the vapor. In principle, on the basis of the known characteristics of this Raman-scattering technique, it should be possible to measure concentrations down to the desired parts-per-billion level and to resolve concentrations of different gases in a mixture.

The intensity of the Raman-scattering signal depends upon the nature of the substrate: oxides of silver, iridium, and lead are candidate substrate materials for the development of practical detectors. Initial tests with electrochemically fabricated substrates demonstrated dynamic detection ranges from 60 parts per billion to > 35 parts per million and response times of about 40 seconds. The adsorption of hydrazine on electrochemically prepared silver oxide substrates was demonstrated to be reversible. The lifetimes of sensors made with silver oxide substrates were found to be approximately 2 weeks.

Contemplated subjects of further development include optimization of substrate-fabrication procedures, networks of sensor substrates distributed at positions to be monitored and connected to lasers and spectrometers via optical fibers, and the use of filters (instead of bulkier, more-expensive monochromators) to resolve Raman spectra. Similar systems could also be developed to detect nitrogen oxides and other gases.

This work was done by Martin W. Rupich and Michael M. Carrabba of EIC Laboratories, Inc. for **Kennedy Space Center**. *For further information, Circle 30 on the TSP Request Card.*
KSC-11516

Two-Dimensional Laser-Speckle Surface-Strain Gauge

Surface strains in two dimensions would be measured by an extension of Yamaguchi's method.

Lewis Research Center, Cleveland, Ohio

A proposed extension of Yamaguchi's laser-speckle surface-strain-gauge method would yield data on two-dimensional surface strains in times as short as fractions of a second. Laser-speckle measurement is intended to replace strain-gauge measurement of surface strain at high temperatures that degrade the accuracies, lifetimes, and reliabilities of strain gauges. The extended Yamaguchi method might be used, for example, to monitor strains and changes in strains induced by hot-forming and the subsequent cooling of steel.

The figure illustrates the essential optical scheme of the original version and the proposed extended version of Yamaguchi's method. The original version yields the linear surface strain in one dimension. In this version, two thin laser beams are channeled through beam-steering and beam-switching optics to strike the same measurement spot on the specimen sequentially at equal but opposite angles of incidence in the same plane of incidence (the *x*–*z* plane). The resulting speckle patterns are recorded by a linear array of photodiodes aligned parallel to the plane of incidence. The specimen is strained, and the measurement is repeated at the same spot, yielding a second pair of speckle patterns that are displaced from the speckle patterns of the first measurement along a displacement vector. This vector depends on the strain and the rigid-body translation of the specimen between the first and second measurements.

The cross-correlation between the speckle patterns of the first and second measurements is computed, yielding the displacement of each pattern. The difference between the displacements is proportional to the component of linear surface strain parallel to the plane of incidence, and the effect of rigid-body translation is automatically canceled out in the subtraction. In a prior extended version of Yamaguchi's method, the optical apparatus was rotated about the *z* axis in 45° increments to measure speckle patterns in three different planes of incidence, yielding data on the principal strains in two dimensions. This prior extended version entailed long data-acquisition times (about 10 seconds), stringent requirements on alignment, and decorrelation caused by displacements of speckle patterns perpendicular to the axis of the linear array.

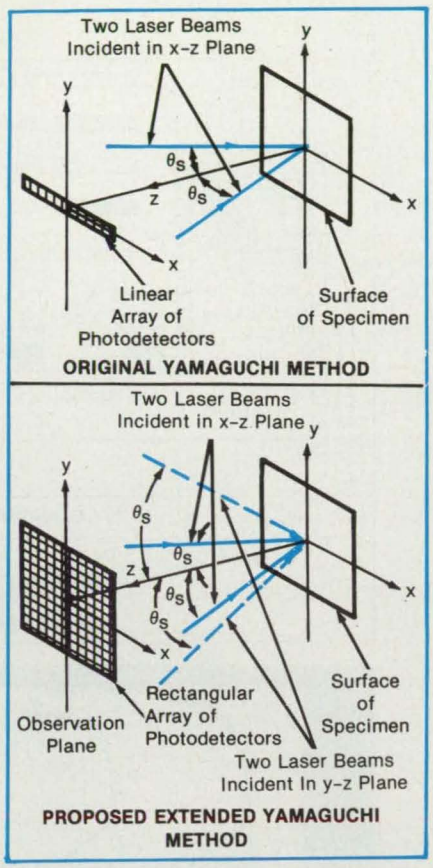

Laser Beams Probe a Rough Spot on the surface of a specimen before and after processing. Changes in the speckle pattern of laser light reflected from the spot are indicative of changes in surface strains during processing.

The proposed extended version of Yamaguchi's method would provide data on two linear strains along orthogonal axes and on the shear strain between those axes. In this version, the apparatus would not be rotated; instead, additional beam-steering optics would be installed so that the apparatus could generate laser beams in two orthogonal planes of incidence (*x*–*z* and *y*–*z*). The linear array of photodiodes would be replaced by a rectangular array of photodetectors (e.g., a charge-coupled device), which would be used to measure the speckle patterns.

Displacements of speckle patterns would be determined by computing cross-correlations, except that the cross-correlations would be two-dimensional instead of one-dimensional as before. Then the appropriate differences between displacements would be calculated, and the differences would be summed, yielding the linear strains along the *x* and *y* axes and the shear strain between them. Next, the magnitudes and directions of the principal strains can be calculated from these measured strains by use of the fundamental equations for the components of strains.

If the rectangular array of photodetectors were a charge-coupled device operating at the standard frame rate of 30 Hz, the laser beams could be steered during the transfer-gate period (about 30 μs) of vertical blanking. The total time necessary to acquire the four speckle patterns would be only four frame periods — about 0.13 s.

This work was done by John P. Barranger of **Lewis Research Center** *and Christian Lant of Sverdrup Technology, Inc. Further information may be found in NASA TM-103162 [N90-22784], "Two-Dimensional Surface Strain Measurement Based on a Variation of Yamaguchi's Laser-Speckle Strain Gauge."*

Copies may be purchased [prepayment required] from the National Technical Information Service, Springfield, Virginia 22161, Telephone No. (703) 487-4650. Rush orders may be placed for an extra fee by calling (800) 336-4700.
LEW-15337

GaAs Optoelectronic Integrated-Circuit Neurons

These devices consume less power than do prior optoelectronic neurons.

NASA's Jet Propulsion Laboratory, Pasadena, California

Monolithic GaAs optoelectronic integrated circuits are being developed for use as artificial neurons. A neural-network computer would contain planar arrays of optoelectronic neurons, and the variable synaptic connections between neurons would be effected by diffraction of light from a volume hologram in a photorefractive material. The basic principles of neural-network computers of this type were explained more fully in "Optoelectronic Integrated Circuits for Neural Networks"

(NPO-17652), *NASA Tech Briefs*, Vol. 14, No. 5 (May 1990), page 28.

Each optoelectronic neuron is basically a nonlinear processing element whose output is an amplified and thresholded version of the input. The optoelectronic neurons described in the noted prior article included double-heterojunction bipolar transistors as the amplifier. In the present circuits, these devices are replaced by metal/semiconductor field effect transistors (MESFET's), which consume less power. This decrease in power consumption is necessary for the development of large, single-chip integrated circuit array of optoelectronic neurons.

The optical input to each optoelectronic neuron is detected by the phototransistor, which is in series with a biasing MESFET (see Figure 1). If the input light becomes bright enough, the current through the phototransistor becomes sufficient to raise the source-to-drain voltage across the biasing MESFET. This turns on the output MESFET, which drives the light-emitting diode.

The turn-on threshold can be raised or lowered by raising or lowering the bias voltage on the biasing MESFET. The saturation of the output is provided by the finite swing of the gate voltage in the output MESFET. The differential gain (change in output optical power ÷ change in the input optical power) of the neuron between turn-on and saturation is determined by the slopes of the current-vs.-voltage curves of the phototransistor and the biasing MESFET. If the slopes were both zero, the differential gain of the optoelectronic neuron would be infinite.

The leftmost experimental curve in Figure 2 represents a differential gain of 6. In another experiment of optoelectronic neuron in which the phototransistor was replaced by an optical field-effect transistor (OPFET), a differential optical gain of 80 was obtained when a 54-nW beam incident on the OPFET caused the output of the light-emitting diode to rise by 4.3 μW. The optical switching energy and the power consumed by this circuit are only 38 pJ and 1.8 mW, respectively.

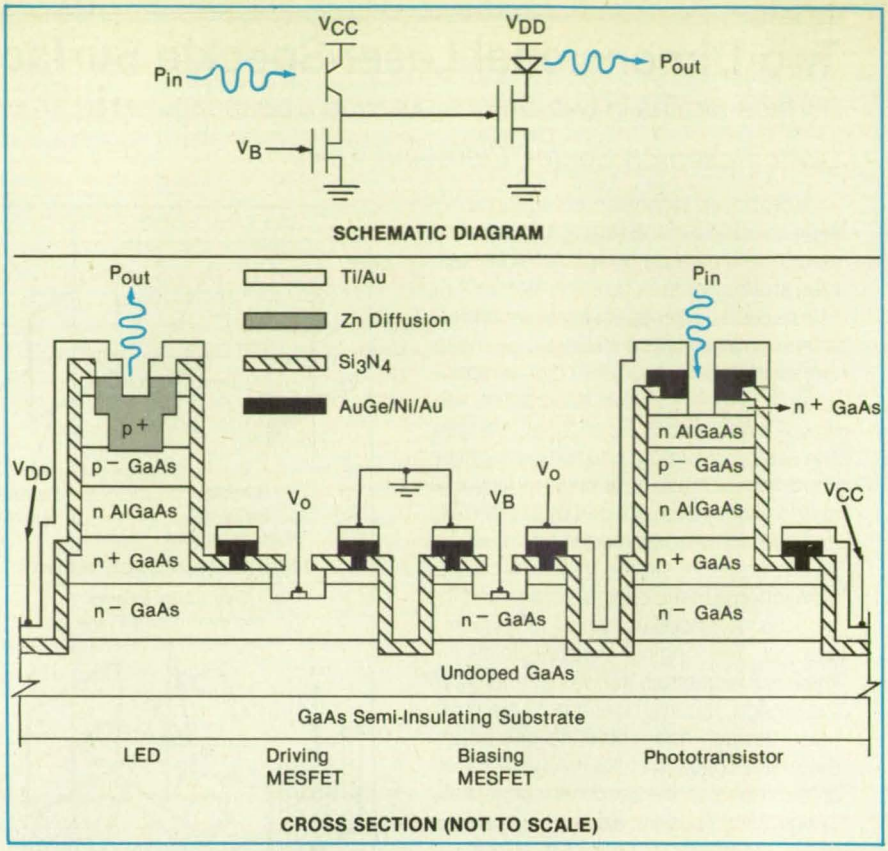

Figure 1. **The Optoelectronic Neuron** is an integrated circuit that contains low-power GaAs MESFET's and a LED.

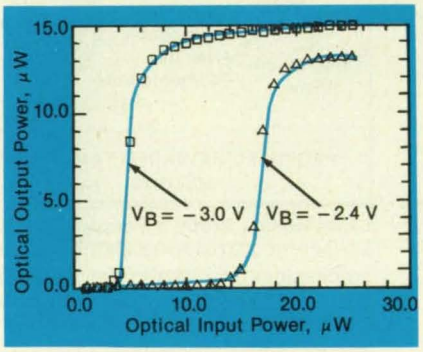

Figure 2. The **Threshold Input Power** can be adjusted by changing the bias voltage, V_B.

This work was done by Steven H. Lin, Jae H. Kim, and Demetri Psaltis of Caltech for **NASA's Jet Propulsion Laboratory**. *For further information, Circle 12 on the TSP Request Card.*

This invention is owned by NASA, and a patent application has been filed. Inquiries concerning nonexclusive or exclusive license for its commercial development should be addressed to the Patent Counsel, NASA Resident Office - JPL [see page 20]. Refer to NPO-18497.

Ball Lenses Collimate and Focus Diode-Laser-Array Beams

Low cost, low loss, and simplicity outweigh spherical aberration.

NASA's Jet Propulsion Laboratory, Pasadena, California

Ball lenses can be used to collimate and focus pump light from an array of diode lasers onto the input face of a solid-state laser (see figure). Preliminary experiments have shown that in this application, ball lenses perform as well as, or better than, the multiple-element lenses supplied heretofore as parts of commercial arrays of diode lasers.

A ball lens is simply a polished solid sphere of glass, quartz, sapphire, or any other material that is highly transparent at the laser wavelength. The surface can be coated to suppress reflections; ball lenses with transmittance greater than 99.95 percent can be fabricated readily. In comparison with conventional multiple-element lenses, it offers the advantages of relative simplicity and ease of fabrication, lower cost, lower weight, and less sensitivity to misalignment.

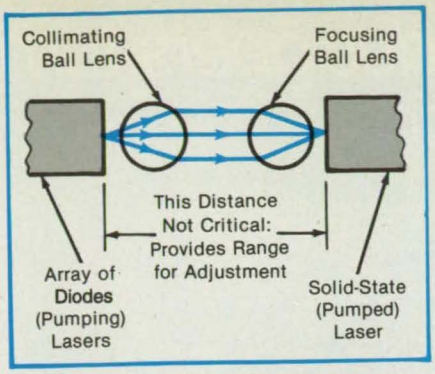

Two Ball Lenses in a collimating-and-focusing arrangement offer advantages of relatively low cost and simplicity.

The diameter of the lenses in a collimating-and-focusing pair should be sufficient to provide an adequate focal length and working distance between the output facets of the diode laser(s) and the lens and to assure the capture of all of the highly divergent laser beam. The working distance would ordinarily be approximately the focal length, which is given by $nr/2(n-1)$, where r is the radius of the sphere and n is its index of refraction. Typical diameters would probably lie between 5 and 10 mm.

The numerical aperture (a measure of the angle of divergence within which the lens captures light) of a ball lens can be made larger than that of a typical commercial diode-laser collimating lens; that is, a spherical lens can be made to capture more of the divergent laser beam. For example, a ball lens of $n = 1.8$ has a numerical aperture > 0.8, while some of the best commercial lenses designed for use with diode lasers have numerical apertures of about 0.6.

The one disadvantage of ball lenses is that they introduce some spherical aberration. This is not a serious disadvantage in the laser-pumping application, because the quality of the image of the diode laser(s) on the face of the pumped solid-state laser is not very critical. Furthermore, spherical aberration can be reduced by slight defocusing or by use of lenses of greater n.

This work was done by Hamid Hemmati of Caltech for **NASA's Jet Propulsion Laboratory**. *For further information, Circle 16 on the TSP Request Card.*

Inquiries concerning rights for the commercial use of this invention should be addressed to the Patent Counsel, NASA Resident Office – JPL [see page 20]. Refer to NPO-18469.

Where product and network designers turn for a helping hand in fiber optics.

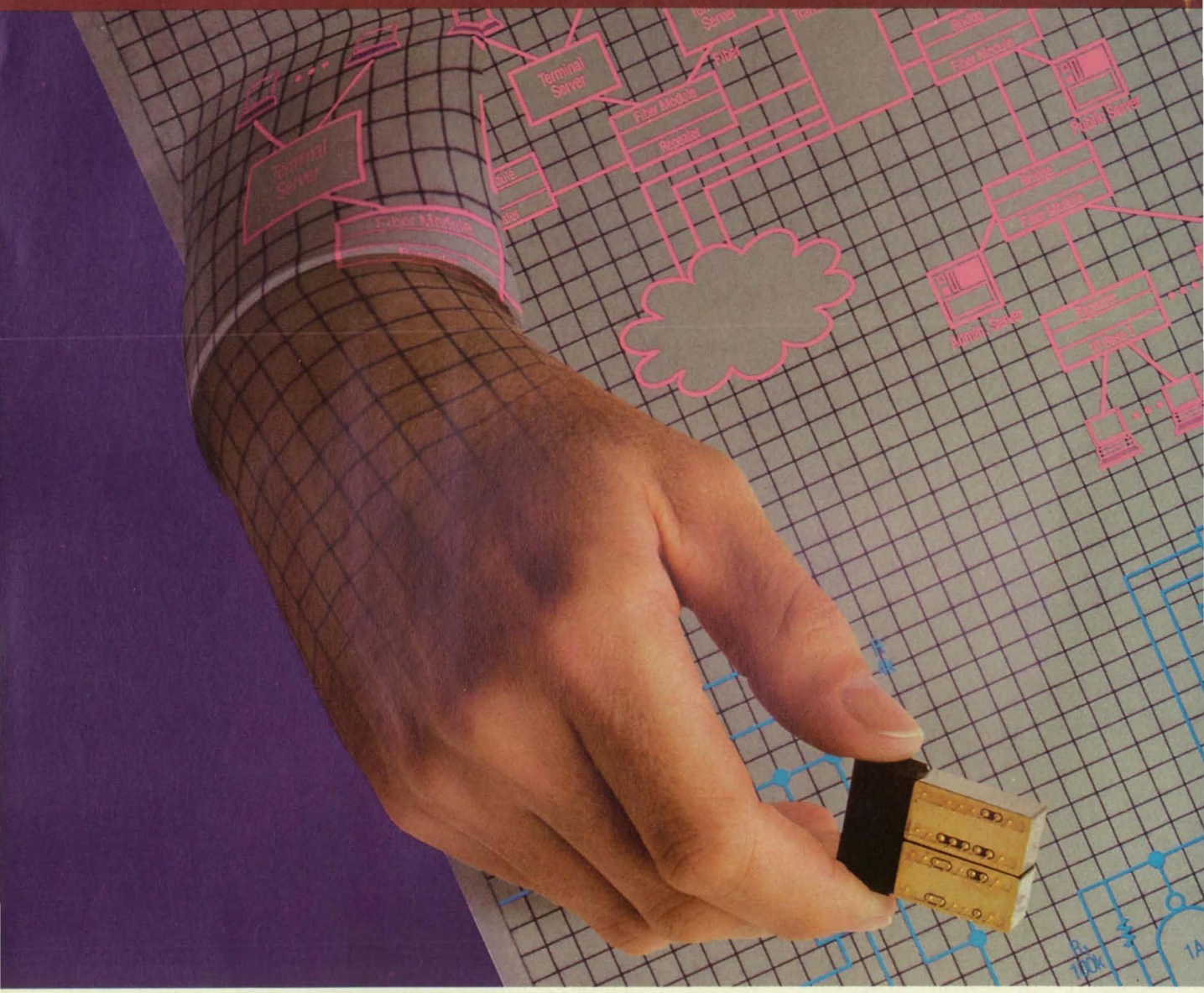

Product design and network implementation sometime seem to lie on opposite ends of the fiber spectrum; practitioners of each can spend an entire career without meeting.

Where do they find common ground? For AMP customers, the answer is simple: one supplier. One supplier who understands both sides of the fiber equation. Who has pursued fiber technology from its beginnings. Who has played and continues to play a major role in key standards organizations. Who ultimately provides a bridge of technology and support between the hardware side and the transport side of today's fiber networks.

AMP LEDs, laser diodes, and detectors are an easy way to make the transition from pcb, panel, or bulkhead to cable. Our data links contain everything you need for a logic-to-logic interface, and come with today's popular FDDI, ST, SC, and other connectors built in. They're about as close as you

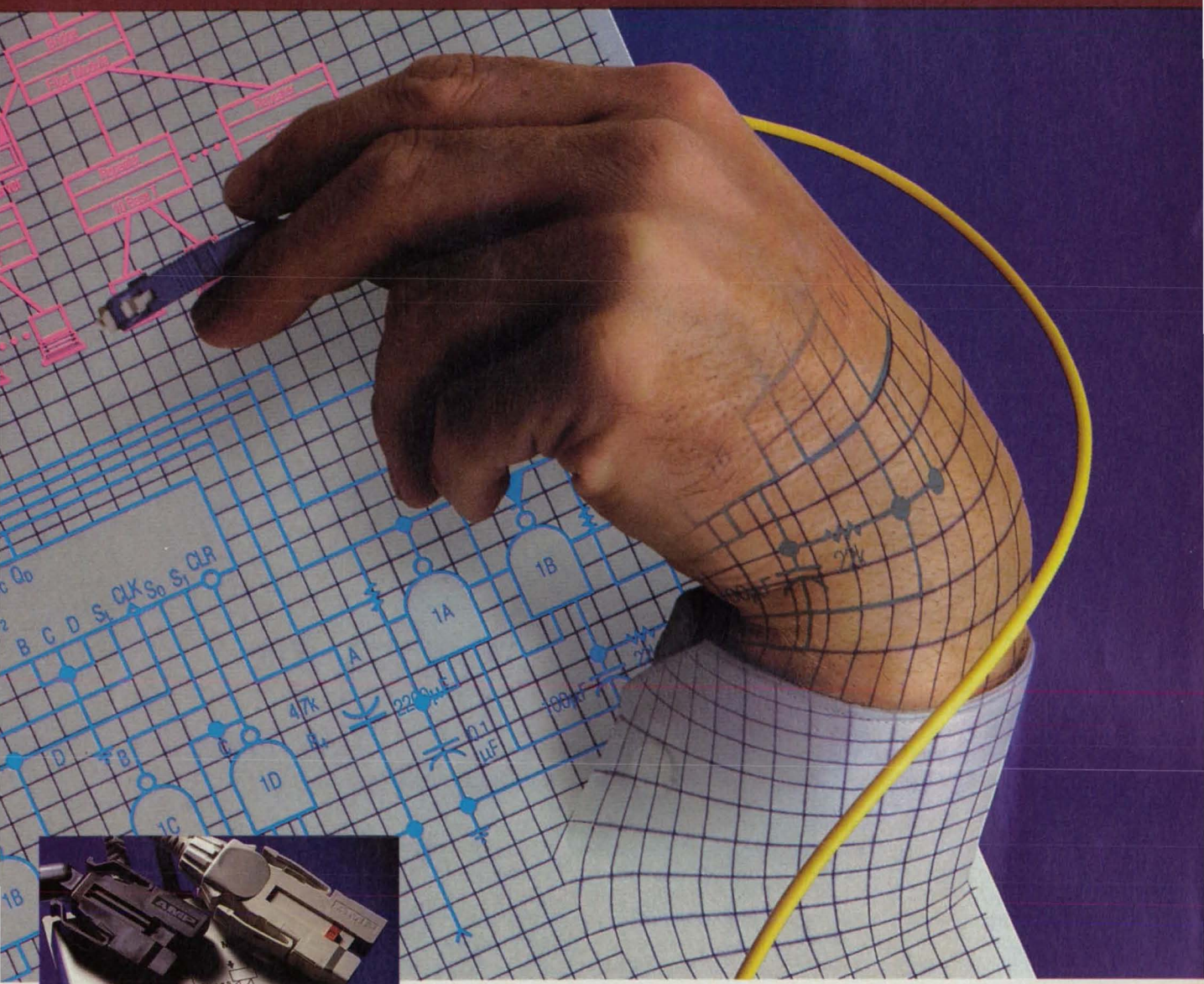

can get to a plug-and-play fiber link.

Our general fiber and network products include multiple connector families, a wide variety of cables, associated tooling, complete cable assemblies, and distribution accessories such as patch panels and splice boxes.

We also offer a wide range of network-specific products, including a complete selection of FDDI products. Our Dual Bypass Switch Module, for instance, provides a fail-safe FDDI network interface.

Whether you're building fiber into boards or networks, you can get all the support you need. Call our Product Information Center at 1-800-522-6752 (fax 717-986-7575). AMP Incorporated, Harrisburg, PA 17105-3608. In Canada, call 416-475-6222.

For More Information Circle No. 657

THIS IS AMP TODAY.

AMP

Protecting Li/TiS_2 Cells Against Overcharge

An electrolyte additive reacts electrochemically at both electrodes.

NASA's Jet Propulsion Laboratory, Pasadena, California

A new electrolyte additive, N,N,N',N'-tetramethyl-1,4-phenylenediamine (TMPD), helps to protect lithium/titanium disulfide rechargeable cells against overcharge. TMPD is a redox couple: during overcharge, it undergoes electrochemical reactions at both electrodes and thereby takes up the excess input charge. Without TMPD, overcharge results in oxidative degradation of the nonaqueous electrolyte, leading to loss of rechargeability and to safety problems. Li/TiS_2 cells are currently being considered for spacecraft and military applications.

The following properties of TMPD make it useful in protecting against overcharge of Li/TiS_2 cells:

- TMPD has a standard reduction potential of about 2.90 V, which is positive to that of the cathode (TiS_2) at the end of charge. Therefore, as a redox additive, it comes into operation at the end of charge.
- TMPD is highly soluble in the organic electrolyte (EC-2MeTHF): a concentration as high as 1 M is readily achieved.
- TMPD appears to be stable in contact with lithium (except as described below), titanium disulfide, and the organic electrolyte.
- Experiments in charge/discharge cycling have demonstrated that TMPD has no tendency to intercalate into the cathode during discharge.
- Rapid kinetics for the electrochemical reaction during overcharge are deduced from the high overcharge rate of 0.5 mA/cm^2 observed with TMPD.
- The cell-voltage profiles observed during charge and discharge reveal that TMPD has minimal effect on the conductivity and viscosity of the electrolyte.

To evaluate the performance of TMPD as an additive for protection against overcharge, laboratory Li/TiS_2 cells that contained EC-2MeTHF/1.5 M $LiAsF_6$ electrolyte, a mixture of ethylene carbonate and 2-methyl tetrahydrofuran containing lithium hexafluoroarsenate at a concentration of 1.5 M, with 0.8 M TMPD as additive were subjected to charge/discharge cycles. The cells were charged at 0.5 mA/cm^2, taken into the overcharge regime (2.7 to 3.2 V), and then discharged at 1.0 mA/cm^2.

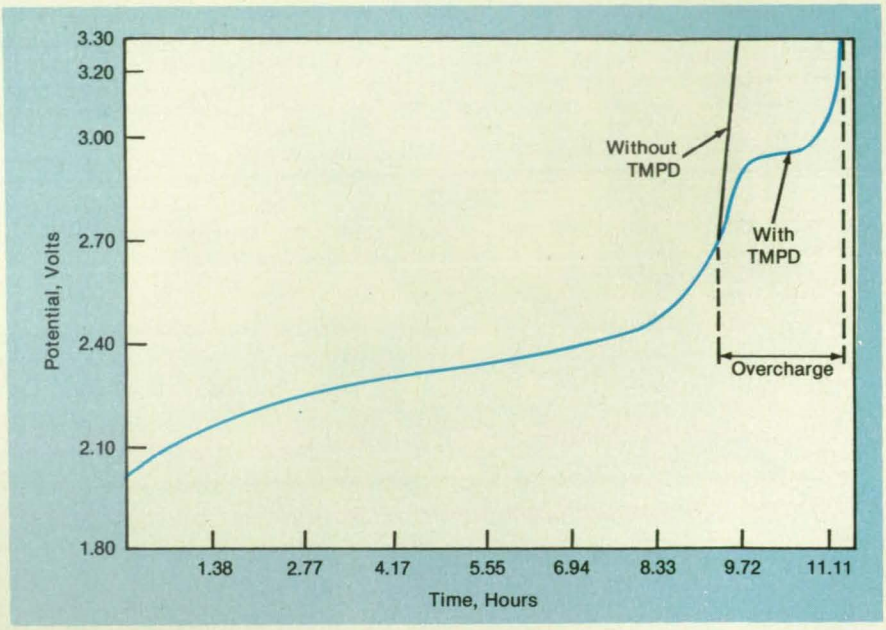

The **Potential During Charge and Overcharge** of an Li/TiS_2 cell with and without TMPD was measured at a cathode-current density of 0.5 mA/cm^2.

The figure shows a typical variation of voltage during charge, with and without the redox additive. The excess input charge accommodated during overcharge when TMPD is present corresponds to about 10 to 15 percent of the theoretical capacity of the cell; in the absence of TMPD additive, no excess input charge is accommodated. The capability of taking up to 15 percent overcharge, at the normal charge rate, offers the possibility of complete protection in many common applications in which the capacities of individual cells in a battery are matched within 2 percent.

The overcharge behavior shown in the figure had been reported to be reproduced over 10 cycles when this article was written, and extended cycling studies were reported to be continuing. The decline in the capacities of the cells in the presence of additive was found not to be significantly different from that of cells without the additive.

Microcalorimetric measurements were made to study the reactivity of the additive toward metallic lithium. The heat output observed in these experiments was marginally higher than that observed with the electrolyte that did not contain the additive, but the order of magnitude of the heat outputs was the same in both cases.

This work was done by S. R. Narayanan, Subbarao Surampudi, and Alan I. Attia of Caltech for **NASA's Jet Propulsion Laboratory**. *For further information, Circle 49 on the TSP Request Card.*

Inquiries concerning rights for the commercial use of this invention should be addressed to the Patent Counsel, NASA Resident Office – JPL [see page 20]. Refer to NPO-18490.

Active Electrical-Transient Damper

Weight, volume, and cost are less than those of an equivalent passive damper.

Marshall Space Flight Center, Alabama

The figure shows an active circuit that damps switching transients and other electrical noise of the sort that is generated by switching power supplies, sudden changes in electrical loads, and the like. Damping circuits are needed to dissipate such noise and thereby prevent it from adversely affecting the various pieces of electrical and electronic equipment connected to a com-

CyberResearch PC Products for Scientists & Engineers

NEW VRK Rack-Mount Computer Systems with Pull-out Keyboard & VGA Color Monitor

Select a Turn-Key System Configuration

The new VRK model is just 10.5" (6 rack spaces) tall. (*including* built-in monitor and keyboard.)

NEW Rugged High-Performance Rack-Mount PC's at Desktop Prices! VRK's Include:

- Your choice of 80386 or '486 microprocessor. From affordable 386sx models to Ultimate-Performance 50MHz EISA-Bus Computers.
- 4MB of RAM (2MB on 386sx model).
- 10" VGA High-Resolution Color Monitor, with VGA Card included at no extra charge.
- Eight Expansion Slots. Features Heavy-Duty metal case for EMI/RFI protection.
- **Industrial Keyboard** pulls out and locks — does not move while typing. A protective door keeps keys safe from foreign materials when not in use.
- 1.2MB (5.25") or 1.44MB (3.5") Floppy Drive.
- 3 Full-access Drive Bays for Floppy Drives, etc.
- Hold-Down keeps Expansion Cards Firmly Seated.
- Floppy Drive & IDE Hard Disk Controller included.
- Dual-Fan Cooling System w/Honeycomb Filter.
- Rack-Mounting Slide Rails Included FREE.

Call or FAX for the latest VRK pricing, quantity discounts, and more detailed information.

For More Information Circle No. 390

19" Ruggedized Rack-Mount Keyboards

If you usually use a standard keyboard with your rack-mount system, you know what a nuisance and a hazard it can be. Our industrial keyboards are designed to fit easily into any EIA 19" rack. Rugged and reliable, these keyboards are made in the U.S.A. Features Include:

- 101-key layout with full-travel keys; unit pulls out & locks into position. Solid, tactile feel is perfect for comfortable touch-typing.
- **#OIX 3010** drawer-mounted/**#OIX 6010** (shown) slides out with locking door in front.
- Occupies only 1 rack space (1.75" high).

#OIX 3010 Low-cost, Drawer-Mounted Rack-Mount Keyboard (not shown).....**$295**
#OIX 6010 Slide-out, Heavy-Duty Rack-Mount Keyboard w/locking slides.....**$395**

For More Information Circle No. 391

Keithley Metrabyte Sets the Standard — AGAIN

The DAS 16 analog converter board has always set the standard for PC-based data acquisition. **Keithley Metrabyte** has now set a new standard for price and performance. A total redesign using ASIC architecture has resulted in complete backwards compatibility, reductions of cost, size, and power consumption, and the addition of many new features, including:

- Programmable gains
- Demand-mode DMA
- Burst-mode timing
- 16 Analog inputs, 2 analog outputs, 32 digital I/O lines, 3 counter/timers
- BASIC drivers and pop-up control panel software included free.

#DAS 1601 100KHz, 16-Channel DAS Board w/Hi-Level Gains (1, 10, 100, 500).....**$895**
#DAS 1602 100KHz, 16-Channel DAS Board w/Lo-Level Gains (1, 2, 4, 8).....**$895**
#ASO 1600 Advanced Software Option – Windows, C, Visual Basic Drivers.....**$99**

For More Information Circle No. 392

DAS Boards w/DMA offer Acquisition to 400KHz

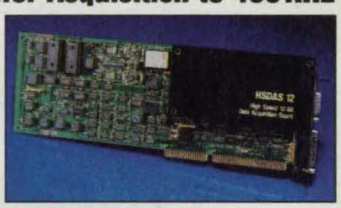

Our selection of high-performance A/D boards from **Analogic** allow continuous data acquisition. Direct Memory Access (DMA) allows these boards to transfer data directly to your PC's memory at high speed. For use in AT or EISA-bus PC's only. The 16-bit DAS boards offer the greatest resolution (1 part in 65536), while the HSDAS 12 resolves to 1 part in 4096. Each board is supplied with utility software, and all three are fully supported by *LABTECH NOTEBOOK, Snapshot, SnapMaster, DriverLINX,* and *IPC Xpert* software packages.

#HSDAS 12 400KHz, 12-Bit Data Acquisition Board with High-Speed DMA **$2295**
#HSDAS 16 200KHz, 16-Bit High Resolution DAS Board w/High-Speed DMA...**$1695**
#LSDAS 16 50KHz, 16-Bit High Resolution DAS Board w/High-Speed DMA.....**$1395**

For More Information Circle No. 393

Complete Data Acquisition System for just $995

Our A/D boards from **Advantech** have made data acquisition more affordable. Despite the PCL 812G's low cost, it hasn't sacrificed performance or advanced capabilities. Our Complete Package with **LABTECH NOTEBOOK/OEM** software provides everything you need to set up your PC as a data acquisition station.

- 16 Single-Ended Analog Input Channels
- Up to 30,000 Samples/Sec with 12-bit Resolution
- 2 D/A Channels, 16 Digital Input Lines & 16 Outputs
- **GLT** includes: Terminal Panel; Cables; and BASIC, C, & Pascal Drivers

#PCL 812G 30KHz, 16-Chan. Low-Cost A/D Board w/Programmable Gains.....**$395**
#PCL 812GLT Package of PCL 812G, NOTEBOOK/OEM SW & Terminal Panel.....**$995**

For More Information Circle No. 394

Data Acquisition via your PC's Parallel Port

The PPIO Plugs into the Parallel Port of your PC. It's a new **low-cost** approach to data acquisition and control. Each board is packaged with cables and includes a complete BASIC CALL routine. Analog inputs may be expanded from 8 to 16, 32, up to 128 using optional muliplexer panels. Call for details.

- No need to open up your computer. No Address or Interrupt Conflicts.
- Perfect for Portables or Laptops. Does not require an expansion slot.
- Ideal for Student Lab/Training Stations. Only requires +5V power.

#PPIO AI08 8 Analog Inputs, 4 Digital Outputs/3 Inputs for Parallel Port **$199**
#PPIO D24H 24-Channel Digital I/O w/High Current Sink for Parallel Port.....**$99**
#CBL MOLPS 5V Power Adapter Cable to your PC's Mouse Connector **$25**
#MPS 05-01P Optional 5-Volt, 1A Power Supply (Plugs into 120V wall outlet).....**$49**

For More Information Circle No. 395

FREE

PC Systems Handbook for Scientists & Engineers

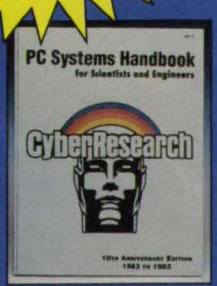

New 1993 Edition

10th Anniversary Edition – 188 Pages
Combination Tutorial/Catalog Includes Many Examples of PC-based Systems

The CyberResearch *PC Systems Handbook for Scientists & Engineers* describes over 1400 unique and hard to find items for PC-based engineering. Packed with useful technical information and easy-to-read diagrams, this invaluable reference should be part of every engineer's library.

Fax, Call, or Write for a complimentary copy.

For A FREE Copy Circle No. 395

The CyberResearch Advantage:

- ☑ FREE Application Engineering
- ☑ Everyday Low Prices
- ☑ Broadest Product Selection
- ☑ 100% Satisfaction Guarantee

CyberResearch

Mailing Address:
P. O. Box 9565
New Haven, CT 06535

Worldwide
(203) 483-8815
Fax: (203) 483-9024

MasterCard VISA American Express Card

(800) 486-8800

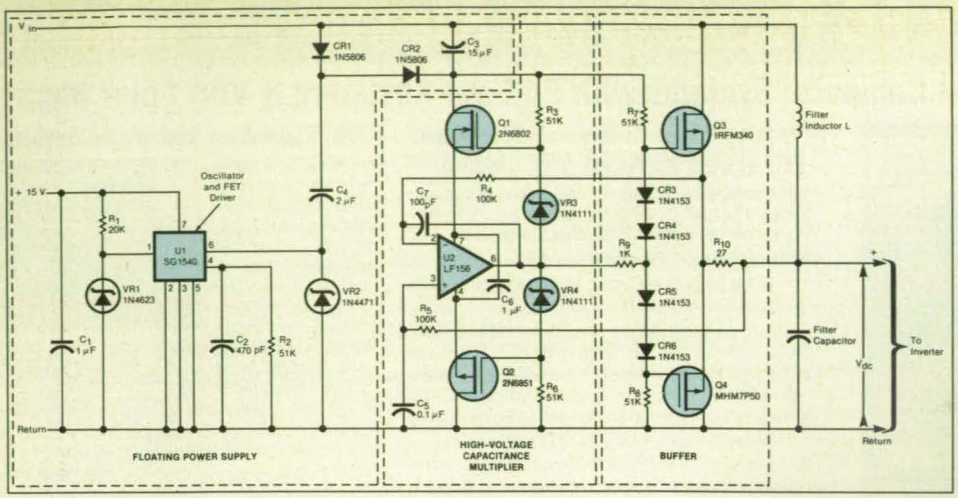

The **Active Damping Circuit** suppresses transients in V_{dc}. It acts like a passive damper that has a capacitance of C_5R_5/R_{10} and a series resistance of R_{10}.

mon power supply (e.g., the equipment aboard an aircraft).

The damping circuits used heretofore have been passive, usually consisting of resistors in series with capacitors. Typically, the size of the capacitor in a passive damper is 4 to 5 times that of the filter capacitor in the associated power supply. This means that the size and cost of the passive damper increase with the rated power of the supply. The active damping circuit functions similarly to a passive damping circuit, but its volume, weight, and cost do not increase nearly as steeply with the rated power as do those of an equivalent passive damper. Thus, the active damper affords advantages of economy that increase with the rated power.

The major functional blocks of the active damping circuit are a high-voltage capacitance multiplier, a buffer, and a floating power supply that generates the bias voltages for the capacitance multiplier and the buffer. Operational amplifier U_2 forces the potential at the source terminals of Q_3 and Q_4 to be the same as that at the junction of R_5 and C_5. As a result, any abrupt transitions of V_{dc} are constrained by the time constant R_5C_5. In effect, the circuit functions as a passive damper that has a capacitance of C_5R_5/R_{10} and a series resistance of R_{10}. During any transient that excites the resonance of the filter inductor and capacitor, Q_3 and Q_4 dissipate the energy stored in the filter inductor, thereby inhibiting ringing in the filter.

Integrated circuit U_1 in the floating power supply contains an oscillator and a field-effect-transistor (FET) driver, which transfers energy through capacitor C_4 into capacitor C_3. The frequency of oscillation is made high (200 kHz) so that C_4 can be made small.

This work was done by Carlisle R. Dolland of Allied-Signal Aerospace Co. for **Marshall Space Flight Center**. *For further information, Circle 10 on the TSP Request Card.*

Inquiries concerning rights for the commercial use of this invention should be addressed to the Patent Counsel, Marshall Space Flight Center [see page 20]. Refer to MFS-26195.

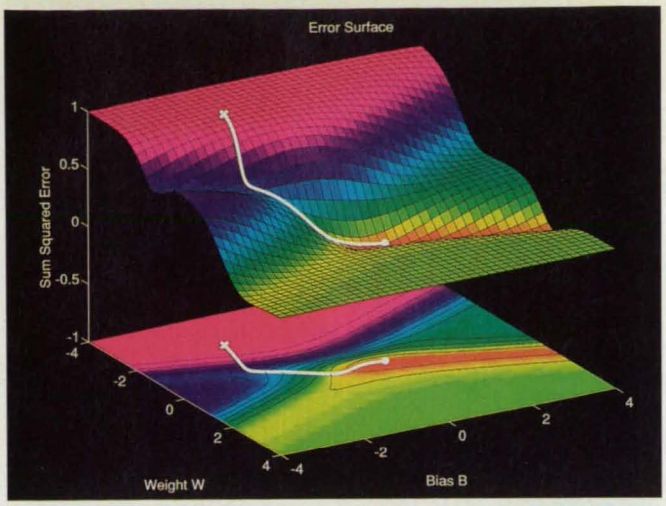

Graphics enhance understanding of neural network behavior. This surface and contour plot shows the descent of a backpropagation network from initial conditions to the minimum error.

Take command with neural networks, whether or not you've completed basic training.

Both newcomers and experts will find the MATLAB® Neural Network Toolbox to be ideal for the design, training, and simulation of neural networks in fields as diverse as signal processing, pattern recognition, nonlinear control, and financial forecasting.

Extensive Functionality

Within the Neural Network Toolbox, you can choose from a comprehensive set of proven paradigms, including backpropagation, associative, Hopfield, and self-organizing networks.

You can design recurrent or feedforward networks, using supervised or unsupervised training.

Finally, with no limits on network size or architecture, you can implement networks as complex as your application demands.

The first Neural Network Engineering Environment

Departing from the traditional "canned" approach of other neural network packages, the MATLAB Neural Network Toolbox is actually a comprehensive engineering environment for neural network research, design, and simulation.

Flexible data import and transformation capabilities simplify preprocessing of network training data. Powerful analysis and visualization functions help you understand network behavior and evaluate performance.

Also, you can use other MATLAB application toolboxes and nonlinear simulation to compare neural networks with other methods to create optimum solutions.

The only truly open system

The Neural Network Toolbox is truly open and extensible. You can easily customize the built-in functions or even add new paradigms—all in the high-level MATLAB environment, without having to write a single line of C or Fortran.

Not just for experts

You don't have to be an expert to put the MATLAB Neural Network Toolbox to immediate use. The comprehensive User's Guide makes learning a breeze, with examples of how to solve real world problems.

Your choice of platforms

The MATLAB Neural Network Toolbox runs on PC, Macintosh, UNIX workstations, VAX/VMS, and supercomputers, and your neural network applications can be easily moved between them.

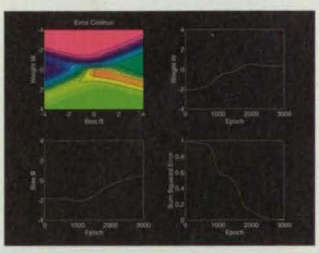

Evaluate performance at a glance with the help of built-in diagnostic routines and graphs—or create your own

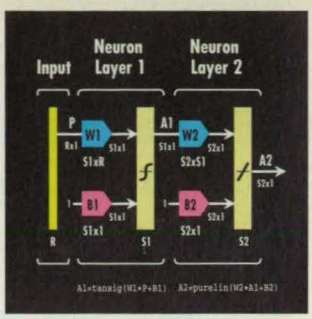

Concise notation makes it easy for all to understand complex network architecture.

So, whether you are an expert or just getting started, discover the true power MATLAB brings to neural networks. Call us now for more information,

508/653-1415.

MATLAB Neural Network Toolbox

- *Extensive proven paradigms for supervised and unsupervised networks, including:*
  - *Perceptron*
  - *Widrow-Hoff*
  - *ADALINE/MADALINE*
  - *Backpropagation (with momentum, adaptive learning)*
  - *Associative networks*
  - *Hopfield networks*
  - *Self-organizing networks including feature map*
- *Competitive, limit, linear, and sigmoid transfer functions*
- *Feedforward & recurrent architecture*
- *Performance analysis functions & graphs*
- *Unlimited layers, elements, & interconnections*
- *Acclaimed "textbook quality" user guide*

The MATH WORKS Inc.

24 Prime Park Way/Natick, MA 01760
Tel: 508/653-1415 Fax:508/653-2997
Email info@mathworks.com

France: Scientific Software, +33-1-45-34-23-91
Germany: Bausch-Gall GmbH, +49-89-995-9010
Israel: Omikron Delta, +972-3-561-5151
Japan: Cybernet Systems, +81-3-3982-4641
Scandinavia: CSEAB, +46-8-15-30-22
Switzerland: COMSOL AG, +41-31-961-70-11
U.K.: Cambridge Control, +44-223-421-920
U.K.: Rapid Data Ltd., +44-903-202-819

Multiple Pages Intentionally Left Blank

Microrover Operates With Minimal Computation

A small robotic vehicle responds to a variety of situations.

NASA's Jet Propulsion Laboratory, Pasadena, California

Small, light, highly mobile robotic vehicles called "microrovers" use sensors and artificial intelligence to perform complicated tasks autonomously. A vehicle of this type navigates, avoids obstacles, and picks up objects by use of a reactive (as distinguished from deliberative) control scheme in which it selects from among a few preprogrammed behaviors to respond to the environment (e.g., go around obstacles) while executing the assigned task (e.g., carry an object to a designated position).

Microrovers are programmed by use of a behavior-description language that requires less computation than do other approaches to artificial intelligence. Relatively simple microcontroller and memory integrated circuits are adequate to implement the control. A microrover can therefore be small and light: a 15-kilogram microrover can have the capabilities of an older 1,500-kilogram robotic vehicle.

Now under development for exploration and mining of other planets, microrovers may also be useful in firefighting, cleaning up chemical spills, and delivering materials in factories. The reactive control scheme and the principle of the behavior-description language may be useful in reducing computational loads in prosthetic limbs and automotive collision-avoidance systems.

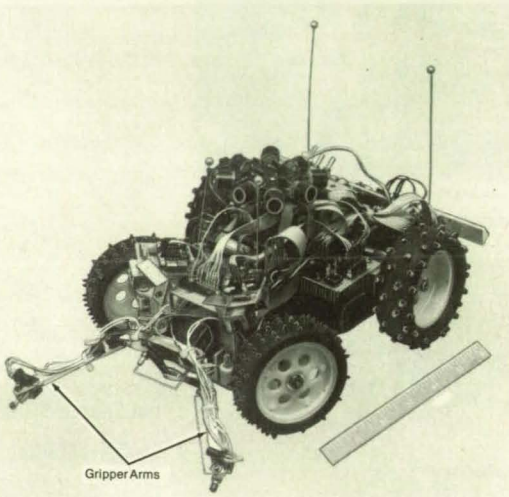

This **Demonstration Microrover** includes two gripper arms, which close on an object between them when a break-beam infrared sensor on the arms detects the object. The vehicle can execute such simple tasks as carrying the object to a designated position marked by a beacon.

The relatively small amount of computation required is illustrated by the example of a demonstration microrover, which contains only 4K bytes of memory and two 8-bit control microprocessors. This microrover (see figure) is 30 centimeters long and 20 centimeters wide. It employs front-wheel steering and rear-wheel drive. A forceps-like gripper at its front picks up small objects. It includes ten 1-bit sensors: five bump sensors, two grasp sensors, two proximity sensors, and one infrared break-beam sensor that detects an object in the gripper. There are also 10 analog sensors: 8 cadmium sulfide photocells and a tachometer on each rear-wheel drive motor. The microrover explores a test course in a laboratory, avoiding walls and such obstacles as trash cans and desks. When the vehicle encounters any of several small cylindrical test objects in its path, it picks it up and deposits it at a central point beneath a 150-watt light bulb, which serves as a beacon.

One of the control microprocessors is connected to the drive and steering motors, bump sensors, and infrared proximity sensors. It implements behaviors for coordinating the drive and steering motors and for dealing with such contingencies as veering or backing away from obstacles, recovering from a stalled motor, escaping endless loops, and getting out of dead ends.

The other control microprocessor is con-

Analysis Simplified!

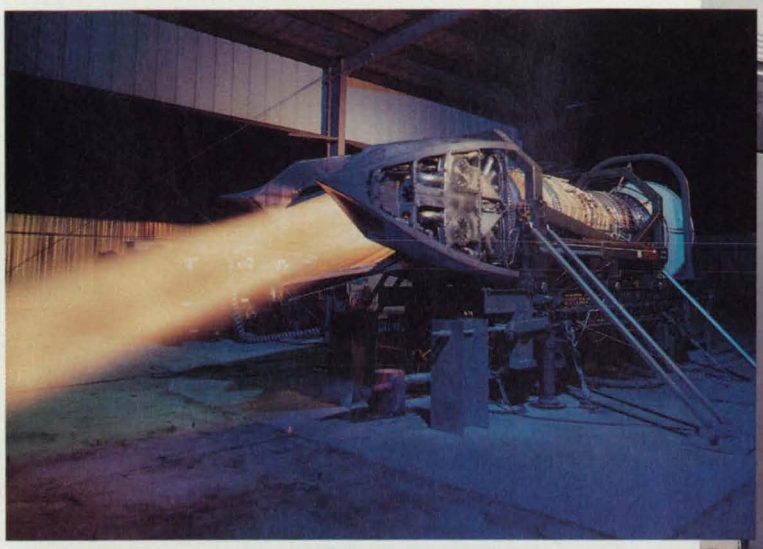

Testing and measurement shouldn't be complicated. That's why Scientific-Atlanta's SD390 Dynamic Signal Analyzer is designed to make every measurement simple to perform.

The SD390's dc to 100 KHz frequency range and up to eight input channels make data acquisition easy and the intuitive Microsoft® Windows™ interface makes every step, from setups to analysis, a "point and click" operation.

Not only does the SD390 simplify data analysis, it's embedded personal computer lets you process that data with the most powerful and specialized software available such as SMS StarModal®, MathCAD® and Microsoft Excel®.

The SD390 also lets you go where the action is. It's rugged, portable and designed for field use. On site, the SD390 packs all the power you need to handle real-world analysis problems whether you're analyzing machinery, designing electronics or controls, measuring sound and vibration or testing structures.

No other dynamic signal analyzer is as easy to use and offers these features:

- All new digital Signature Ratio® order tracking
- True digital octave analysis that meets ANSI S1.11-1986 standards
- Input memory for up to 1.8 million data samples
- Full 32-bit signal processing performance
- Advanced digital and analog filtering with 16-bit analog to digital converter
- Dedicated sampling, triggering and tachometer inputs
- Modular, expandable architecture

The SD390 Dynamic Signal Analyzer: Keeping it simple.

Find out how the SD390 can do more for you now and keep up with your needs in the future. Call us for a competitive price at (800) 426-8887 or (619) 679-6465.

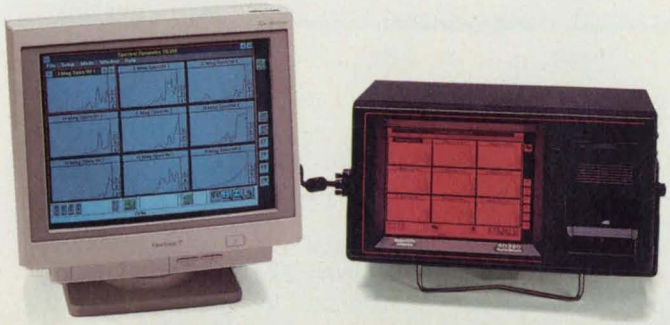

Scientific Atlanta

Our customers are the winners.

For More Information Circle No. 548

nected to the photocells and the gripper control. It implements behaviors for picking up a test object, dropping it near the beacon, and guiding the vehicle toward and away from the beacon. The two control microprocessors communicate over a serial link.

A promising possibility is having microrovers cooperate in autonomous teams. One vehicle would be designated the leader, and others would fall into formation after it. Such teams would work together in moving materials, for example.

This work was done by David P. Miller, John L. Loch, Erann Gat, Rajiv S. Desai, Colin Angle, and Donald B. Bickler of Caltech for **NASA's Jet Propulsion Laboratory**. *For further information, Circle 37 on the TSP Request Card.*
NPO-18543

Ultrasonic Imaging of Bond Layers Through Bond Layers

Pictures of obscured layers would be clearer.

Goddard Space Flight Center, Greenbelt, Maryland

A proposed combination of hardware and software would help an ultrasonic C-scan inspection system create images of a bond layer in a laminated composite material, even when it is obscured by another bond layer. Ordinarily, imaging a bond layer is a straightforward process. An ultrasonic transducer is scanned across the face of the specimen, and a plot is made of the amplitude of the ultrasonic reflection versus position. Because the transmitted signal is the same at all locations, the strength of the reflection is a measure of the integrity of the bond layer. An $x-y$ plot or intensity image of the amplitude of the reflection thus reveals debonded areas.

When a bond layer lies under another bond layer, the situation is more complicated. The transmitted signal that reaches the lower layer has been modified by the upper layer. Thus, a flaw in the upper layer can give rise to a strong signal that masks or distorts the signal from a less-severe flaw in the lower layer. Therefore, the image of the lower layer can easily be misinterpreted. Often, the quality of the lower layer cannot be determined.

The proposed system would produce an image of both layers in a single scan; it would not require a lengthy double scan as older postprocessing schemes do. The proposed system would include the usual components: an ultrasonic transducer, a pulser/receiver, a mechanical scanner, and a personal computer as controller (see figure). The system would also include electronic circuitry that would gate the first and second peak signals (representing the reflections from the upper and lower bond layer, respectively) independently, detect the peaks, and feed the resulting amplitude data to the computer. The computer would normalize the second peak with respect to the first, thereby compensating the second peak for the influence of the first reflection.

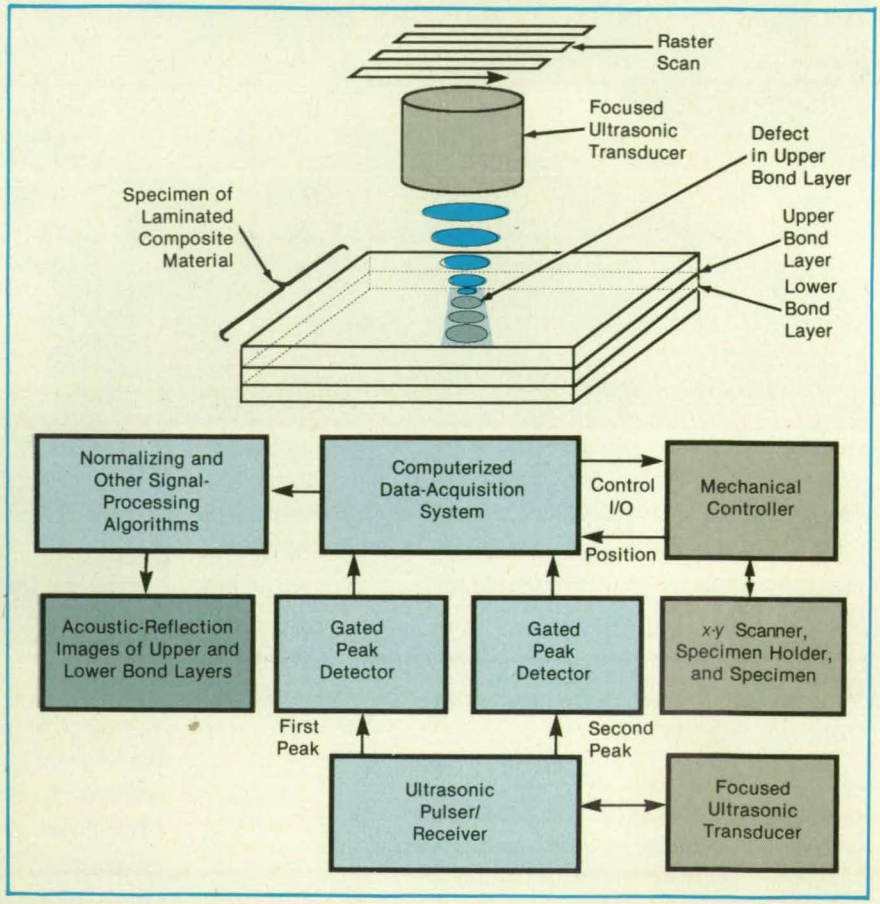

While the Ultrasonic Transducer Scans, the reflections from bond layers in the specimen would be gated separately, and their peaks would be detected. Data from the first reflection peak would be used in a normalizing subalgorithm of the signal-processing algorithm to compensate data on reflections from the lower bond layer for effects of reflections from the upper bond layer.

This work was done by E. James Chern of **Goddard Space Flight Center**. *For further information, Circle 87 on the TSP Request Card.* *GSC-13511*

Constant-Frequency Pulsed Phase-Locked-Loop Measuring Device

This device measures changes in phase velocities in both solids and liquids.

Langley Research Center, Hampton, Virginia

There is a need to characterize states of metals and other materials by measuring changes in ultrasonic phase velocities as functions of thermodynamic variables. One of the problems associated with previous techniques for measuring phase velocity, such as the pulse-echo overlap method, is that automation would be difficult. Blume-related* and previous pulsed phase-locked-loop methods include phase-comparison techniques, but involve changes in phase effected via changes in

frequency to obtain quadrature between the acoustic signals and the driving electronic signals. In these cases, the changes in frequency prevent measurement of changes in true phase velocity, and make the measurements sensitive to the frequency dependences of the characteristics of transducers, bonds, and electronics.

On the other hand, the constant-frequency pulsed phase-locked-loop measuring device is sensitive to small changes in phase velocity and can be easily automated. This device is based on the use of a fixed-frequency oscillator in measuring small changes in ultrasonic phase velocity when a sample is exposed to such changes in the environment as changes in pressure and temperature. It automatically balances electrical phase shifts against acoustical phase shifts to obtain accurate measurements of the acoustical phase shifts.

As shown in the figure, the output of the fixed-frequency oscillator is sent to a logic and timing circuit, a gate, and a phase-shifting circuit. An electrical tone burst supplied to a transducer is converted into an acoustical tone burst, which echoes through the sample, thereby producing an electrical echo signal that is fed through a gate and preamplifier to one of the two input terminals of a mixer. The output of the phase-shifting circuit is fed to the other input terminal of the mixer. The mixer compares the phases of its two input signals and produces an error signal in the form of a voltage, to which an adjustment voltage is added. The resulting voltage is supplied as a control voltage to the phase-shift circuit. The error signal is present until a quadrature condition is reached.

With the constant-frequency pulsed phase-locked-loop measuring device, there are no frequency changes to cause phase shifts that would result in erroneous readings. Since the drive frequency remains fixed, all possible phase shifts, except those caused by changes in acoustic parameters, remain fixed. This means that the measuring system can monitor true phase changes in the acoustical system. Moreover, corrections for the presence of bonds and phase-adjusting mechanisms make it possible to use this device to determine true phase velocity and its changes as functions of changes in the thermodynamic parameters with an enhanced sensitivity not previously attained. Laboratory measurements of the speed of sound in ultrapure water made by use of this device showed agreement with accepted values within 0.18 percent.

*R. J. Blume, *review of Scientific Instruments*, volume 34, page 1,400, 1963.

This work was done by William T. Yost and John H. Cantrell of **Langley Research Center** *and Peter W. Kushnick of PRC Kentron. For further information, Circle 83 on the TSP Request Card.*

This invention is owned by NASA, and a patent application has been filed. Inquiries concerning nonexclusive or exclusive license for its commercial development should be addressed to the Patent Counsel, Langley Research Center [see page 20]. Refer to LAR-13823.

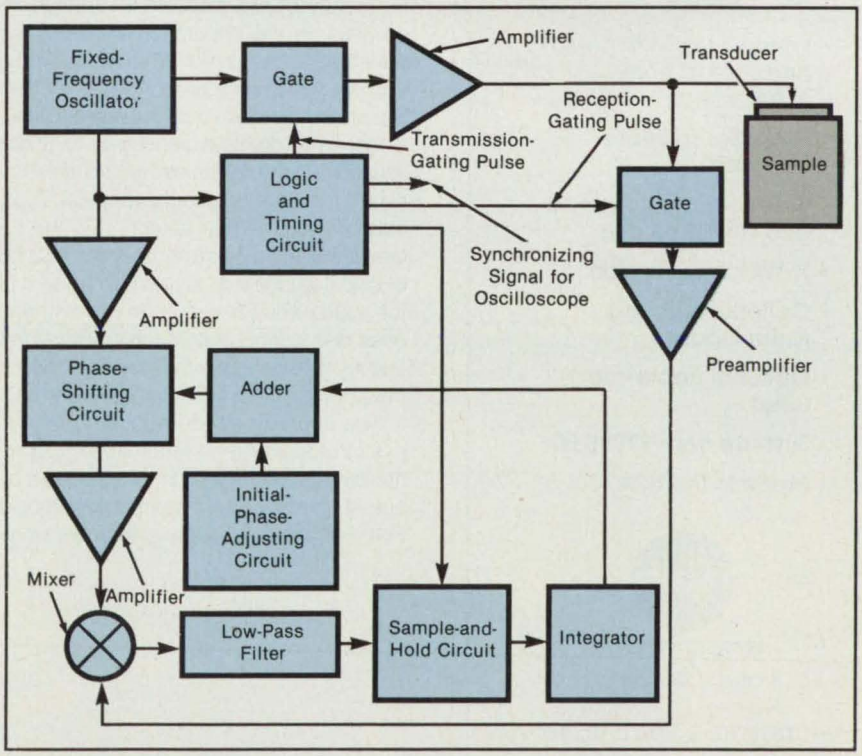

The **Constant-Frequency Pulsed Phase-Locked-Loop Measuring Device** monitors changes in acoustic parameters.

Books and Reports

These reports, studies, handbooks are available from NASA as Technical Support Packages (TSP's) when a Request Card number is cited; otherwise they are available from the National Technical Information Service.

Errors in Synthetic-Aperture Interferometric Radiometry

Streaks in the reconstructed scene can be partly removed by image-enhancement techniques.

A report presents an analysis of errors in the image of a scene reconstructed from the output of a synthetic-aperture interferometric radiometer (SAIR). Receiving at a typical frequency of 1.4 GHz, a SAIR is an airborne or spaceborne instrument that includes several antennas aimed at the nadir and arrayed along a line perpendicular to the trajectory, such that the antennas scan a swath along the ground track in "pushbroom" fashion.

SAIR imaging is based on the Fourier-transform relationship between the interferometric outputs and the distribution of microwave brightness in the scene, which relationship manifests itself partly in the spatial-filtering characteristics of interferometer pairs of antennas. The effective antenna pattern formed by two separated antennas, the outputs of which are cross-correlated, contains a sinusoidally varying series of interference maximums and minimums, enveloped by the individual patterns of the two antennas. The spatial frequency of the sinusoidal variation increases as the separation between the antennas is increased. When used with a microwave radiometer receiver, this effective antenna pattern acts as a spatial filter; it results in greatest sensitivity to those variations in the brightness distribution that exhibit the same sinusoidal variation. Thus, coherent quadrature detection in the receiver essentially extracts the sine and cosine components of that component of the spatial Fourier transform of the brightness distribution that lies at a spatial frequency determined by the spacing between the antennas in each interferometer pair.

The approximate distribution of brightness in the scene is reconstructed from the outputs of the interferometer pairs by use of an algorithm that incorporates the Fourier-transform relationship and calibration measurements of the interferometric patterns of antenna pairs at an antenna-testing range. The algorithm solves for that distribution of brightness that minimizes the squared error between the actual interferometric outputs and the interferometric outputs predicted by use of the assumed distribution of brightness and the calibrated interferometric patterns.

The analysis in this report shows that the image thus reconstructed is affected by systematic offsets and stochastic noise in the receiver outputs, errors in the calibration of interference patterns, multipath scattering from the antenna-support structure, mutual coupling between nearby antennas, and small differences among the individual patterns of the antennas. These errors are shown to produce crosstrack brightness ripple; that is, streaks parallel to the trajectory axis in the image. It is shown that the ripple can be reduced greatly by incorporating, into the image-reconstructing algorithm, a transformation of the subspace of brightness distributions spanned by the interference patterns. This transformation consists of an element-pattern-based renormalization of the interference patterns. The correction attainable via this approach is limited by the small differences among the radiation patterns of the various antennas.

Multipath scattering of the incoming signal is shown to produce interference patterns with strong primary harmonic components and significant secondary distributions of effective interferometer-pair spacings. This coupling of spatial harmonics between the receiver outputs introduces a very strong correlation between the noise components in the image at widely separated pixels. This correlation also appears as streaks parallel to the trajectory. In principle, this correlation can be detected by covariance analysis of the image, and then the image can be corrected accordingly. However, the cross-coupling between spatial harmonics can also be reduced by improvements in design; e.g., reduction in the profile of the antenna-support structure and the use of corrugated skirts to decouple adjacent antennas from each other.

This work was done by Christopher S. Ruf of Caltech for **NASA's Jet Propulsion Laboratory**. *To obtain a copy of the report, "Synthetic Aperture Interferometric Radiometer Image Reconstruction Error Analysis," Circle 8 on the TSP Request Card. NPO-18561*

Thinner, More-Efficient Oxygen-Separation Cells

Better gas-distribution plates can be fabricated more easily.

NASA's Jet Propulsion Laboratory, Pasadena, California

An oxygen-separation cell has been redesigned to make it more efficient, smaller, lighter, and easier to manufacture. Potential applications include use as gas separators, filters, and fuel cells.

The cell includes a layer of zirconia solid electrolyte between two electrodes of strontium-doped lanthanum manganate (LSM), a porous, electrically conductive ceramic. When current is supplied to the cell through its electrodes, the zirconia acts as a membrane that selectively passes oxygen. Thus, when a stream of air flows over one side, pure oxygen is collected on the other side. Cells are stacked to provide the requisite capacity.

In the old design (see Figure 1), the three gas streams — air, oxygen, and depleted air — are carried through manifolds in the outer rim of a stack of cells. This configuration requires three internal channels in each of the distribution plates (also of LSM and made nonporous by firing to full density). The distribution plates separate the cells and provide parallel gas and series electrical connections. As a result, the distribution plates of the old configuration are thick.

The fabrication of the old, thick plates was problematic. They were made by slip casting LSM in plaster molds with wax inserts to create the internal channels. Because of their thickness, the plates tended to warp during firing and to crack, both before and during firing. The resulting scrap rate was unacceptably high. Moreover, the fabrication process was labor-intensive.

In the new version (see Figure 2), the internal channels are eliminated by routing the inlet air through a manifold at the outer rim. The depleted air leaves through a hollow central shaft in the stack of cells. The oxygen flows through a manifold on the opposite side of the sandwich and leaves through vertical channels at the outer rim.

The thickness of the distribution plates in the new design is less than 10 percent of that of the prior design. The new distribution plate can be fabricated by tape casting, which is more suitable for mass production than slip casting is. Moreover, an intricate pattern of ribs can be embossed in a distribution plate to guide the flow of gas and distribute electrical current more uniformly, thereby increasing efficiency.

The new distribution plates are made from ceramic powder suspended in a plastic binder solution. A tape-casting machine is used to cast long, thin tapes from the suspension, each about 4 inches (10 centimeters) wide. After the solvent has evaporated, disks destined to become distribution plates are cut from the tapes. The disks are embossed with the rib pattern by pressing them between die plates in a hydraulic press. The disks are then fired. Because less ceramic material is used in the new plates, they weigh less and are better able to take advantage of the self-heating effect of the oxygen-separation

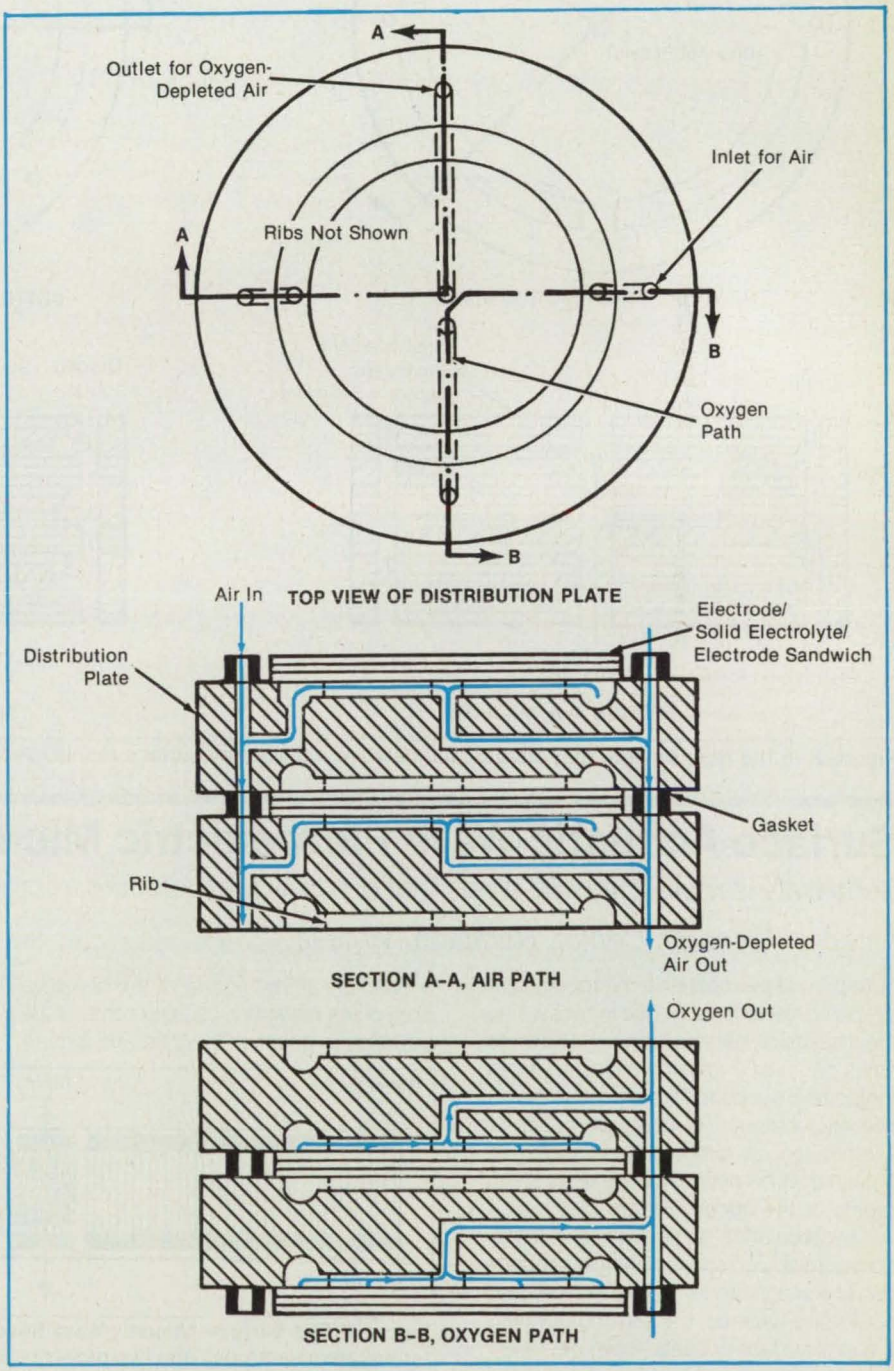

Figure 1. The **Old Design** features thick distribution plates with internal channels.

process. This increases energy efficiency.

This work was done by Douglas J. Clark, Leo M. Galica, and Robert W. Losey of Caltech for **NASA's Jet Propulsion Laboratory**. *For further information, Circle 100 on the TSP Request Card.*

In accordance with Public Law 96-517, the contractor has elected to retain title to this invention. Inquiries concerning rights for its commercial use should be addressed to

Edward Ansell
Director of Patents and Licensing
Mail Stop 305-6
California Institute of Technology
1201 East California Boulevard
Pasadena, CA 91125

Refer to NPO-18093, volume and number of this NASA Tech Briefs *issue, and the page number.*

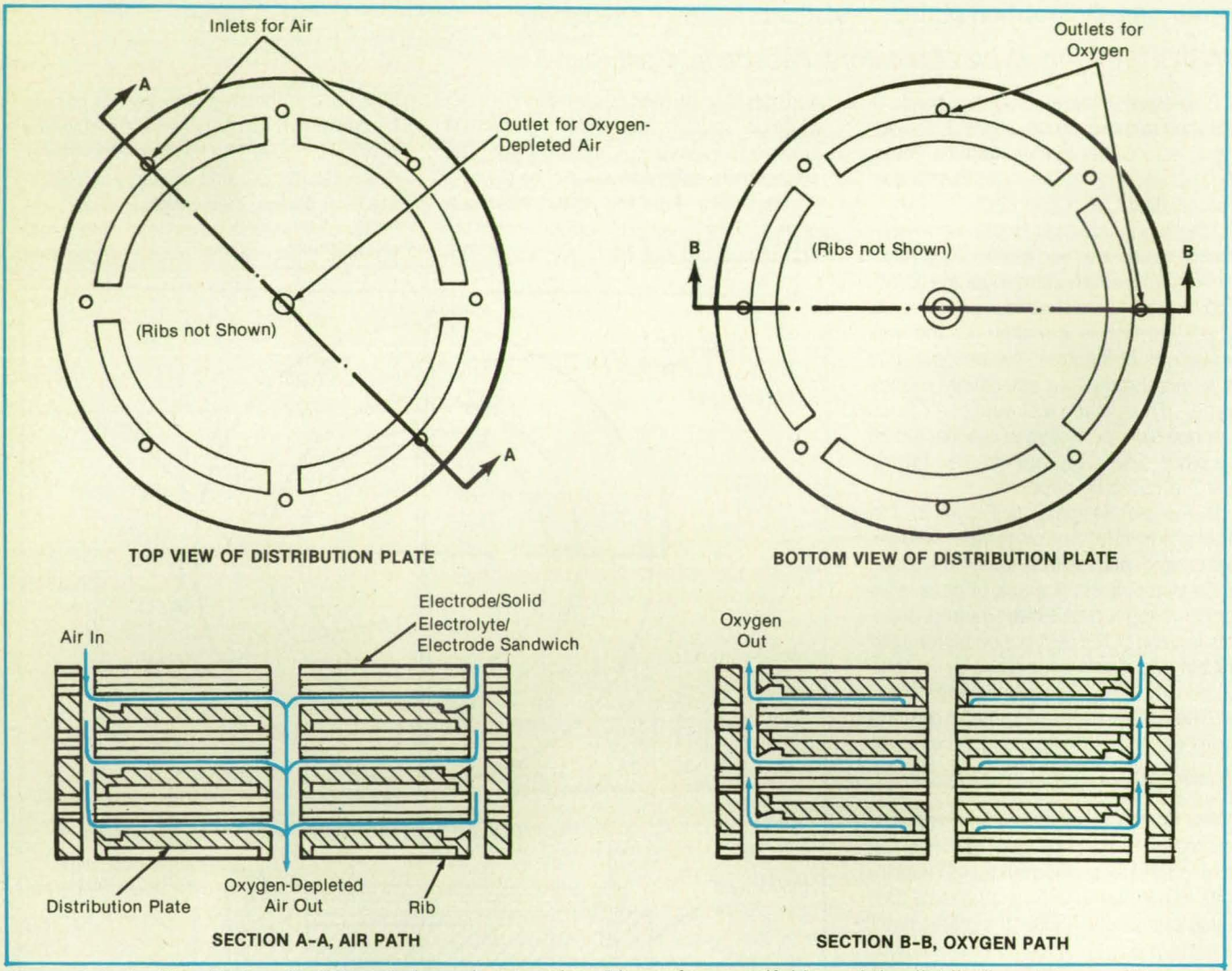

Figure 2. In the **New Design**, the internal channels are replaced by surface manifolds, and the distribution plates are thinner.

Surface-Acoustic-Wave Piezoelectric Microbalance

Sensitivity is more than 400 times that of a bulk piezoelectric microbalance.

Langley Research Center, Hampton, Virginia

Improved piezoelectric microbalances are being developed for use in measuring the masses of volcanic, aerosol, and other small particles (including associated gas molecules) suspended in the air. A sensitive microbalance of this type could be used to analyze airborne particles in real time in environments as diverse as clean rooms or the upper atmosphere.

"Microbalance" is something of a misnomer inasmuch as the principle of operation of a weighing device of this type does not involve balance: the sensing device is a quartz surface-acoustic-wave piezoelectric resonator (see Figure 1). A jet of the sampled atmosphere is directed through a carefully aimed nozzle at the sensitive area of the resonator, causing some of the particles in question to strike and adhere to its surface. The mass of the adhering particles causes a reduction in the frequency of resonance.

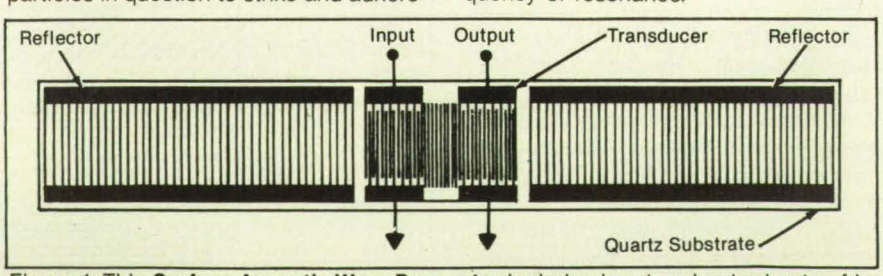

Figure 1. This **Surface-Acoustic-Wave Resonator** includes input and output sets of interdigitated electrodes and two passive conductive patterns that act as reflectors. The mechanical energy travels both ways out from the middle and is reflected back toward the middle.

The complete microbalance contains two surface-acoustic-wave resonators: the sensing device, which is exposed to the sample jet; and a reference device, which is identical except that it is not exposed to the sample jet. The mass of particles adhering to the sensing device is deduced from the difference between the resonant frequencies of the two devices, which is measured directly as the beat frequency (see Figure 2).

The prototype microbalance operates at a nominal resonant frequency of 200 MHz. It is expected to provide about 400 times the mass sensitivity per unit area of a prior quartz bulk piezoelectric microbalance that operated at 10 MHz (the mass sensitivity is proportional to the square of the resonant frequency).

This work was done by Raymond L. Chuan and William D. Bowers of Femtometrics for **Langley Research Center**. *No further documentation is available.*

In accordance with Public Law 96-517, the contractor has elected to retain title to this invention. Inquiries concerning rights for its commercial use should be addressed to

Dr. W. D. Bowers
Femtometrics
1001 W. 17th Street, Ste. R
Costa Mesa, CA 92627

Refer to LAR-14476, volume and number of this NASA Tech Briefs *issue, and the page number.*

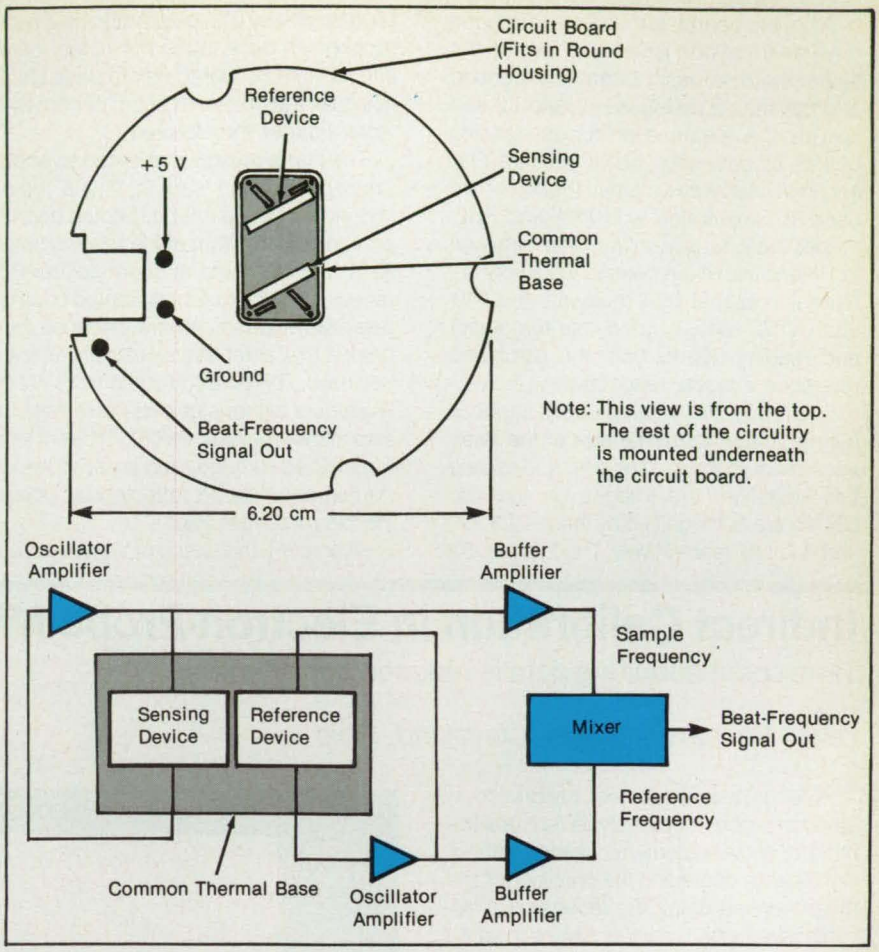

Figure 2. The **Microbalance** and associated circuitry fit in a small package. The circuit draws only 80 mA at 5 V.

Real-Time Optical Correlator Based on GaAs

Frame rates as high as 1,000 s^{-1} should be achievable.

NASA's Jet Propulsion Laboratory, Pasadena, California

An experimental apparatus performs the correlation between an input image and a reference image in real time by means of degenerate four-wave mixing in a photorefractive crystal, which serves as a real-time holographic medium. Gallium arsenide was chosen to be the photorefractive material in this application because at the frame rate and level of illumination used in the experiments, it offers adequate diffraction efficiency. (Typically, in the selection of a photorefractive material, it is necessary to trade diffraction efficiency against speed of response; to increase both in a given material, it is necessary to increase the illumination.)

The apparatus implements the Vander Lugt correlation method, which involves the following principle of operation: The hologram is written by interference between (1) a non-spatially-modulated laser beam (called the "reference beam") and (2) another laser beam (called the "object beam") that bears the Fourier transform of the input image. The hologram is read by another laser beam that bears the

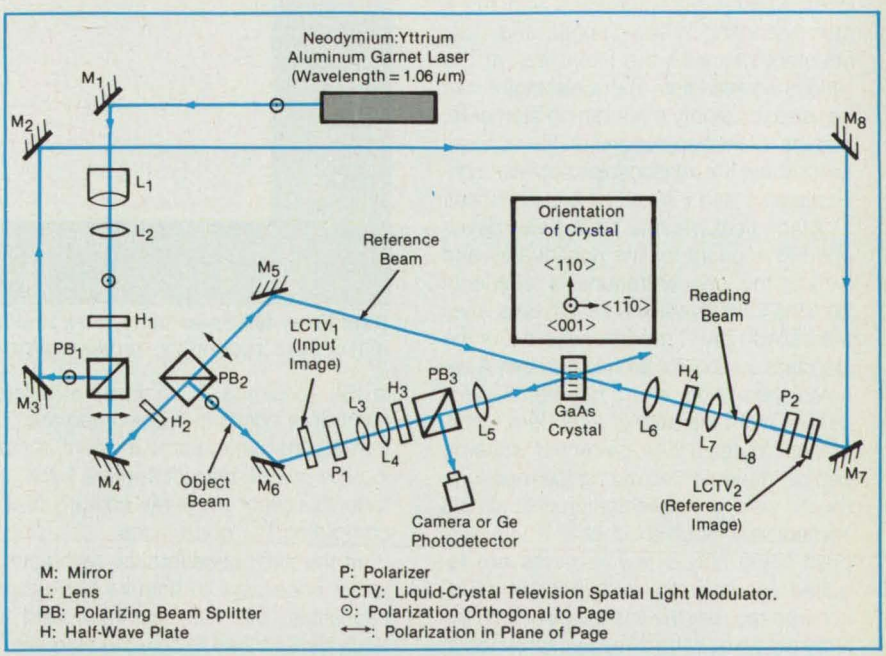

The **Experimental Optical Correlator** implements the Vander Lugt method of correlation. The GaAs crystal, which is photorefractive, serves as a real-time holographic medium.

Fourier transform of the reference image.

All of the beams are obtained from the main beam of one laser. As shown in the figure, the main laser beam is expanded and collimated by lenses L1 and L2 and split into the reference, object, and reading beams by polarizing beam splitters PB1 and PB2. Half-wave plates H1 and H2 are used in conjunction with PB1 and PB2, respectively, to adjust the ratio between the intensities of the beams. Liquid-crystal television spatial light modulators LCTV1 and LCTV2 spatially modulate the object and reading beams with the input and reference images, respectively.

The Bragg diffraction process imposes a limit on the horizontal size of the reference image in the reading beam. To escape this limitation, the images on the two LCTV's are demagnified by lenses (L3, L4) and (L7, L8), respectively. The images are then Fourier transformed by lenses L5 and L6, respectively. The output diffracted beam propagates back along the object beam and through Fourier-transform lens L5. By doing so, the diffracted beam becomes inverse Fourier transformed.

The GaAs crystal is oriented to enable cross-polarization readout; that is, the polarization of the output diffracted beam is perpendicular to that of the reading beam. As a result, polarizing beam splitter PB3 reflects only the output diffracted beam (s-polarized) into the camera, because other beams that enter this beam splitter are p-polarized. This polarization scheme not only yields a higher signal-to-noise ratio but also allows most of the object beam to be transmitted through, and most of the diffracted beam to be reflected by, polarizing beam splitter PB3.

At present, the speed of the optical correlator is limited by the frame rate of the LCTV's, which are commercial units designed to operate at the standard video rate (30 frames per second). The shortest measured response time of the GaAs crystal under the experimental conditions was 0.8 ms; this response time could accommodate any frame rate up to about 1,000 s^{-1}.

This work was done by Tsuen-Hsi Liu and Li-Jen Cheng of Caltech for **NASA's Jet Propulsion Laboratory**. *For further information, Circle 93 on the TSP Request Card.*

This invention is owned by NASA, and a patent application has been filed. Inquiries concerning nonexclusive or exclusive license for its commercial development should be addressed to the Patent Counsel, NASA Resident Office-JPL [see page 20]. Refer to NPO-18379.

Indirect Calibration in Electron-Probe Microanalysis

Time spent acquiring data is reduced considerably.

Lewis Research Center, Cleveland, Ohio

A technique for indirect calibration in electron-probe microanalysis reduces the number of measurements needed without significantly degrading the precision of the measurement data. The technique is advantageous when many analyses must be performed; for example, in determining the varying chemical composition at many positions across a specimen of a multicomponent alloy.

In electron-probe microanalysis, the spot of interest on a specimen is struck by a thin beam of electrons that have sufficient kinetic energy to excite x-ray emissions from elements of interest in the specimen. Crystal diffractometers sort the x rays according to wavelength, and x-ray counters measure the intensities at the various wavelengths. The wavelengths can be used to identify the emitting elements, and the intensities depend on the concentrations, but the relationships between concentrations and intensities are nonlinear.

Theoretical models have been developed to account for the nonlinearity and extract the concentrations of elements from the intensity-vs.-wavelength data. They are called "ZAF" models (where Z is the standard symbol for atomic number, A denotes absorption, and F denotes fluorescence). With the help of a modern small, fast computer, a ZAF correction scheme can be implemented during the measurements, yielding concentration data almost immediately. Such a scheme is very efficient when only a few analyses are required. However, the calibration of a ZAF scheme requires the intensities of both the x-ray peaks and the x-ray backgrounds at the wavelengths of interest for all elements in the specimen. If analyses at a large number of points in a specimen are performed, then much time is spent in moving the crystal diffractometers back and forth to collect the x-ray spectra and in computing the corrections.

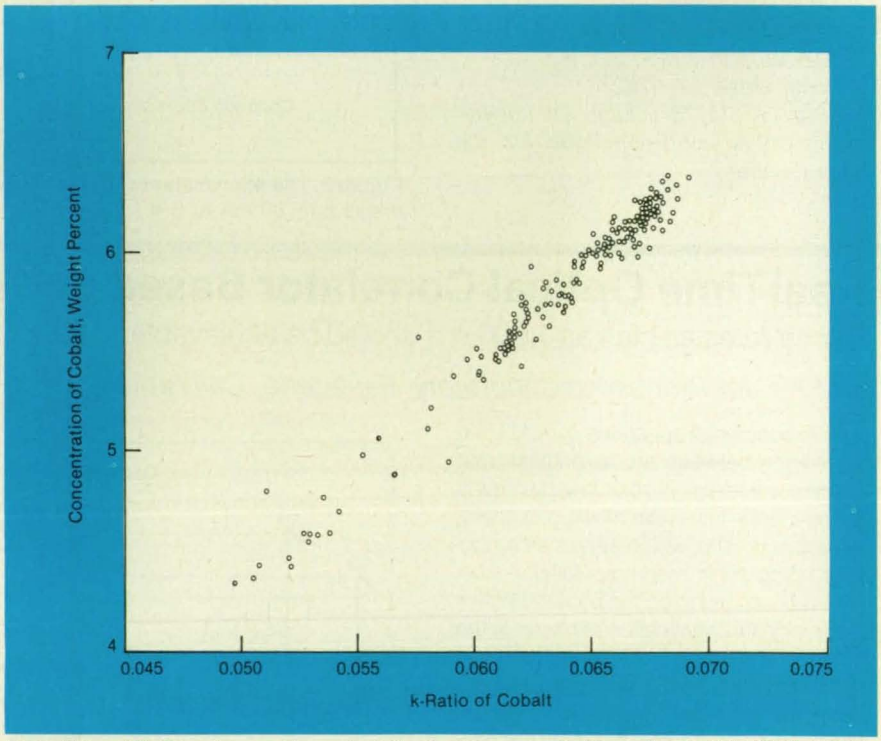

Data From 199 Specimens show that the local concentration of cobalt in PWA-1480 (a nickel-base superalloy) varies approximately linearly with its *k*-ratio.

In the indirect-calibration technique, it is not necessary to acquire background intensities from the specimen, and the analysis is limited to only the elements of interest; that is, it is not necessary to collect and process data on all the elements in the specimen. The technique requires data both on the intensities of x-ray peaks from the specimen to be analyzed and on the x-ray peaks and backgrounds from standard specimens of the pure element and previous specimens of the same alloy. The "*k*-ratio," which is the ratio between the peak x-ray intensities from every specimen and the corresponding intensities from the standard specimen, is com-

puted for each element.

The data from the previous specimens are processed through a full ZAF correction scheme to obtain the concentrations of the elements. It turns out that when the data for each specimen and element are plotted statistically in the form of concentration vs. *k*-ratio, the data points fall very nearly on a straight line (see figure). A linear equation that relates the concentration to the *k*-ratio can be obtained by a least-squares best fit. Thereafter, the concentration of an element of interest in a specimen to be analyzed can be obtained by measuring its *k*-ratio and inserting this ratio in this simple equation.

This work was done by F. M. Terepka of **Lewis Research Center** *and M. Vijaykumar and S. N. Tewari of Cleveland State University (with partial support under a cooperative agreement NAG-8-091 from Marshall Space Flight Center). Further information may be found in NASA TM-102393 [N90-14335], "Calibration Approach to Electron Probe Microanalysis: A Study With PWA-1480, a Nickel Base Superalloy."*

Copies may be purchased [prepayment required] from the National Technical Information Service, Springfield, Virginia 22161, Telephone No. (703) 487-4650. Rush orders may be placed for an extra fee by calling (800) 336-4700.
LEW-15107

Automated Recognition of Melt Lines in Phase-Change Paints

Two-color measurements with a modified color television camera yield isothermal contours.

Langley Research Center, Hampton, Virginia

A technique has been developed to reduce data quickly and objectively in images of phase-change paints (PCP's). Phase-change paints are coats designed to become transparent at certain raised temperatures. Such coats offer visual information on the evolution of isotherms and thus provide valuable temperature-versus-time data when used on aerothermodynamic wind-tunnel test models.

In the past, wind-tunnel PCP data have been recorded on cinematic film and later reduced manually by projecting individual frames on paper and tracing melt lines with colored pencils. This technique has been extremely labor-intensive. Previous attempts to automate the image-data-reduction process have failed to detect paint melt lines accurately in the presence of variable surface lighting. These techniques rely on the processing of monochromatic images to determine transition gray values for the identification of melt lines and involve difficulties in the interpretation of data in the presence of glare, shadows, or any contrast in surface illumination. For such reasons, past automated data-processing systems have proven inadequate for wind-tunnel applications.

The new technique involves the use of a three-tube color-camera system. The camera is modified so that the separate red (R), green (G), and blue (B) video outputs contain complete framing information and can be recorded and digitized by use of standard video format. Camera-signal levels, lighting, the selection of paints, and the color of the model are adjusted so that a relative camera signal between any two of the color outputs (R, G, or B) varies significantly, depending on whether paint is unmelted or melted within a picture element. In this manner, an image-data-processing algorithm is simply an image-subtracting routine that identifies a positive and negative image region, representing unmelted and melted paint surfaces.

In a demonstration of the new technique, PCP was coated on a red model and tested

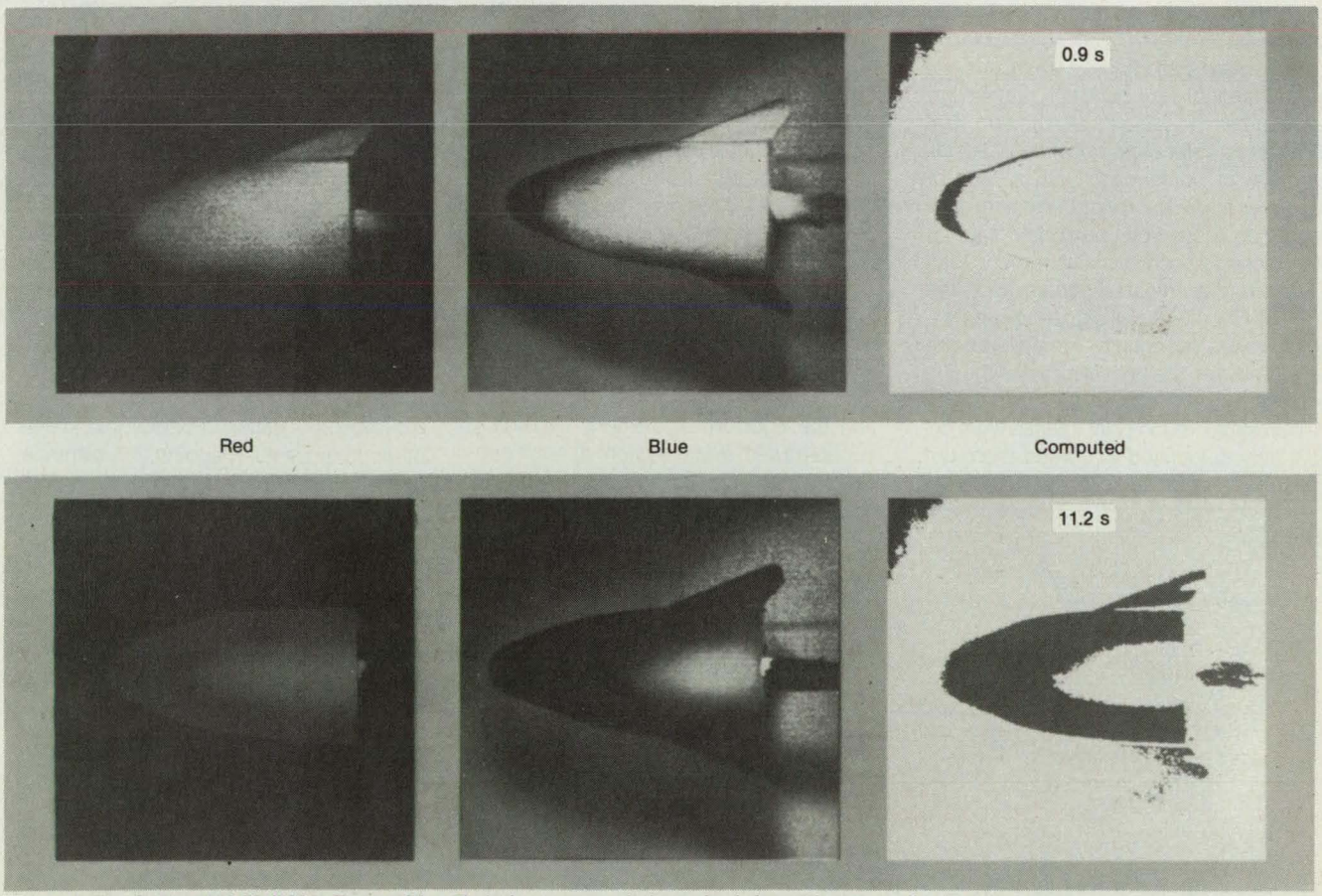

Figure 1. The **Automated Melt-Line-Recognition Technique** uses relative-color information to outline painted regions.

in NASA Langley Research Center's 31-in. (79-cm) Mach-10 Wind Tunnel. The images in Figures 1 and 2 illustrate the process in which an image-subtracting routine was used to generate positive/negative computer images from the blue and red digitized images. Successive positive/negative images in time can be subtracted from each other, and each step colored to produce an isotherm map. The various PCP's, applied to a red model and illuminated with a 150-W spot lamp, have all resulted in success in the use of this technique.

This technique was proven very simple and repeatable. While the original application is in the detection of a specific temperature on the surface of an object in a wind tunnel, the technique could be used wherever rapid and accurate remote temperature-profile measurements are desired; for example, for test objects in inaccessible, toxic, or other hostile areas.

This work was done by Gregory M. Buck of **Langley Research Center**. *No further documentation is available.*
LAR-14127

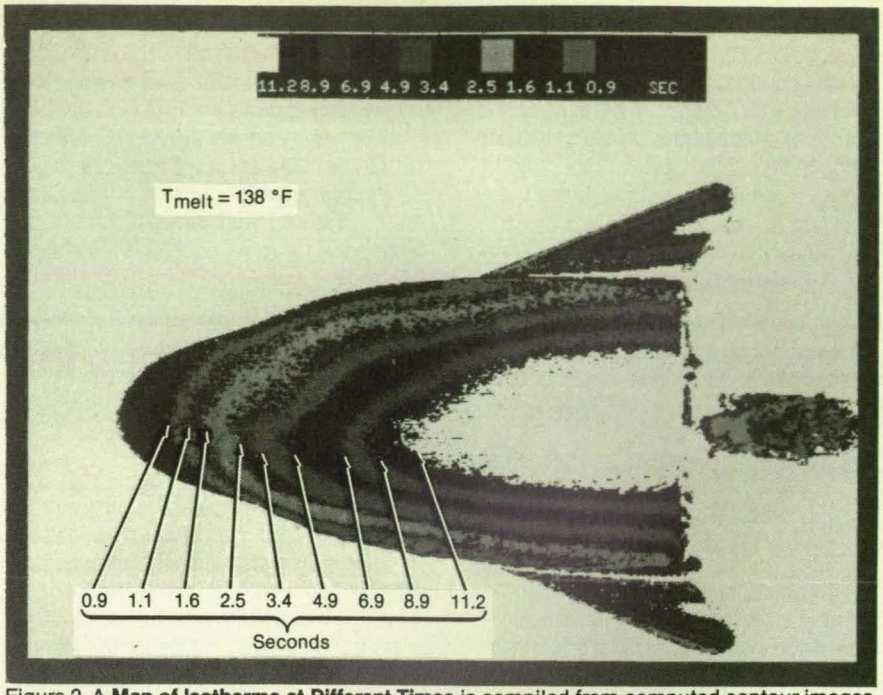

Figure 2. A **Map of Isotherms at Different Times** is compiled from computed contour images by use of standard image-processing algorithms.

Phase-Scrambler Plate Spreads Point Image

An array of small prisms can be retrofit to an imaging lens.

Goddard Space Flight Center, Greenbelt, Maryland

The phase-scrambler plate is an optical component that can be installed on an imaging lens to alter the point image of a star, laser beam, or other distant source of light into a focused spot image of square, round, or other arbitrary shape. The flux in the image can be made essentially uniform. The phase-scrambler plate might be used, for example, in conjunction with a lens of square aperture to produce a square spot of light on a quad-cell photodetector in a star-tracking or surveying instrument. With a uniformly illuminated square spot, the output of the quad-cell signal-balance circuitry varies essentially linearly with the angle between the optical axis and the line of sight to the source.

Heretofore, round point images were deliberately defocused to spread them out on quad-cell photodetectors. Operation out of focus makes an instrument extremely sensitive to small thermal and mechanical changes in the focus adjustment. With the phase-scrambler plate, an instrument can be operated at best focus, with consequent large tolerance for mechanical and thermal changes.

The functions of the lens and phase-scrambler plate can be described more precisely as follows. The lens alone focuses the light from a point source onto a single diffraction spot. The angular width of this spot is proportional to the wavelength of the illumination and inversely proportional to the width of the aperture. The phase-scrambler plate is essentially a planar array of small prisms that partition the aperture of the lens into many subapertures, and the prism at each subaperture is designed to divert the relatively large diffraction spot formed by that subaperture to a different, specific point on the focal plane (see figure). The ensemble of the diffraction spots constitutes the desired square, round, or other composite spot image. The number, sizes, and arrangement of subapertures are chosen so that the phases in wave fronts are distributed randomly among the subaperture diffraction spots and adjacent subaperture diffraction spots overlap slightly to yield nearly uniform illumination in the composite spot image.

There are many different spot mappings and corresponding prism arrangements, and there are many different ways of fabricating a phase-scrambler plate to obtain a desired spot pattern. For example, in one particularly useful mapping, the distance of a subaperture spot from the axis in the image is proportional to the distance of the subaperture from the axis. A square pattern with this mapping can be produced by a phase scrambler that consists, in effect, of a back-to-back, crossed pair of surfaces that resemble cylindrical Fresnel lenses. Such surfaces could be formed by compression molding of sheets of plastic, using dies made by machining and polishing the edges of stacked steel plates.

This work was done by Oliver J. Edwards and Tor Arild of Quantic Industries, Inc. for **Goddard Space Flight Center**. *For further information, Circle 80 on the TSP Request Card. GSC-13185*

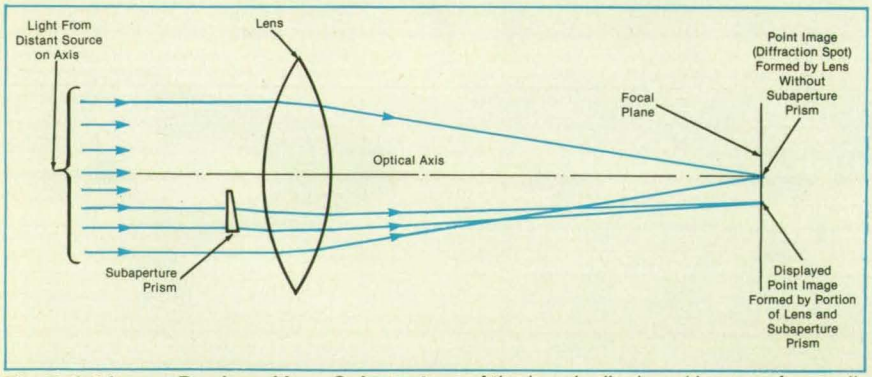

The **Point Image Produced by a Subaperture** of the lens is displaced by use of a small prism at the subaperture.

Locating the Geocenter From GPS Measurements

The center of mass of the Earth can be located within a few centimeters.

NASA's Jet Propulsion Laboratory, Pasadena, California

Two strategies to determine the location of the geocenter from observations of satellites in the Global Positioning System (GPS) have been devised. The geocenter is the center of mass of the Earth; precise knowledge of its position in a terrestrial reference frame tied to observing stations on the surface is necessary for such geophysical measurements as those of plate tectonics. For example, any time-dependent offset, from the geocenter, of the supposed center of the Earth in such a terrestrial frame can result in misinterpretation of some measurements in terms of motions of tectonic plates.

The two strategies involve a fiducial network of two or more ground GPS tracking stations, the positions of which have been determined in a terrestrial coordinate frame to a very high accuracy, usually by very-long-baseline interferometry (VLBI) or satellite laser ranging. Several GPS receivers at other, less-accurately-known, stations also observe the GPS satellites along with the fiducial network. The GPS data can be processed simultaneously to adjust the computed states of the GPS satellites and the computed positions of the nonfiducial sites. The coordinate frame of the fiducial network can be used to express the adjusted GPS-satellite orbits and the locations of the nonfiducial stations to greater accuracy.

In the first strategy, the filtering algorithm used to process the GPS data adjusts the baselines between a reference site (one of the fiducial sites) and all nonfiducial sites along with GPS orbits and the absolute coordinates of the reference site. This implicitly entails the adjustment of the computed location of the geocenter. In this strategy, one or two fiducial baselines are fixed or constrained by their a priori uncertainties.

The orientation of the adopted coordinate frame is defined by the fixed baselines. The absolute scaling can be fixed either by the lengths of these baselines or by the gravitational constant of the Earth, GM. Both are known to an accuracy of about 1 part in 10^8. The absolute scale derived from the fixed baseline lengths makes the coordinate frame thus established consistent with the VLBI frame of the fiducial baselines.

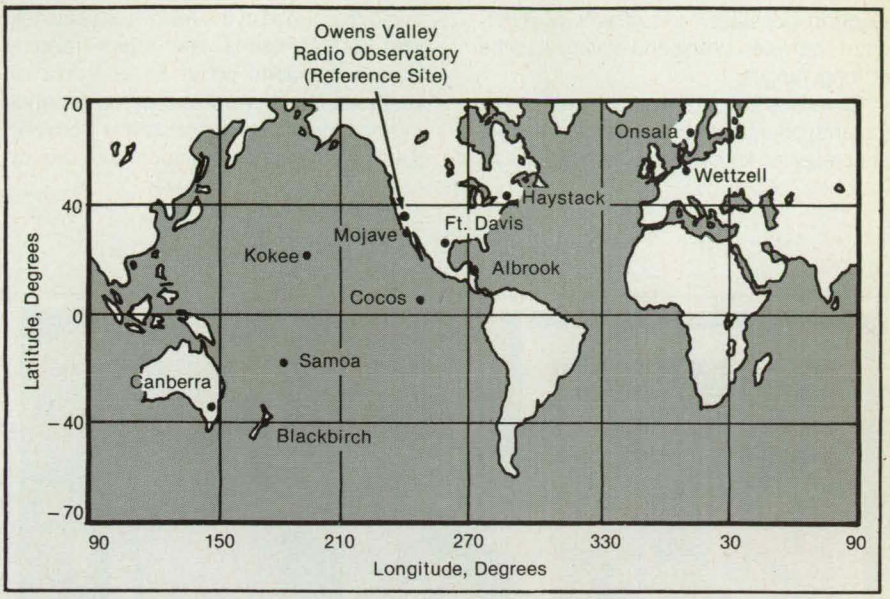

The **GPS Tracking Stations** indicated by dots collected the data used to compute the location of the geocenter according to the two strategies.

In the second strategy, only the longitude of a reference site is held fixed; all other coordinates of this site are adjusted simultaneously along with the states of the GPS satellites. The absolute scale is provided by GM of the Earth. The geocentric radius at a station can be obtained from the adjusted periods of GPS orbits and GPS pseudorange measurements. The time signature of the measurements defines the latitude. The coordinate system thus defined will be centered and fixed in the Earth.

The two strategies were tested by applying them to data acquired in a GPS experiment conducted from January 18 to February 5, 1988. Twelve globally distributed ground stations and seven satellites were used in the experiment (see figure). The geocenters computed by use of the two strategies differed from each other by 42, 49, and 5 cm along three perpendicular coordinate axes, with a root-mean-square difference of 37 cm along each axis. With anticipated future improvements in the quality of GPS data, better GPS satellite constellations, and more nearly even distribution of tracking stations, it should be possible to determine the location of the geocenter with an error of no more than a few centimeters.

This work was done by Rajendra P. Malla and Sien C. Wu of Caltech for **NASA's Jet Propulsion Laboratory**. *For further information, Circle 4 on the TSP Request Card. NPO-18398*

Books and Reports

These reports, studies, handbooks are available from NASA as Technical Support Packages (TSP's) when a Request Card number is cited; otherwise they are available from the National Technical Information Service.

Charged-Particle Calibration of Spacecraft-Ranging Signals

Selection of optimal calibration strategies is discussed.

A report discusses the determination of effective densities of electrically charged particles along the paths of microwave signals transmitted to and from a spacecraft and the use of those densities to calibrate the measured signal-propagation times, which are used to compute the distances between ground stations and the spacecraft. The discussion is oriented toward the selection of a method of calibration that is optimal with respect to three criteria: (1) minimization of the range error and of the root-mean-square uncertainty in the range error; (2) minimization of the amount, complexity, and/or cost of equipment; and (3) capability of calibrating changes in group velocities of signals on the ranging channel.

The charged particles in question are the electrons and ions of the solar-wind, outer-space, and ionospheric plasmas. To a close approximation, the time of propagation along a path through a plasma increases by amount that is proportional to the column abundance of electrons along

the path and inversely proportional to the frequency of the signal. The report discusses the contributions of delays of this type to the measured total round-trip propagation time, including the effects of different uplink and downlink frequencies, effects of temporal and spatial variations of electron densities, and effects of differences between uplink and downlink paths at long ranges.

Equations for range errors, based on the (column-abundance)/(frequency)^2 delays, are presented for cases in which the spacecraft is tracked by one or by two ground stations. Methods of calibration are then compared by use of the tracking-error equations. Next, methods of calibration are compared in terms of the inherent capabilities of the methods and of the equipment required for each method. Following a detailed discussion of the relative advantages and disadvantages, the report recommends the adoption of several optimal methods, the applicable method depending on how far the spacecraft is from the Earth and whether it is tracked by one or two ground stations. These methods involve various combinations of single and dual uplink frequencies, dual downlink frequencies, and/or, in the case of two stations, measurements of Faraday rotation between the spacecraft and the ground station.

This work was done by Tien M. Nguyen of Caltech for **NASA's Jet Propulsion Laboratory**. *To obtain a copy of the report, "Optimal Charged-Particle Calibration Techniques for Ranging Data Channels," Circle 26 on the TSP Request Card.*
NPO-18292

Nonvented Filling of a Cryogenic Tank

Chilling before filling reduces ullage.

A report describes experiments on nonvented filling of a tank designed to store cryogenic liquids. The experiments showed that if the tank is first chilled and evacuated — i.e., to less than atmospheric pressure — it can then be filled to more than 90 percent of its capacity without venting, provided that the conditions of chilling, initial tank pressure, and filling are chosen properly.

On Earth, a tank is vented during filling to remove vaporized liquid and enable the use of the entire volume to store liquid. In outer space, however, liquid and vapor do not separate as they do under the influence of gravity, and a large amount of liquid could be lost through the vent, along with the vapor. Nonvented filling is intended to reduce the loss of liquid in the absence of gravity.

The essence of the strategy of nonvented filling is to reduce the excessive buildup of vapor in the tank while it is not vented and thereby maximize the portion of the volume in the tank that can be filled with liquid of a given supply temperature and pressure. First, the tank is cooled to reduce the vaporization of incoming liquid by heat from walls. This is done by repeatedly spraying small amounts of the cold liquid into the empty tank and venting briefly to remove the evaporated liquid. The vent on the chilled tank is then closed, and the liquid is pumped in through an internal spray nozzle that promotes condensation of evolved vapor on the incoming liquid.

In the experiments, the chilling-and-nonvented-filling procedure was performed with liquid nitrogen and liquid hydrogen in a 5-ft^3 (0.14-m^3) insulated tank. With liquid nitrogen at a temperature of 126 °R (70 K) at the inlet and the inner wall chilled initially to 273 °R (152 K), 98-percent fill was achieved. The transfer of liquid hydrogen was more difficult: it was necessary to reduce the temperature of the liquid at the

inlet to 34 °R (19 K) and the initial temperature of the inner wall to 103 °R (57 K) to achieve a 91-percent fill.

Although this procedure was developed for space applications, it may also be useful in ground-based operations where venting is impractical or hazardous.

This work was done by David J. Chato, Matthew E. Moran, and Ted W. Nyland of **Lewis Research Center** *and Shigeo Nakanishi of Analex Corp. Further information may be found in NASA TM-103155 [N90-26728], "Initial Experimentation on the Nonvented Fill of a 0.14 m^3 (5 ft^3) Dewar With Nitrogen and Hydrogen."*

Copies may be purchased [prepayment required] from the National Technical Information Service, Springfield, Virginia 22161, Telephone No. (703) 487-4650. Rush orders may be placed for an extra fee by calling (800) 336-4700. LEW-15336

Measuring Density of Air by Ultraviolet Rayleigh Scattering

A pulsed excimer layer would probe air in the vicinity of the reentering Space Shuttle.

A report presents theoretical and experimental studies directed toward the development of an optoelectronic instrument to measure the density of air at altitudes from 50 to 90 km and possibly beyond. The instrument would be mounted in the Space Shuttle orbiter and would be operated during reentry into the atmosphere. The data to be gathered by the instrument are needed because the density of the upper atmosphere is highly variable in space and time and this variability affects the aerodynamic behavior and trajectory of the reentering Shuttle. Of course, the variations in density are also meteorologically significant.

The instrument would measure the density of air indirectly by Rayleigh scattering of an ultraviolet laser beam. The theoretical study addresses such instrument-design factors as signal-to-noise ratio, Rayleigh-scattering cross sections of air molecules, efficiency of the scattered-light-collecting optics, sensitivity of the photodetector, and solar background radiation. The source of ultraviolet light chosen to satisfy the preliminary design requirements (though not necessarily the final flight design requirements) and for use in a laboratory prototype of the instrument is a commercial pulsed ArF excimer laser that operates at a wavelength of 193 nm and that puts out an average power of 5 W at a pulse-repetition rate of 100 Hz (50 mJ/pulse). The photodetector is a commercial photomultiplier tube with a CsTe solar-blind photocathode and an ultraviolet-transmissive fused-silica envelope.

The laser beam would be sent out through a Space Shuttle window along a line of sight perpendicular to the fore-and-aft axis. Laser light scattered back from air molecules during each pulse would be focused onto the photocathode by the collecting optics, which would be attached to the inside of the window. The collecting optics are arranged and configured to collect only light scattered from a distance greater than the thickness (about 2 m) of the shock layer around the Space Shuttle.

The output of the photomultiplier is integrated during a selected interval following each pulse to obtain a signal indicative of the total energy of light scattered from that pulse. This signal, normalized by the energy of the pulse, is proportional to the density of the air along the observed length of the laser beam.

The laboratory prototype has been tested by using it to probe the air in a 21-m-long vacuum chamber that can be pumped down to pressures typical of altitudes up to 125 km. This facility duplicates the signal levels (except those due to solar background and scattering from aerosol particles) of the flight environment. The results of the tests indicate that a flight version of the instrument could measure the density of air with an uncertainty of less than 1 percent and with a spatial resolution of 1 km along the flightpath, at altitudes from 50 to 90 km. The instrument could also be used

at altitudes from 90 to 100 km, but there it would yield greater uncertainty and less resolution.

This work was done by Robert L. McKenzie of **Ames Research Center**. *Further information may be found in NASA TM-100056 [N88-22337], "A Method of Atmospheric Density Measurements During Space Shuttle Entry Using Ultraviolet-Laser Rayleigh Scattering."*

Copies may be purchased [prepayment required] from the National Technical Information Service, Springfield, Virginia 22161, Telephone No. (703) 487-4650. Rush orders may be placed for an extra fee by calling (800) 336-4700. ARC-12233

Calculating Shocks in Chemically Reacting Flows

A total-variation-diminishing dissipation operator results in crisp shocks.

A report discusses a method for the numerical simulation of shocks in hypersonic, chemically reacting flows. It introduces a mathematical model of gas of as many as three species (e.g., nitrogen and oxygen molecules and oxygen atoms) for which the species-conservation equations are coupled with the gas-dynamic equations.

The dynamic equations for a one-dimensional, inviscid flow of the model gas are initially stated in the form of the conservation of density, momentum, energy, and the mass fraction of each species. The pressure is found from the sum of partial pressures of the species according to Dalton's law. Using the model definition of the total energy per unit volume, the temperature is calculated from conserved quantities and from the chemical-reaction energies. The gas is presumed to be in local thermal equilibrium, though not necessarily in local chemical equilibrium.

The production and consumption of chemical species (e.g., the dissociation and recombination of oxygen) are expressed in conventional chemical-rate equations, in terms of products of concentrations, temperature-dependent forward and reverse rate constants, and heats of reaction. These rate equations are used to form the species source terms on the right side of the conservation equations for the mass and momemtum densities of the species.

The coupled dynamic and species conservation equations are hyperbolic and are solved by an explicit finite-difference method. However, to suppress spurious numerical oscillations that would inhibit the capture of simulated shocks, the convective-flux terms on the left side and the source terms on the right side are treated differently. The convective terms are integrated by a first-order, total-variation-diminishing, numerical-dissipation model, while the source terms are evaluated by the use of fourth-order Runge–Kutta time differencing.

The coupled equations have been solved for a mach-30 shock in two model reacting gases: one gas of a single species of dissociating diatomic molecules, and one gas consisting of one nondissociating and one dissociating diatomic species having mass fractions resembling those of nitrogen and oxygen in air. The solution method is successful in capturing strong, crisp shocks and in specifying the concentrations of the species. The method is independent of the number of species, and one or more species can be allowed to vanish without introducing new errors or singularities. Future studies will be directed toward the validation of the method by the use of realistic gas parameters and comparison of the numerical results with experimental data from shock tubes.

This work was done by Scott Eberhardt and Kevin Brown of **Ames Research Center**. *Further information may be found in AIAA paper 86A-22683, "A Shock Capturing Technique for Hypersonic, Chemically Relaxing Flows."*

Copies may be purchased [prepayment required] from AIAA Technical Information Service Library, 555 West 57th Street, New York, New York 10019, Telephone No. (212) 247-6500. ARC-11747

Local Gravitomagnetism

In a quasi-inertial reference frame, geodetic precession is a gravitomagnetic phenomenon.

A report presents a theoretical analysis of gravitomagnetism as perceived by an observer in a quasi-inertial reference frame near a spinning body. "Quasi-inertial" as used here means falling freely or in orbit about the spinning body but fixed in orientation with respect to distant celestial objects. Gravitomagnetism is an effect predicted by the theory of general relativity: it is so named because it is a space-time/gravitational effect and its relationship with mass currents bears some resemblance to the well-known relationship between electromagnetism and charge currents.

A reference frame moving with the Earth in free fall around the center of mass of the solar system is approximately quasi-inertial. The study addresses the manifestations of gravitomagnetism in this reference frame, with emphasis on two measurable phenomena: the precession of a gyroscope in orbit about the Earth and perturbation of the trajectory of a satellite in orbit around the Earth.

The analysis begins with the calculation of the space-time metric tensor in the center-of-mass reference frame. The quasi-inertial reference frame moving with the

Multiple Pages Intentionally Left Blank

Earth is defined. Standard tensor-transformation laws are used to compute the components of the metric tensor in this frame up to third order in v/c (where v = speed of the object in question and c = the speed of light).

The precession of a gyroscope in free fall or in orbit around the Earth, as seen by an observer in the quasi-inertial reference frame, is caused by gravitational torques. This precession is computed by use of the metric in the quasi-inertial frame; the gravitomagnetic component is identified and found to account for the precession in its entirety. It is also found that (1) in the absence of preferred-reference-frame effects, the gravitometric field attributable to the motion of the Earth around the center of mass of the solar system can be deduced from analysis of measurements, by ground-based laser ranging stations, of distances to satellites in orbit around the Earth, but that (2) to observers in the local quasi-inertial reference frame, conclusion (1) is a mere consequence of Einstein's principle of equivalence.

This work was done by Bahman Shahid-Saless of Caltech for **NASA's Jet Propulsion Laboratory**. *To obtain a copy of the report, "Local Gravitomagnetism," Circle 55 on the TSP Request Card. NPO-18405*

Polarized-Cathodoluminescence Study of Stress in GaAs/Si

Near microcracks, stresses are primarily uniaxial tensile; elsewhere, they are primarily biaxial tensile.

A report describes experiments in which linearly polarized cathodoluminesce scanning electron microscopy, in both imaging and spectroscopic forms, was used to analyze spatial variations in the stress tensors in specimens of GaAs/Si. The specimens were fabricated by atmospheric-pressure metallo-organic chemical vapor deposition of GaAs to a thickness of 4 μm on Si substrates. The combination of the mismatch between the Si and GaAs crystal lattices and the differential thermal contraction of these materials from the deposition temperature (700 °C) to room temperature gives rise to stresses in the GaAs layer. The experiments were conducted to contribute to understanding of the effects of these stresses and the ramifications thereof for the fabrication of electronic devices in the GaAs/Si system.

The experiments yielded data on strain-induced splitting of the heavy-hole and light-hole valence bands. Previous studies had revealed local variations in luminescence, caused by variations in stress, near microcracks. The use of a linear-polarization detection scheme in this study provided an enhancement in that it made possible a quantification of the intensities of the exciton luminescence and the energies of the excitons in the cathodoluminescence spectra; this led to a definitive evaluation of the heavy-hole and light-hole characters in the strain-split valence bands on a microscopic scale. This approach, in conjunction with polarization selection rules that depend on the form of the stress tensor, enabled determination of the spatial distribution of stress.

Scanning monochromatic cathodoluminescence images of one of the specimens revealed a polarization anisotropy across the specimen. Analysis of the data from the experiments revealed that regions near and far from microcracks were subject to primarily uniaxial and primarily biaxial tensile stresses, respectively. The data from a transition region where biaxial stress changed gradually with position to uniaxial stress were analyzed and shown to reveal mixing of the heavy-hole and light-hole characteristics in the strain-split valence bands.

This work was done by Daniel H. Rich, Alexander Ksendzov, Robert W. Terhune, Frank J. Grunthaner, and Barbara A. Wilson of Caltech for **NASA's Jet Propulsion Laboratory**. *To obtain a copy of the report, "Polarized Cathodoluminescence Study of Uniaxial and Biaxial Stress in GaAs/Si," Circle 101 on the TSP Request Card. NPO-18453*

New Synthesis of Poly(1,3,4-Oxadiazoles)

Synthesis via aromatic nucleophilic displacement yields new high-molecular-weight polymers.

Langley Research Center, Hampton, Virginia

Novel poly(1,3,4-oxadiazoles) (POX) have been prepared by the aromatic nucleophilic displacement of di(hydroxyphenyl)-1,3,4-oxadiazole monomers with activated aromatic dihalides or activated aromatic dinitro compounds. The polymerizations were carried out in polar aprotic solvents such as sulfolane or diphenylsulfone, using alkali metal bases such as potassium carbonate, at elevated temperatures, under nitrogen. The di(hydroxyphenyl)-1,3,4-oxadiazole monomers were synthesized by reacting 4-hydroxybenzoic hydrazide with phenyl-4-hydroxybenzoate in the melt. These monomers were also synthesized by reacting aromatic dihydrazides with phenyl-4-hydroxybenzoate in the melt.

The polymers exhibited good mechanical and thermal properties. Some of the properties of the polymers are shown in the table. The inherent viscosities (η_{inh}) of the POX ranged from 1.02 to 1.71 dL/g, and the glass-transition temperatures (T_g) ranged from 182 to 242 °C. Several of the polymers exhibited crystalline melting temperatures (T_m) by differential scanning calorimetry. These temperatures ranged from 265 to 390 °C. Thermogravimetric analysis showed no loss of weight at temperatures below 300 °C, and a 5-percent loss of weight at approximately 500 °C, in both air and nitrogen.

This synthetic route has provided high-molecular-weight POX of new chemical structure, is potentially more economically favorable than other routes and, because of the availability of a large variety of activated aromatic dihalides, facilitates the variation of chemical structures. The polymers exhibit properties that make them useful as films. They could also be useful in coatings, adhesives, moldings, and composites because of their good high-temperature properties.

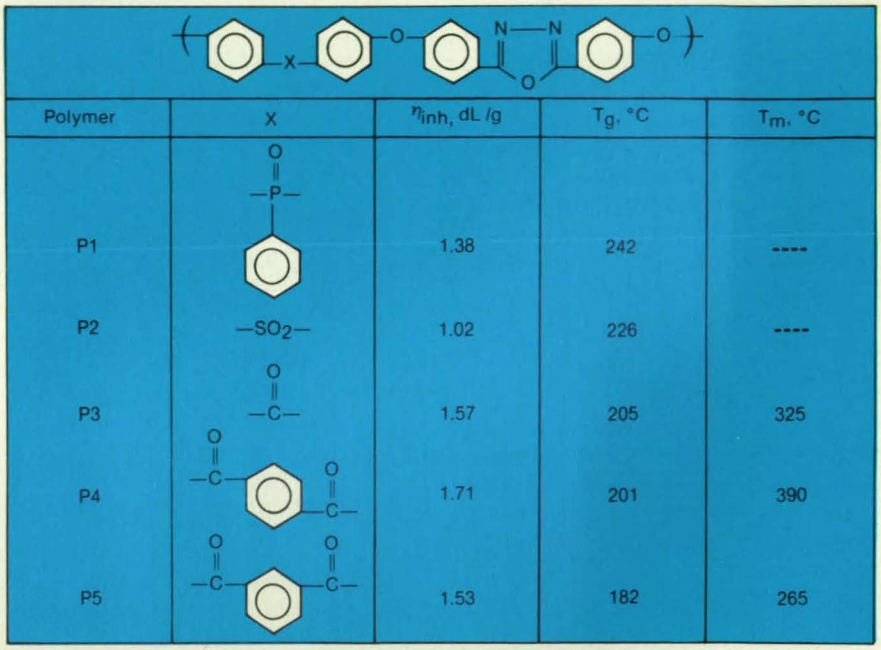

Polymer	X	η_{inh}, dL/g	T_g, °C	T_m, °C
P1		1.38	242	----
P2	$-SO_2-$	1.02	226	----
P3		1.57	205	325
P4		1.71	201	390
P5		1.53	182	265

Chemical Structures and Some Properties of the new poly(1,3,4-oxadiazoles) are shown.

This work was done by John W. Connell and Paul M. Hergenrother of **Langley Research Center** *and Peter Wolf of BASF Corp. For further information, Circle 42 on the TSP Request Card.*

This invention is owned by NASA, and a patent application has been filed. Inquiries concerning nonexclusive or exclusive license for its commercial development should be addressed to the Patent Counsel, Langley Research Center [see page 20]. Refer to LAR-14427.

Fluorescence Reveals Contamination From Adhesives

Highly fluorescent dopants may not be needed.

Marshall Space Flight Center, Alabama

Contamination of nearby surfaces from ingredients in some adhesive materials would be detected by ultraviolet illumination and observation of the resulting fluorescence, according to a proposal. The identification of contaminants via telltale fluorescence is not new; rather, the significance of the proposal lies in the method of implementation and the potential extension to a wider variety of materials and applications.

In a demonstration, fiber-optic sensors and illumination with ultraviolet light at wavelengths from 1,930 to 2,490 Å were used to excite and characterize the fluorescence of contaminants on surfaces. The surfaces in question were those of composite cases and insulation of Space Shuttle solid-fuel rocket motors, and the contaminants in question were ingredients of adhesives in liners in the motors.

The fiber-optic sensors detected the contaminants in concentrations as low as 600 $\mu g/in.^2$ (93 $\mu g/cm^2$). One implication of this finding is that in the rocket-motor application, it may not be necessary to dope the adhesives with highly fluorescent dye to facilitate detection. Similarly, it may not be necessary to dope potential contaminants in other applications — e.g., it may not be necessary to dope cutting fluids used in machining components that are required to be subsequently cleaned and rigorously inspected.

This work was done by William Nikolia of Hercules Aerospace Co. for **Marshall Space Flight Center**. *No further documentation is available.*
MFS-28622

NEW FROM INCO SPP...

EXTRA FINE NICKEL POWDER

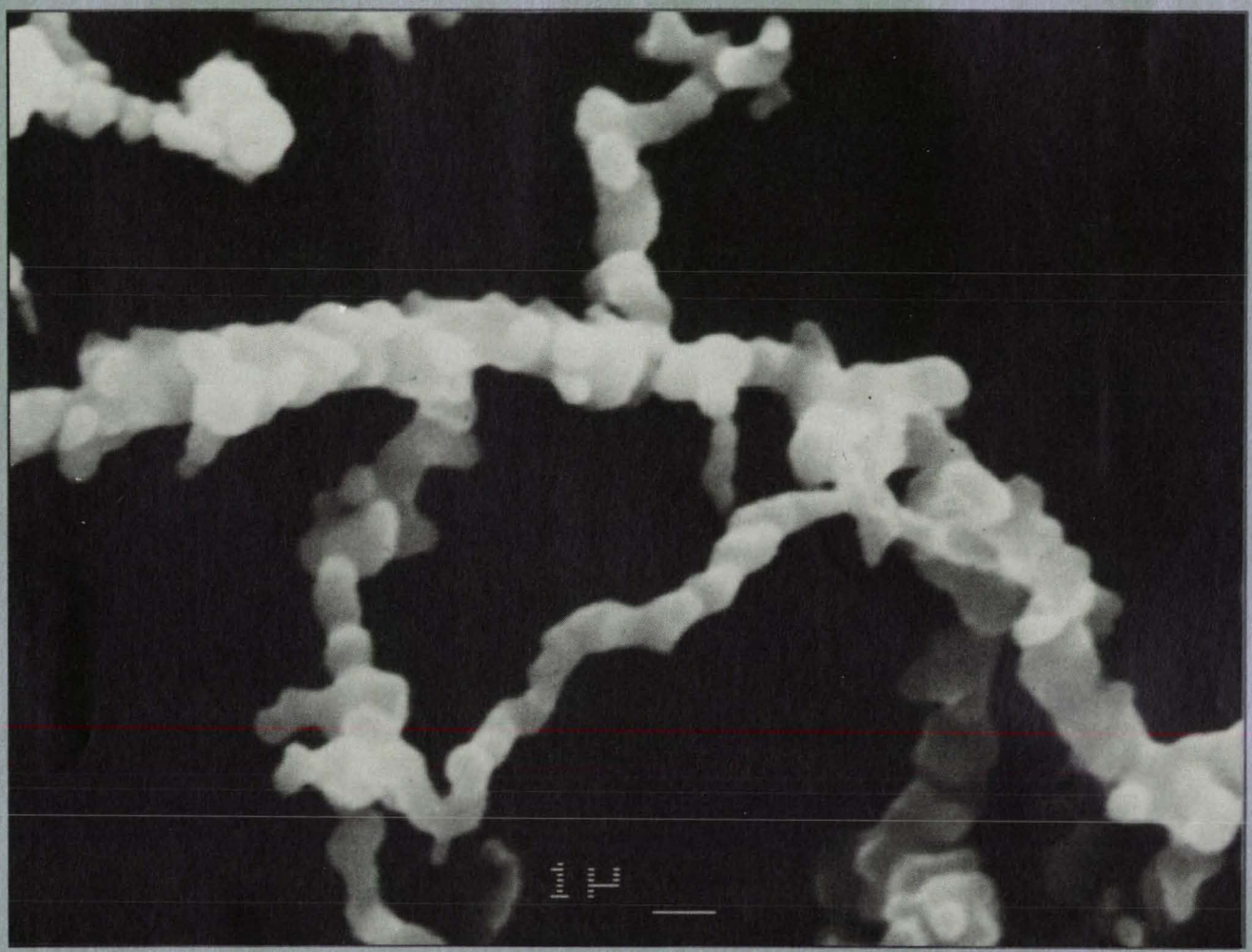

Inco Type 210 Nickel Powder

JUST ADD YOUR IMAGINATION

SEND FOR YOUR FREE SAMPLE TODAY

INCO SPP

Park 80 West-Plaza Two, Saddle Brook, NJ 07662
Shin-Muromachi Building, 4-3 Nihonbashi-Muromachi 2-Chome, Chuo-ku, Tokyo 103 Japan
1-3 Grosvenor Place, London SW1X7EA England
15/Fl Wilson House, 19-27 Wyndham Street Central, Hong Kong

For More Information Circle No. 652

Plasma-Spraying Ceramics Onto Smooth Metallic Substrates

Rough metal/ceramic interfaces are no longer necessary.

Lewis Research Center, Cleveland, Ohio

In an experimental fabrication process, plasma-sprayed ceramic coats (e.g., zirconia/yttria-based thermal-barrier coats) are bonded strongly to smooth metallic surfaces (see figure). The principal use of such coats is in protecting metal parts in the hot-gas paths of advanced gas turbine engines.

Heretofore, plasma-sprayed ceramic coats have been adherent and durable only when applied over rough, plasma-sprayed metallic bond coats. This limitation is sometimes undesirable; for example, when a design calls for a particular oxidation-resistant bond coat that has to be applied by a method other than plasma spraying. The new process would be appropriate for many applications in which thermally insulating coats are needed on smooth metal substrates, as well as for other applications that involve such different types of ceramic coats as wear coats.

The new process consists of (1) the application of an initial thin layer of ceramic on a smooth surface by low-pressure-plasma spraying (LPPS) followed by (2) the application of a layer of conventional, low-thermal-conductivity atmospheric-pressure plasma-sprayed (APPS) ceramic. The smooth surface can be an uncoated oxidation-resistant alloy, a metallic diffusion coat, or even a plasma-sprayed metallic coat that has been ground smooth; it can be nonoxidized or lightly preoxidized.

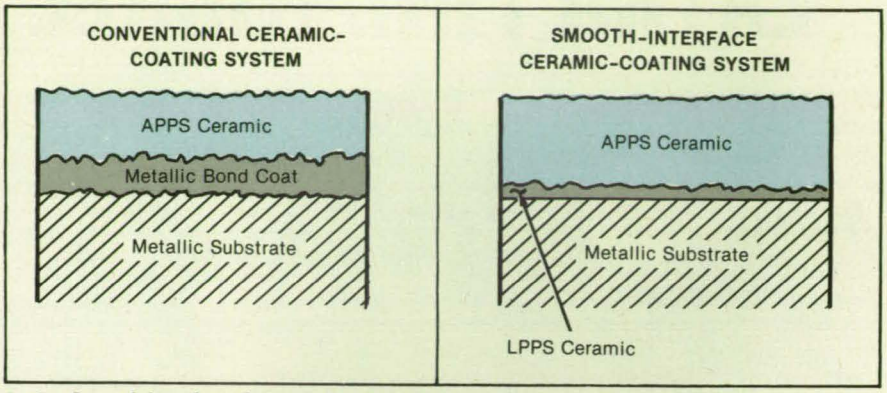

In the **Smooth-Interface Ceramic-Coating System** (right) a smooth metallic substrate is first coated with a thin layer of LPPS ceramic, which is then coated with a thicker layer of APPS ceramic. In the conventional ceramic-coating process (left), a metallic substrate is coated with a metallic-bond coat, the rough surface of which is then coated with the APPS ceramic layer.

When correctly processed, the LPPS ceramic layer adheres to any of these smooth surfaces. However, this initial layer is rather dense and, therefore, less insulating and less tolerant of stresses and strains when thick than conventional plasma-sprayed ceramic coats are. Therefore, the LPPS ceramic is applied to a thickness of only about 1 mil (25 μm). This initial layer is sufficiently rough to enable the final layer of conventional APPS ceramic to adhere.

This work was done by Robert A. Miller, William J. Brindley, and Carl J. Rouge of **Lewis Research Center** *and George Leissler of Sverdrup Technology, Inc. For further information, Circle 46 on the TSP Request Card. LEW-15164*

Improved Sprayable Insulation

New formulations and care in processing yield superior ablative materials.

Marshall Space Flight Center, Alabama

MSA-2 and MSA-2A are two similar improved versions of Marshall sprayable ablator, an insulating material developed at Marshall Space Flight Center to replace both sheets of cork and MSA-1, the first-generation ablative sprayable insulation on the Solid Rocket Booster of the Space Shuttle. MSA-2 and MSA-2A are also suitable for use on other large vehicles and structures that may be exposed to fire or other sources of heat by design or accident. The ablative insulation turns into a strong char when exposed to high temperature — a highly desirable property in the original spacecraft application and possibly in some terrestrial applications.

The development of the improved materials was motivated by two shortcomings of MSA-1: (1) attempts to apply MSA-1 in thicknesses exceeding ¼ in. (about 6 mm) resulted in cure-stress cracking, yet the design called for greater thicknesses; and (2) chunks of MSA-1 fell off in flight. MSA-2 and MSA-2A can be applied in thicknesses up to ½ in. (about 13 mm) and chunks do not fall off in flight.

Nonvolatile Components	MSA-2 Weight, Grams	MSA-2A Weight, Grams
Phenolic Microballoons	4,590	same
Epoxy Resin/Catalyst (Clear Amber)		
EC2216B (or Equivalent)	3,004	same
EC2216A (or Equivalent)	3,005	same
Hollow Glass Spheres (Diameters 30 to 300 μm	1,800	same
Bentone 27 (or Equivalent) Colloidal Clay	495	same
Milled Glass Fibers, 1/16 in.	450	same
Ground Cork, 20/40 Screen	435	same
Chopped Glass Fibers, 1/4 in.	180	same
Solvents		
Methylene Chloride	24,268	none
Perchloroethylene	19,661	none
Ethanol (Bentone Accelerator)	495	same
1,1,1-Trichloroethane	none	36,494

The **Two Versions** of the improved sprayable ablative insulation differ only in the solvents used in the sprayable mixture. After spraying, the solvents evaporate.

The ingredients of MSA-2 and MSA-2A (see table) differ from those of MSA-1 in several respects: most notably in the substitution of a flexible epoxy and the incorporation of ground cork, both of which are essential to the required increases in strength and thickness. The two versions differ only in the solvents, which serve as carriers that fluidize the ingredients for spraying, and which evaporate after application. MSA-2 contains methylene chloride and perchloroethylene, whereas MSA-2A contains 1,1,1-trichloroethane, which is somewhat less toxic. Cured MSA-2 and MSA-2A coats are practically indistinguish-

able: the difference being that when methylene chloride and perchloroethylene are used, the amount of each can be adjusted to optimize fluidity and tackiness during spraying and the rates of subsequent drying and curing.

The other ingredients serve the following purposes:

- Phenolic microballoons contribute low density and, at high temperatures, decompose to a highly desirable carbonaceous residue.
- Hollow glass spheres contribute low density and fuse at high temperatures into a binder that strengthens the char.
- Glass fibers add strength to the insulation and the char.
- Bentone 27 (or equivalent) colloidal clay acts to suspend the other solid ingredients in a uniform, sprayable mixture.
- Ethanol activates the colloidal clay and controls the viscosity.

The mixture can be sprayed robotically or by hand. To maximize the strength of the insulation, spraying should be followed by heating according to a specified temperature-vs.-time schedule. The sprayed material can also be cured at room temperature, but this takes 30 to 45 days. The cured material resists damage from normal handling. Tests show that when the underlying surface is aluminum, the insulation is nonflammable and self-extinguishing.

This work was done by W. F. Hill, M. H. Sharpe, C. N. Lester, Sherman Echols, W. G. Simpson, J. D. Lambert, W. F. Norton, and J. P. McLemore of **Marshall Space Flight Center** *and A. K. Patel, S. V. Patel, C. H. Shockney, G. R. Adams, M. R. Kelly, and W. T. White of United Technologies, Corp. For further information, Circle 73 on the TSP Request Card.*
MFS-28587/MFS-28600

Common Criterion for Failure of Different Materials

Tensile failures of different rubbery propellants can be characterized by similar plots.

Marshall Space Flight Center, Alabama

A common scaling criterion has been found to relate some physical quantities that characterize tensile failures of three different solid propellant materials. The propellants are denoted by their rubbery binders; namely polybutadiene/acrylic acid/acrylonitrile (PBAN), hydroxyl-terminated polybutadiene (HTPB), and nitrate ester polyether (NEPE). The tensile tests were conducted at temperatures from −20 to 120 °F (−29 to 49 °C), gauge pressures from 0 to 1,000 psi (0 to 6.9 MPa), various constant loads, constant rates of increase of loads, and constant crosshead speeds (in effect, constant rates of stretch) from 0.2 to 200 in. per min. (85 μm/s to 85 mm/s).

The results of tensile-failure tests of each material under different conditions are summarized by a plot of $(S_{max}/P)^n$ versus log t/a_T (see figure), where S_{max} is the maximum tensile stress, P is the absolute pressure of the atmosphere in the test chamber, t is the time to failure of a specimen under the given conditions, a_T is a time/temperature shift factor that is characteristic of the material, and t/a_T is called the "reduced time." The exponent n is determined by a "best" fit to the data.

This approach to the characterization of tensile failure is attractive in that it conveniently incorporates the effects of time, temperature, and surrounding pressure to reduce all data to a single monotonic curve for each material. Such curves are consistent with the viscoelastic nature of the materials in question.

This work was done by Rodney B. Beyer of Atlantic Research Corp. for Science Applications International Co. under contract to **Marshall Space Flight Center**. *For further information, Circle 71 on the TSP Request Card.* *MFS-28624*

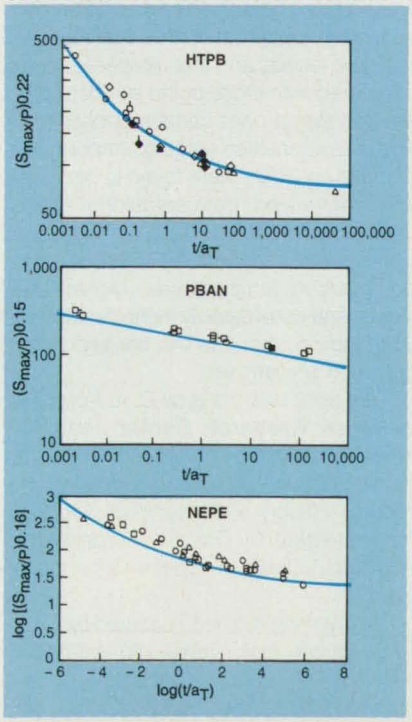

Data From Tensile-Failure Tests of three rubbery propellant materials are plotted to exhibit simple scaling laws.

Books and Reports

These reports, studies, handbooks are available from NASA as Technical Support Packages (TSP's) when a Request Card number is cited; otherwise they are available from the National Technical Information Service.

Parametric Study of a Ceramic-Fiber/Metal-Matrix Composite

Effects of degradation of constituents on properties of the composite are examined.

A report describes a computer-model parametric study of the effects of degradation of the constituent materials upon the mechanical properties of a ceramic-fiber/metal-matrix composite material. This kind of study contributes to understanding of the weakening effects of large changes in temperature and mechanical stresses in fabrication and use. This study was concerned mainly with the influences of the in situ fiber and matrix properties (defined here as the properties of the fiber and matrix in their degraded conditions within the composite) upon the behavior of the composite. Particular attention was given to the influence of the in situ matrix strength and the influence of interphase degradation. ("Interphase degradation" denotes the growth of intermediate layers by chemical reaction between fibers and the matrix, degradation of coating layers deliberately applied to the fibers, or both.)

The material-property data selected for use in this study were those of a composite of silicon carbide fibers in an alloy matrix of 76 percent titanium, 15 percent vanadium, and 3 percent each of aluminum, chromium, and tin — a composite that is a candidate for some high-temperature applications in the National Aerospace Plane. The Metal Matrix Composite Analyzer (METCAN) computer program was used to study the behavior of this material at room and high temperatures. In METCAN, nonlinear properties of the materials are treated at the fiber, matrix, and interphase levels by a "material-behavior-space" mathematical model of the dependency of these properties upon temperature, time, and stress. The properties of the composite are then synthesized from those of the constituents via mathematical models of the micromechanics and macromechanics of the composite.

The composite was treated in this study as a unidirectional laminate with a fiber-volume fraction of 0.4. The study was conducted in two parts. In the first part, there was no interphase, and computations were performed for three different in situ matrix strengths: 100 percent, 50 percent, and 25 percent of the nominal strength at room temperature. In the second part, there was an interphase with a thickness of 1 percent of the diameter of the fiber and computations were performed for in situ interphase strengths of 100 percent, 50 percent, and 25 percent of the matrix strengths.

The numerical results led to the following conclusions, among others, for the range of in situ properties considered:

- The reduction in the transverse strength of the composite is in direct proportion to the reduction in the in situ matrix strength.
- The longitudinal tensile/compressive strength of the composite is reduced by 10 to 20 percent by the reduction in the in situ matrix strength.
- The reduction of the in situ matrix strength reduces the in-plane shear strength by as much as 50 percent.
- The influence of the interphase degradation on the longitudinal tension/compression and in-plane shear behavior is negligible.
- Both the ultimate strength and the ultimate strain in transverse tension/compression are reduced substantially by the interphase degradation.
- In general, the decrease of the in situ matrix strength and the presence of a weak interphase dramatically affect matrix-dominated aspects and have negligible effects on the fiber-dominated aspects of the behavior of the composite.

This work was done by P. L. N. Murthy, D. A. Hopkins, and C. C. Chamis of **Lewis Research Center**. *Further information may be found in NASA TM-102302 [N89-26924], "Metal Matrix Composite Micromechanics: In-Situ Behavior Influence on Composite Properties."*

Copies may be purchased [prepayment required] from the National Technical Information Service, Springfield, Virginia 22161, Telephone No. (703) 487-4650. Rush orders may be placed for an extra fee by calling (800) 336-4700. LEW-15098

Phosphorus Moieties Make Polymers Less Flammable

Phosphorus is incorporated into epoxies and polyamides via a curing agent.

According to a report, the use of 1-[di(2-chloroethoxyphosphinyl)methyl]-2,4- and -2,6-diaminobenzene (DCEPD) as the curing agent for epoxies and polyamides makes these polymers more fire-retardant than are the corresponding polymers made with standard curing agents that do not contain phosphorus. Although epoxy resins are widely used in coating, adhesives, floorings, laminating, and casting, their flammability is a major hazard. In previous studies, epoxies were made less flammable by use of additives that contain phosphorus.

In the experiments described in this report, the phosphorus was incorporated into the polymers via the DCEPD. The DCEPD molecule includes a di(2-chloroethoxyphosphinyl)methyl group bound to *m*-phenylenediamine (MPD), which is widely used as a curing agent for epoxy resins. Therefore, the DCEPD combines the characteristics of a curing agent for epoxy resins with those of an efficient phosphorus-containing fire retardant, and should yield a highly crosslinked polymer of high thermal stability.

In the experiments on epoxies, one epoxy equivalent weight (EEW) of specimens of each of three epoxy resins was polymerized with 0.25 mole of the DCEPD. For comparison, each epoxy resin was also polymerized with common curing agents like MPD and 4,4'-diaminodiphenylsulphone (DDS).

The polymerization reactions were studied by use of a differential scanning calorimeter. DCEPD was found to be less reactive toward all three epoxy resins than MPD is; this is attributed to the presence of the electron-withdrawing phosphinyl group in the DCEPD molecule.

The pyrolysis properties of the epoxies were studied by differential scanning calorimetry and thermogravimetric analysis. The polymers of DCEPD exhibited lower onset decomposition temperatures, higher char yield, and higher limiting oxygen indices than did the corresponding epoxy resins of common curing agents.

In the experiments on polyamides, copolyamides that contain phosphorus were prepared from 1-[(dialkoxyphosphinyl)methyl]-2,6-diaminobenzenes. These polyamides were also characterized by differential scanning calorimetry and thermogravimetric analysis, and their properties were compared with those of the standard polyamides that do not contain phosphorus. The glass-transition melting temperatures of these polymers were found to decrease with increasing concentrations of the phosphorus moieties. The polyamides that contained phosphorus exhibited lower decomposition temperatures, higher char yields, and considerably higher limiting oxygen indices than did the corresponding common polyamides.

This work was done by D. A. Kourtides of **Ames Research Center** *and J. A. Mikroyannidis of the University of Patras, Patras, Greece. To obtain a copy of the report, "History of Phosphorus Additives for Protection of Thermal Properties of Polymers," Circle 13 on the TSP Request Card.*

This invention has been patented by NASA (U.S. Patent Nos. 4,864,050, 4,689,421, 4,886,896). Inquiries concerning nonexclusive or exclusive license for its commercial development should be addressed to the Patent Counsel, Ames Research Center [see page 20]. Refer to ARC-11796.

Properties of Plasma-Deposited Amorphous Hydrogenated Carbon

Characteristics range from diamondlike to graphitic, depending on deposition conditions.

A report reviews experimental research on plasma-deposited films of hydrogenated amorphous carbon (a-C:H). Such films can exhibit electrical resistivity, semi-transparency, mechanical hardness, and chemical inertness. They are useful as gate dielectrics and passivating layers in semiconductor devices, insulators for metal/insulator/metal devices, and masks in nanometer lithography. In addition, they show promise as wear-resistant, hard solid lubricating coats for bearings and optical components.

The report focuses upon the chemical, physical, and tribological characteristics of a-C:H films grown by plasma chemical-vapor deposition at 30 kHz on substrates of Si_3N_4, GaAs, Si, and fused SiO_2. The report is divided into two main parts. The first part discusses experiments in which the influences of growth conditions on the chemical and physical properties of these films were studied by measurements of hardness, Auger electron spectroscopy, secondary ion mass spectroscopy, x-ray photoelectron spectroscopy, ellipsometry, and N^{15}-nuclear-reaction techniques. The nuclear-reaction techniques provide the information on the concentration of hydrogen.

The second part of the report discusses studies that have been conducted to improve understanding of those chemical and physical properties that affect the tribological behavior of an a-C:H film when the film is in contact with a ceramic material. In these studies, the friction, wear, and lubricating behaviors of a-C:H films were examined with flat specimens (each composed of an a-C:H film and Si_3 substrate) in contact with Si_3N_4 riders in two processes. Some of these experiments were performed in dry nitrogen gas and some in moist air to determine the environmental effects on friction and resistance to wear of the a-C:H films. Others of these experiments were performed in vacuums to determine the effect of temperature on adhesion and friction of a-C:H films.

An analysis of the data in the first part of the report shows that the main properties of an a-C:H film are defined by the concentration of hydrogen and by the ratio between the number of sp^2 bonds and the number of sp^3 bonds. A film that contains more sp^3 tends to be more like diamond; that is, to have more tetrahedral bonding and a higher optical band gap. A film that contains more sp^2 tends to be more like graphite.

An analysis of the data in the second part shows that the tribological properties are correlated with the other physical properties described in the first part. Specifically, films of a-C:H deposited at low power tend to be more like diamond and to have frictional properties similar to those of diamond, while those deposited at higher power tend to be more like graphite and to have frictional properties like those of graphite.

This work was done by Kazuhisa Miyoshi, John J. Pouch, and Samuel A. Alterovitz of **Lewis Research Center.** *Further information may be found in NASA TM-102379 {N90-11880}. "Plasma-Deposited Amorphous Hydrogenated Carbon Films and Their Tribological Properties."*

Copies may be purchased [prepayment required] from the National Technical Information Service, Springfield, Virginia 22161, Telephone No. (703) 487-4650. Rush orders may be placed for an extra fee by calling (800) 336-4700.
LEW-15095

Computer Programs

COSMIC: Transferring NASA Software

COSMIC, NASA'S Computer Software Management and Information Center, distributes software developed with NASA funding to industry, other government agencies and academia.

COSMIC's inventory is updated regularly; new programs are reported in *Tech Briefs*. For additional information on any of the programs described here, circle the appropriate TSP number.

If you don't find a program in this issue that meets your needs, call COSMIC directly for a free review of programs in your area of interest. You can also purchase the annual *COSMIC Software Catalog*, containing descriptions and ordering information for available software.

COSMIC is part of NASA's Technology Transfer Network.

COSMIC®—*John A. Gibson, Director,*
Phone (706) 542-3265; FAX (706) 542-4807
The University of Georgia, 382 East Broad Street,
Athens, Georgia 30602

Computer Programs

These programs may be obtained at a very reasonable cost from COSMIC, a facility sponsored by NASA to make computer programs available to the public. For information on program price, size, and availability, circle the reference number on the TSP and COSMIC Request Card in this issue.

Mechanics

Program Simulates Spacecraft Missions

IMP computes principal parameters of trajectories, maneuvers, and events.

IMP is a simulation language that is used to mathematically model spacecraft missions around the Earth, Moon, Mars, or other planets. Simulated missions are controlled by the user through selection from a large menu of events and maneuvers. As many as three simulated spacecraft can be used: a main, a target, and an observer. The simulation can begin at lift-off or in suborbital or orbital phases.

IMP incorporates a Fehlberg 7th-order, 13-evaluation Runge–Kutta integrator with error and step-size (maximum of 360 seconds) control to integrate the equations of motion numerically. The user can choose oblate or spherical gravity for the central body (Earth, Mars, Moon, or other), while a spherical model is used for the gravity of an additional perturbing body. Sun gravity and pressure and Moon gravity effects are selectable by the user. Earth and Mars atmospheric effects can be included.

The optimum thrust guidance parameters are calculated automatically. Events and maneuvers can involve many changes in velocity, and these changes can be impulsive or of finite duration. Aerobraking to orbit is also an option. Other simulation options include line-of-sight communication guidelines, a choice of propulsion systems, a soft landing on the Earth or Mars, and rendezvous with a target vehicle.

The input and output are in metric units, with the exception of thrust and weight, which are in English units. Input is read from the user's input file to minimize real-time keyboard input. Output includes the state of the vehicle, orbital and guide parameters, events and total velocity changes, and usage of propellant. The main output is to the print file defined by the user, but during execution, part of the input and output is also displayed on the screen. The code is double precision.

IMP is written in FORTRAN 77 for DEC VAX-series computers running VMS. The main memory requirement is 250K. An executable code is provided. This package of software is available in DEC VAX BACK-

UP format on a 9-track 1,600-bit/in. (630-bit/cm) magnetic tape (standard distribution medium) or on a TK50 tape cartridge. Documentation is included on the tape. IMP was developed in 1991.

DEC, TK50, VAX, and VMS are trademarks of Digital Equipment Corp.

This program was written by V. A. Dauro of **Marshall Space Flight Center**. *For further information, Circle 6 on the TSP Request Card.*

Inquiries concerning rights for the commercial use of this invention should be addressed to the Patent Counsel, Marshall Space Flight Center [see page 20]. Refer to MFS-28606.

Mathematics and Information Sciences

Computer Code Generates Homotopic Grids

HOMAR generates grids by use of algebraic relations.

To solve numerically the partial differential equations that arise in problems in practically all disciplines of engineering and physics, it is necessary to generate appropriate grids. Currently, grids are formed by methods that involve solution of either other differential equations or algebraic equations. By nature, the methods that involve algebraic equations provide means for the rapid construction of grids in domains. Also, homotopic mappings are easily adaptable to algebraic grid-generating techniques. HOMAR is a computer code that uses a homotopic procedure to produce two-dimensional grids in cross-sectional planes, which grids are then stacked to produce quasi-three-dimensional grid systems for aerospace configurations. The program can produce grids for use in both Euler and Navier–Stokes computation of flows.

Prior to execution, HOMAR requires input that specifies the size and other aspects of the geometry of the grid, the locations of the nose and the tail in the case of a blended wing/body configuration, and radii of outer boundaries. The input geometry can either be supplied as a table of point coordinates that define successive cross sections of the body or be generated analytically within the program. Once the input geometry is specified, outer boundaries are defined for each cross section, and the code proceeds to bridge the gap between the inner and outer boundaries by use of a family of transition lines produced by homotopic mapping between the surfaces. Decision parameters or control values are also needed. Decision parameters activate or deactivate processes that determine some aspects of the final grid, and control values furnish various coefficients to control orthogonality and index values that define the specified portion of the grid.

HOMAR efficiently provides grids for complex configurations, making it possible to generate, view, and modify grids rapidly until a desirable grid is obtained. In addition, by providing for redistribution of the homotopy parameter based upon boundary-shape data, HOMAR alleviates the problem caused by the innate inability of an algebraic technique to limit both distortion of cells and propagation of boundary discontinuities. This code also produces nearly orthogonal nonintersecting grid lines while preserving smoothness.

HOMAR is written in FORTRAN 77 for UNIX-based computers. The main memory requirement is approximately 7 Mb for execution. The output of this program is used as input for PLOT3D (ARC-12777). HOMAR is available on a 0.25-in. (6.35-mm) streaming magnetic tape in UNIX TAR format. This program was developed in 1989.

UNIX is a registered trademark of AT&T Bell Laboratories.

This program was written by Anutosh Moitra of High Technology Corp. for **Langley Research Center**. *For further information, Circle 3 on the TSP Request Card.*

LAR-14756

Conservative Grid-Interface Algorithm for Computing Flows

The best features of structured- and unstructured-grid methods are combined.

Ames Research Center, Moffett Field, California

An algorithm for use in finite-volume computations of flows that are governed by the Navier–Stokes equations provides an improved specification of interfaces between adjacent computational grids and enforces the conservation of mass, momentum, and energy at the interfaces. This improvement is important because flows of practical interest often have complicated geometries. It is necessary to divide complicated flow regions into zones of simpler shape, in which flows can be computed more efficiently by use of smaller, simpler zonal grids.

Typically, the grid in each zone is of a type called "structured," meaning that the points of intersection of the grid lines are a well-ordered array of points. Structured grids are preferred for the computation of flows in the zones because methods for the numerical solution of the Navier–Stokes equations on such grids are well developed. Grids of another type are called "unstructured," meaning that the points of intersection are specified arbitrarily. It is easier to generate unstructured grids than to generate structured grids about complicated bodies, but methods of numerical solution on such grids are not yet competitive with those for structured grids.

To compute an entire flow field, one must be able to transfer data across grid interfaces, where gaps and overlaps between the grids (see figure) can give rise to conservation errors. The algorithm combines the best of both structured- and unstructured-grid methods in providing for this transfer. The effects of overlaps and gaps between two zones are eliminated by use of an interfacial surface and grid defined by the union of all the grid points on the facing surfaces of both zones. The interfacial grid is, in effect, an unstructured grid, and the algorithm constructs it from the points by use of unstructured-grid triangulation techniques.

The interfacial cells of the adjacent grids are redefined to conform to the interfacial grid, thereby eliminating the gaps and overlaps. The area-normal vectors and volumes of the redefined interfacial cells are computed, and corresponding adjustments are made in fluxes of conserved quantities across the facets of the gridded interface. The flux across each facet from within each zone is computed by use of the same method of numerical solution as that used throughout the zone. This approach provides for global conservation via balancing of fluxes across the interface.

The algorithm has been incorporated into two three-dimensional Navier–Stokes finite-volume codes and tested in computations of incompressible and compressible flows about simple bodies. Good numerical results have been obtained. The algorithm is general enough that it can be incorporated into other finite-volume codes without restrictions on the complexities of shapes of bodies and zonal interfaces.

This work was done by G. H. Klopfer and G. A. Molvik of MCAT Institute for **Ames Research Center**. *For further information, Circle 59 on the TSP Request Card. ARC-13053*

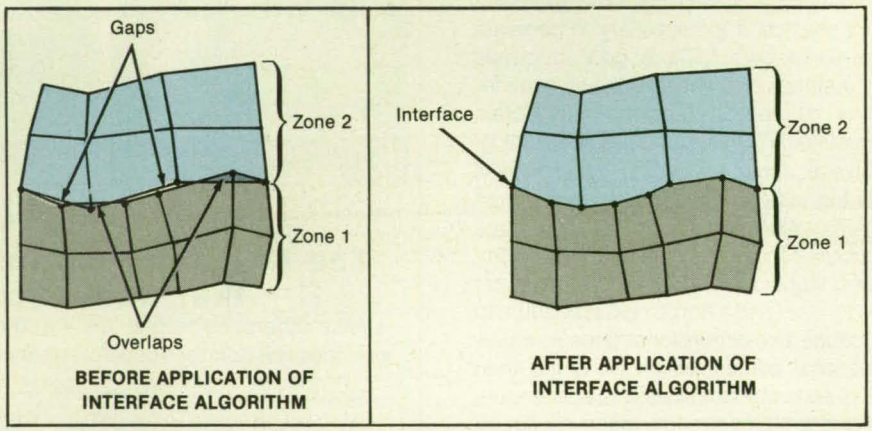

The **Gaps and Overlaps** between zonal grids are eliminated by the grid-interface algorithm, which generates a single interfacial grid and corrects the fluxes of flow quantities accordingly.

Splined Ball-Bearing Carrier

The spline provides a constant deadband and means to establish the desired radial stiffness.

Marshall Space Flight Center, Alabama

A ball-bearing carrier includes a splined outer surface that mates with the slightly larger splined inner surface of a housing and thereby provides a constant deadband, unaffected by movements of other components. The deadband — the gap between the bearing carrier and the housing — is needed to establish the radial spring rate (stiffness) and to provide for axial movement of the bearing for thrust balance. The bearing carrier and bearing are intended for use in a high-pressure turbopump.

Previous bearing-support schemes provided for control of radial deflections between bearings and support housings. The present scheme provides for fixed positioning of a bearing by means that depend only on initial parameters of the bearing-and-housing configuration and are independent of operational movement, caused by thermally or mechanically induced loads, of the bearing-support housing.

With the splines, there is no need to control the slope of the bearing-support housing at the surface of contact with the carrier. The splines restrain the carrier rotationally without such additional antirotation features as shear pins. The radial stiffness of the bearing support can be controlled by altering the spline geometry. The outer race of the bearing is inserted with a tight radial fit into the bearing carrier (see figure).

The radial clearances between the circumferential surfaces of (1) the spline on the carrier and (2) the mating spline slot

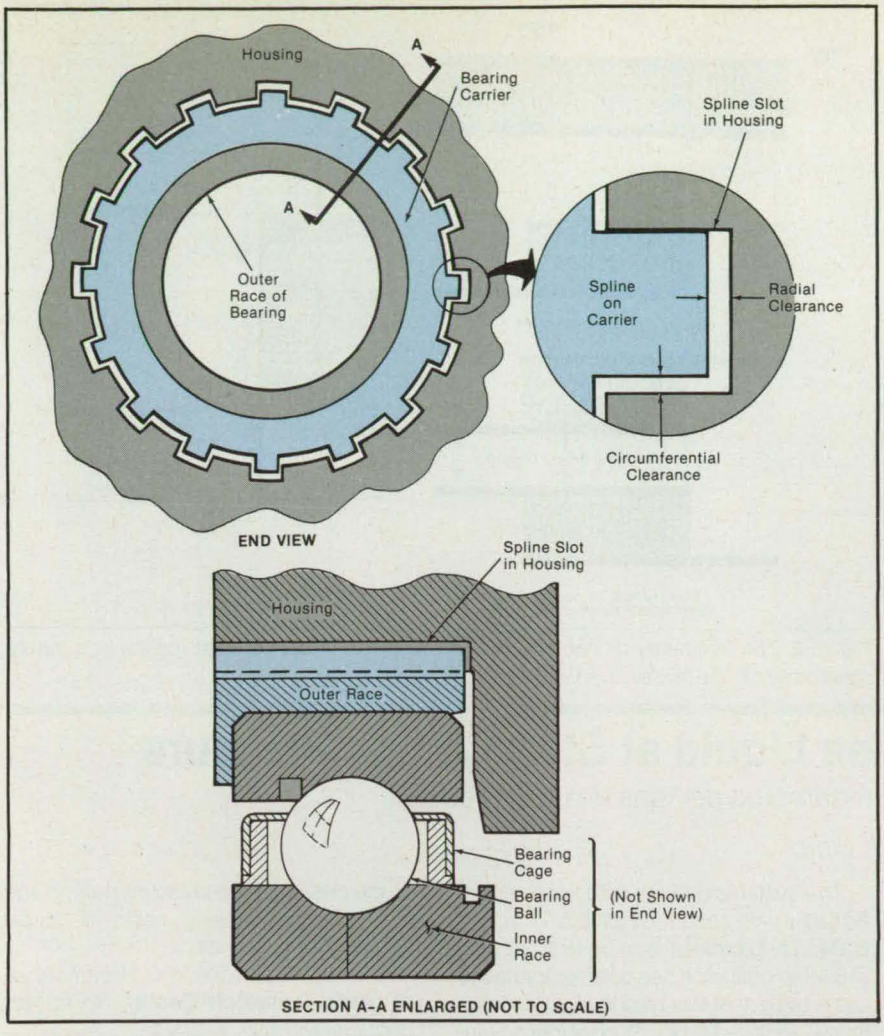

The **Splined Bearing Carrier** provides radial and axial gaps that can be chosen to obtain the desired radial stiffness and other characteristics.

in the housing are larger than the circumferential clearances between the radial surfaces of the carrier and housing splines. This allows radial movement of the carrier until the splines located 90° from the radial direction of movement make contact at the limit of their circumferential clearances. This range of movement is equivalent to the deadband in a conventional bearing support.

Axial movement in the spline is restrained only by friction from contact loading. The radial gap can be increased to create additional cross-sectional area for axial flow of the pumped fluid, so that flow through the bearing is decreased. This reduces the pressure on the bearing cage. Any radial movement of the bearing-support housing results in radial sliding of the housing relative to the carrier but does not impose any radial deflection or slope upon the carrier. The radial stiffness between the rotor and the housing can be chosen by selection of the deadband and the number and width (and, thereby, the stiffness) of the spline tangs.

This work was done by Jerry H. Moore of United Technologies Corp. for **Marshall Space Flight Center**. *No further documentation is available.*

Inquiries concerning rights for the commercial use of this invention should be addressed to the Patent Counsel, Marshall Space Flight Center [see page 20]. Refer to MFS-28629.

Double-Lap Shear Test for Honeycomb Core

Smaller specimens can be tested without spurious tensile or compressive loads.

Marshall Space Flight Center, Alabama

A double-lap test measures the shear strength of a panel made of honeycomb core with 8-ply carbon-fiber/epoxy face sheets. This double-lap shear test was developed to overcome three principal disadvantages of a prior standard single-lap shear test; namely, that (1) the specimen had to be more than 17 in. (43.2 cm) long, (2) metal face sheets (rather than the fiber/epoxy face sheets with which the panel would normally be fabricated) had to be used, and (3) the test introduced torque, with consequent bending and peeling of the face sheets and spurious tensile or compressive loading of the honeycomb (see Figure 1).

The double-lap shear test requires a specimen 13 in. (33.0 cm) long. Thus, it saves material and can be performed on a smaller testing machine. The double-lap shear test can be performed with the carbon-fiber/epoxy face sheets; this is particularly important when there is a need to perform an impact-damage test on one of the face sheets prior to the shear test. The symmetry of the double-lap configuration eliminates the torque and, with it, the spurious bending, peeling, and tensile or compressive loads.

Figure 2 illustrates the preparation of the specimen and the clamping of the specimen in the double-lap shear-testing fixture. Two sections of panel are fabricated in the usual manner except that by use of release films and incisions, portions are cut away to make single-lap shear specimens. The single-lap specimens are then bonded back-to-back to make a double-lap specimen. The double-lap specimen is mounted in a custom-made fixture that enforces the symmetry of the double-lap configuration: the core portion of the specimen is held

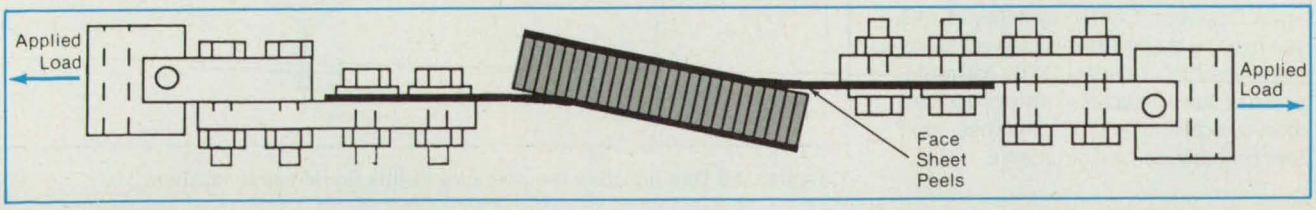

Figure 1. The **Single-Lap Shear Test** caused bending and peeling of face sheets and imposed spurious tensile loads on the core.

loosely between two plates that prevent lateral movement, and the face sheets are clamped tightly at the ends, where a tensile load is applied.

The double-lap shear test has three disadvantages:

1. The fabrication of specimens takes more time than it does in the prior standard single-lap shear test.
2. It takes more time to load specimens into the test fixture.
3. A new fixture has to be built to accommodate any change in the thickness of the core or of the face sheet.

This work was done by Alan T. Nettles and Andrew J. Hodge of **Marshall Space Flight Center**. *For further information, Circle 64 on the TSP Request Card.*

Inquiries concerning rights for the commercial use of this invention should be addressed to the Patent Counsel, Marshall Space Flight Center [see page 20]. Refer to MFS-28553.

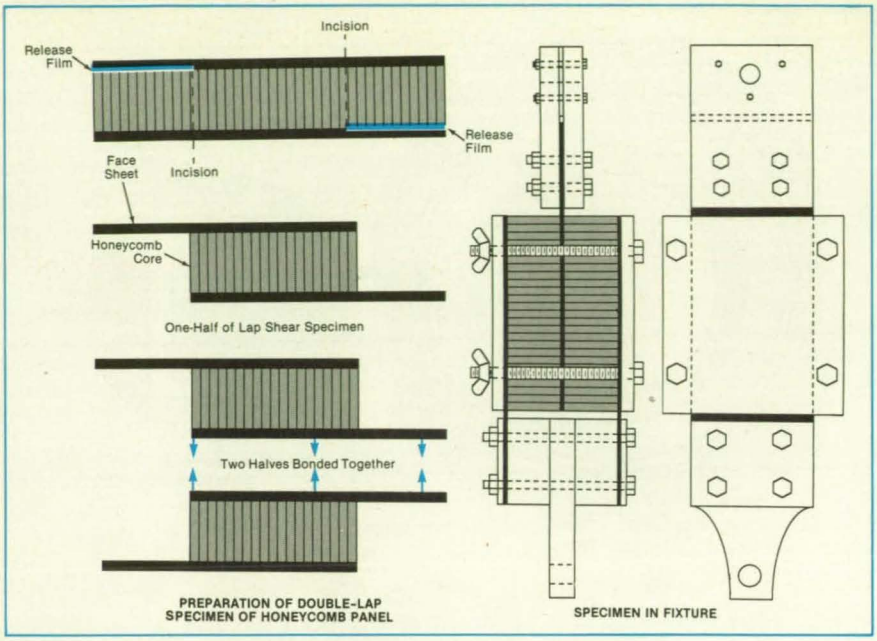

Figure 2. The **Symmetry of the Double-Lap Shear** specimen and test results in a purely shear load on the honeycomb core.

Cheap System Supplies Liquid at Steady High Pressure

High-pressure pumps and pulsation-damping devices are not needed.

Lewis Research Center, Cleveland, Ohio

Systems that supply liquid at high pressure that is free of pulsations have been in use at Lewis Research Center for some time. A system of this type (see figure) includes a tank of suitable pressure rating and capacity for the purpose at hand. The tank is filled with the desired liquid and pressurized with an inert gas to the level required. A dip tube extends down through the upper end of the tank to a point a few inches above the bottom of the tank. The external end of the dip tube is connected to the piping system designed for the desired use.

The pressure in the system is controlled by a regulator valve suitable for the pressurizing gas. Nitrogen has been used in all cases to date because it is readily available, either in bottles or in pressure systems installed in buildings.

The tanks have been made from stainless-steel pipes of suitable schedules fitted with end caps. In all cases, water has been the pressurized liquid and the systems have been filled manually to prevent backflow into the water supply. In one system, a remote refill was accomplished by depressurizing and filling the tank at atmospheric pressure, then repressurizing. At Lewis Research Center, systems of this type have been used for inducing vibrations in propellers in wind-tunnel tests, for visualization of flows of gases in tests of vertical/short-takeoff-and-landing airplanes, and flow calibrations of instruments.

The systems used to date have included tanks with capacities of 4 to 17 gal (15 to 64 L) and pressures of up to 1,100 psig (7.6 MPa, gauge). It has been proposed to use a system of this type to inject alcohol in fuel-additive tests. The principal advantage of systems of this type is elimination of the costs of high-pressure pumps and of the accompanying costs of pulsation-damping devices.

This work was done by C. Robert Morse of **Lewis Research Center**. *No further documentation is available.*
LEW-15189

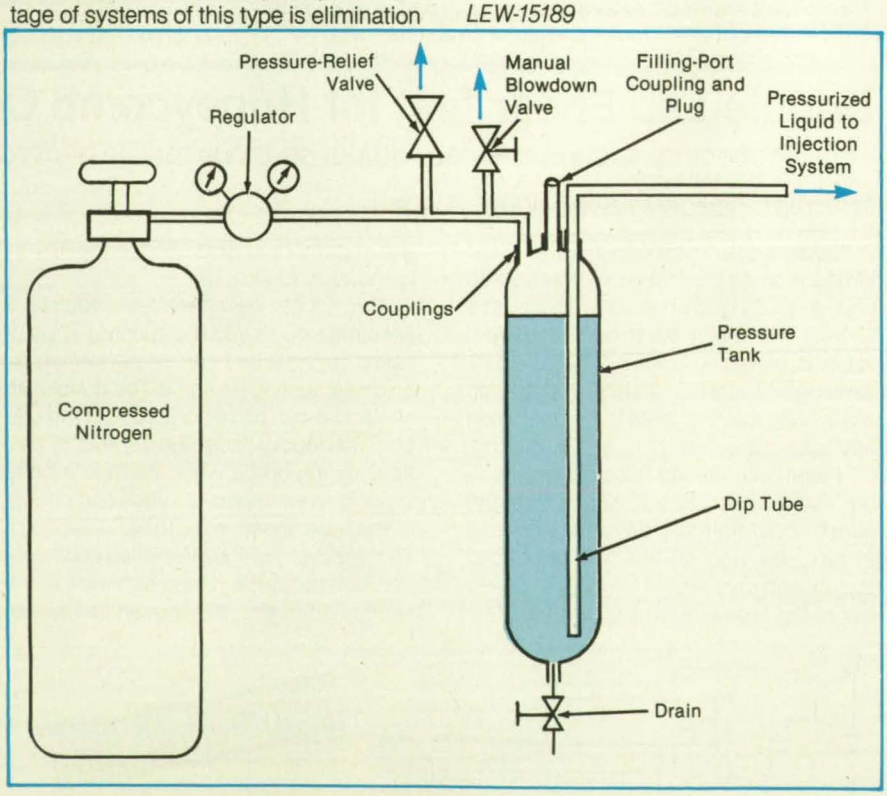

Compressed Gas provides the pressure in this liquid-supply system.

Face-Sealing Butterfly Valve

The valve plate would be made to translate as well as rotate.

Marshall Space Flight Center, Alabama

The figure illustrates a proposed butterfly valve in which a valve plate would rest against a face seal when in the closed position. The valve would be actuated by a shaft that would extend through the valve body. To open the valve, the shaft would rotate clockwise (as viewed in the lower part of the figure). This action would rotate a lever, relieving the force of a spring on the valve plate, and would translate and rotate the plate in such a way that in further clockwise rotation, it could clear the face seal.

When the shaft and lever had been rotated clockwise through 17° from the closed position, a stop on the shaft would engage the plate, so that further clockwise rotation of the shaft would cause an accompanying rotation of the plate toward the open position. To close the valve, the shaft would be rotated counterclockwise, simply reversing the opening movements.

This work was done by John N. Tervo of Allied-Signal Aerospace Company for **Marshall Space Flight Center**. *No further documentation is available.*

Inquiries concerning rights for the commercial use of this invention should be addressed to the Patent Counsel, Marshall Space Flight Center [see page 20]. Refer to MFS-28748.

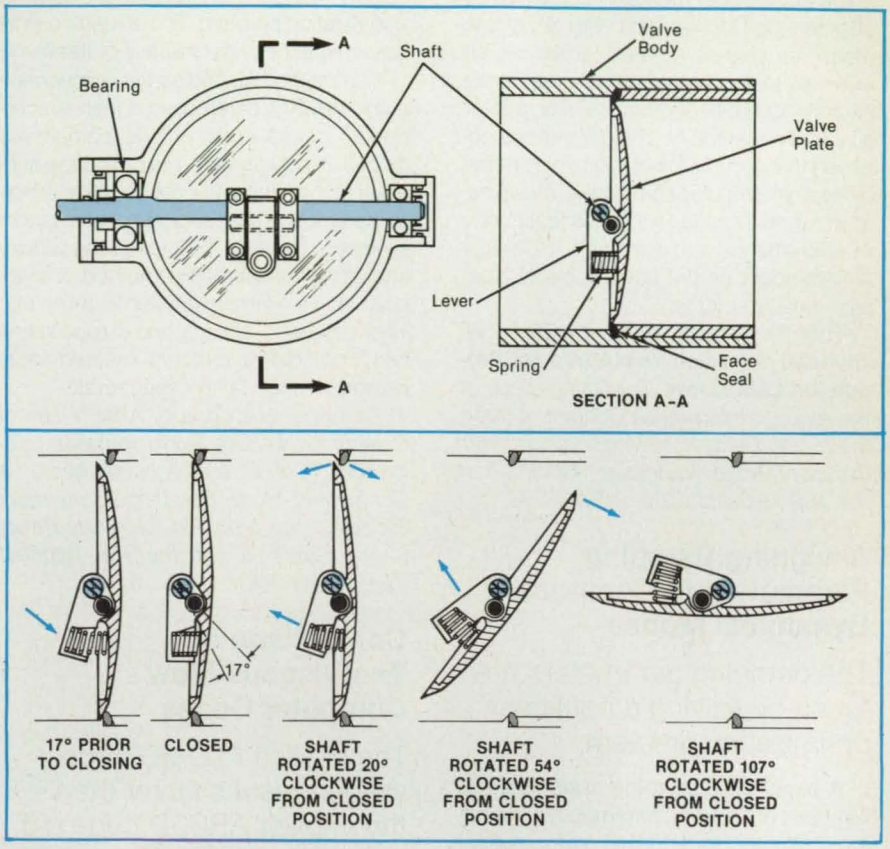

The **Valve Would Be Opened and Closed** by turning the shaft and lever. The interactions among the lever, spring, valve plate, and face seal would cause the plate to undergo a combination of translation and rotation so that the valve plate would clear the seal during parts of the opening and closing motions.

Books and Reports

These reports, studies, handbooks are available from NASA as Technical Support Packages (TSP's) when a Request Card number is cited; otherwise they are available from the National Technical Information Service.

Computing Orbits Around Planets From Differential Doppler Data

The information content of delay-rate measurements of different kinds are analyzed.

A report presents an analysis of the information content of interferometric measurements of rates of change of propagation delay ("delay rates" for short) of radio signals transmitted to and from a spacecraft in orbit around a distant planet. "Information content" as used here can be defined, somewhat loosely, as the contribution of a given measurement or series of measurements to accurate knowledge of the orbit.

The measurements are characterized as "interferometric" or as "differenced Doppler" because they involve differences between times of arrival measured at two widely separated stations on Earth. The types of measurements discussed in the report are (1) differenced one-way Doppler (DOD), in which signals are transmitted by the spacecraft (only) and the difference between the Doppler signals received at the two stations is computed; (2) two-way minus three-way Doppler (2DM3D), in which one Earth station transmits a signal to the spacecraft, which rebroadcasts the signals back to both Earth stations, which then observe the rebroadcast signal by use of the DOD technique; and (3) delta-differenced one-way Doppler (ΔDOD) in which the difference between the times of reception of the one-way signal from the spacecraft and an extra-galactic radio source (quasar) at the two Earth stations is determined.

Of the three methods, ΔDOD is the most complicated and the most accurate. The ΔDOD measurement is accomplished by computation of the difference between two nearly simultaneous DOD measurements: one from the spacecraft, and another from a quasar or other extra-galactic source in the angular vicinity of the spacecraft. This "double-differencing" eliminates the effects of offsets between the clocks at the two Earth stations and greatly reduces the sensitivity of the measurements to errors in the presumed locations of the stations — errors that are sometimes significant in DOD and 2DM3D measurements.

The analysis is directed toward showing how the information content of delay-rate measurements varies with the details of the geometric relationships among the Earth, the two Earth stations, the remote planet, and the orbit of the spacecraft around the planet. The analysis is applicable to DOD, 2DM3D, and ΔDOD, but the focus is on ΔDOD.

An approximate analytic model for delay-rate measurements as functions of classical orbital elements is developed. The resulting expressions are used to show how the information content of the DOD, 2DM3D, and ΔDOD data varies with the size, shape, and orientation of the orbit.

Comparison is made with the information content of Doppler-shift data alone, using sets of orbital elements derived from the Magellan and Mars Observer missions. Results indicate that improvements in the accuracy of navigation obtained by augmenting Doppler data with delay-rate measurements are greatest for spacecraft in low-altitude circular orbits but decrease steadily for orbits of progressively greater size and eccentricity. The differences between the accuracies of orbits computed by use of Doppler-shift (only) measurements and Doppler-shift plus delay-rate measurements were also found to be highly dependent on the accuracies of Doppler measurements.

This work was done by Sam W. Thurman of Caltech for **NASA's Jet Propulsion Laboratory**. *To obtain a copy of the report, "Information Content of Interferometric Delay-Rate Measurements for Planetary Orbiter Navigation," Circle 47 on the TSP Request Card. NPO-18283*

Assigning Damping Parameters to Component Dynamical Modes

The damping parameters are found by solving a nonlinear optimization problem.

A paper discusses the assignment of matrices of damping parameters ("damping matrices," for short) to mathematical models of the vibrations and rotations of the interconnected flexible components of a large, flexible structure. Typically, such models are truncated at the component level to reduce the amount of computation necessary to simulate the dynamics of the structure numerically at both the component and system (overall structure) levels.

Truncation consists of the selection of a limited number of vibrational and coupled vibrational/rotational modes that capture the salient features of the dynamics of each component. Heretofore, it has been common practice to represent damping, after transformation to modal coordinates, by assuming simplified, conservative estimates of component and system damping matrices. In this study, the problem is to choose more-accurate component damping matrices systematically so that when the truncated mathematical models of the components are combined into a mathematical model of the structure, the resulting damping matrix of the structure is close to the damping matrix that would be obtained by analyzing the dynamics of the structure in all its complexity at the system level.

To begin to address this problem, equations that express the relationship between the modal damping matrix of the system and the modal damping matrices of the components are derived from first principles. It is shown that component-mode damping parameters that most nearly satisfy these equations can be obtained by solving a constrained or unconstrained optimization problem. The solution can be obtained either algebraically or iteratively.

This method for finding the component-mode damping parameters is then specialized to cases in which the component modes are obtained by the projection-and-assembly method. (It could also be adapted easily to the balanced-component-mode-synthesis method.) To illustrate the validity and effectiveness of this method, it is applied to five example problems: three that involve masses, springs, and dampers; and two that involve different mathematical models of the Galileo spacecraft.

This work was done by Allan Y. Lee of Caltech for **NASA's Jet Propulsion Laboratory**. *To obtain a copy of the report, "A Component Mode Damping Assignment Technique for Multi-Flexible-Body Structures," Circle 11 on the TSP Request Card. NPO-18401*

Comparison of Two Viscous-Flow Computer Codes

The explicit FLOMG code yielded results faster than the implicit ARC2D code did.

Two viscous-flow computer codes were compared by applying them to five test cases of steady-state transonic viscous flows about transonic airfoils, in a study described in a NASA Technical memorandum. The two codes were (1) FLOMG, which solves the Navier–Stokes differential equations of flow by implementing an explicit, Runge–Kutta (with respect to integration in time), finite-volume, multigrid numerical-integration algorithm and (2) ARC2D, which implements an implicit, finite-difference, approximate-factorization, eigenvector-diagonalization numerical-integration algorithm.

The Navier–Stokes equations in two dimensions were first put in nondimensional, strong-conservation-law form, then transformed to curvilinear two-dimensional curvilinear coordinates fitted to the surfaces of the airfoils. The thin-layer approximation was applied to flows near the surfaces, and an algebraic mixing-length model of turbulence was incorporated. The resulting mathematical model was incorporated into the two computer codes. Because the results of computations can depend on various features of the computational grids and because it was desired to provide the most controlled test of the two codes, the same sets of grids (three for each airfoil) were used in both codes.

Both codes were found to produce essentially the same results. ARC2D required 5 to 10 minutes of central-processing-unit time for each case, whereas FLOMG required only about 1 minute. Computed pressure coefficients were found to be nearly identical, except in some cases near shocks, where differences are attributable to differences between the coefficients of artificial dissipation used in the two codes to suppress unphysical numerical oscillations. The results of the computations agreed well with data from experiments, except for the locations of shocks in flows characterized by large separation zones. The two codes were also found to predict similar skin-friction coefficients, boundary-layer profiles, and displacement thicknesses, and these quantities were found to agree satisfactorily with data from experiments where grids were spaced finely enough near the airfoil surfaces.

Lift coefficients calculated by the two codes were found to be generally within 1 percent of each other, and drag coefficients within 5 percent. For attached flows, both codes predicted lifts within 5 percent of the experimental values, and drags within 10 percent. This accuracy was not found for flows with separation, for which deficiencies in the model of turbulence were found.

This work was done by of C. M. Maksymiuk and T. H. Pulliam of **Ames Research Center** *and R. C. Swanson of Langley Research Center. Further information may be found in NASA TM-102815 [N90-27654], "A Comparison of Two Central Difference Schemes for Solving the Navier–Stokes Equations."*

Copies may be purchased [prepayment required] from the National Technical Information Service, Springfield, Virginia 22161, Telephone No. (703) 487-4650. Rush orders may be placed for an extra fee by calling (800) 336-4700. ARC-12958

Tests of Shear-Flow Model for Acoustic Impedance

Tests were generally successful for both upstream and downstream propagations.

A need for more-efficient acoustic treatments in the ducts of aircraft engines has prompted an abundance of research directed toward understanding the fundamental mechanisms of attenuation of sound in ducts that carry high subsonic flows and multiple high-order acoustic modes. One critical input for all duct propagation models is the liner impedance boundary condition. The desired impedance must be incorporated into a struc-

ture that does not compromise the safety or aerodynamic performance of an operating aircraft. The effective impedance of a duct liner beneath a boundary layer usually depends on both the intrinsic impedance of the liner and its interaction with the local aeroacoustic environment. Thus, in view of the desirability of an optimal design, the improvement of impedance-predicting mathematical models and the application of these to measurement techniques continue to be important.

Tests described in the report were conducted to validate a two-dimensional shear-flow analytical model for determination of the acoustic impedance of an acoustic liner in a grazing-incidence, grazing-flow environment by use of the infinite-waveguide method. The specimen consisted of a rigid matrix of narrow circular channels, each acoustically isolated from the others. This particular structure was chosen to minimize grazing-flow effects so that the analytical model could be expected to produce results nearly the same as those of normal-incidence impedance measurements. The analytical model was exercised by use of three flow profiles in three submodels, each of a different level of complexity: a uniform- (or "plug")-flow submodel, a one-dimensional shear-flow submodel, and a two-dimensional shear-flow submodel.

Impedances for both downstream and upstream propagation of sound generally agreed well with the normal-incidence impedances for all three flow-profile submodels. Consistency of the results suggests that, if due consideration is given to the effects of variability in the measured propagation parameter, then the analytical model can be relied upon to infer changes in the impedance of the specimen when significant two-dimensional-flow effects are involved.

An analysis of the sensitivity of the mathematical model revealed a wide-ranging sensitivity of the grazing-incidence impedance to relatively small changes in the absolute slopes of the axial attenuation and phase profiles over the range of test frequencies. The greatest sensitivity was associated with those frequencies near the antiresonance of the channels of the specimen. Most of the variability in the propagation parameter was attributed to the technique for extracting components of the propagation parameter from the measured attenuation and phase profiles.

This experimental validation of predictions of a finite-element numerical model for determining acoustic impedances in lined ducts is a technically significant contribution to understanding the problem and the numerical model. This work has clear potential for utility in the testing of engine ducts in commercial aircraft.

This work was done by Tony L. Parrot and Willie R. Watson of **Langley Research Center** *and Michael G. Jones of PRC Kentron, Inc. Further information may be found in NASA TP-2679 [N87-20798], "Experimental Validation of a Two-Dimensional Shear-Flow Model for Determining Acoustic Impedance."*

Copies may be purchased [prepayment required] from the National Technical Information Service, Springfield, Virginia 22161, Telephone No. (703) 487-4650. Rush orders may be placed for an extra fee by calling (800) 336-4700.
LAR-14310

Designing Composite Structural Components

Simplified step-by-step procedures for design are presented.

A report summarizes procedures for the design of structural components made of fiber/matrix (e.g., graphite/epoxy) composite materials and of joints between such components. A summary is presented by way of example design cases, using typical numerical values and showing typical results. A simplified form of the applicable step-by-step design procedure, suitable for a preliminary design, is presented for each case. References to detailed descriptions in the literature are provided.

The examples are a rectangular composite panel subjected to combined in-plane loads; a composite tapered, cantilever, multiple-bay box beam subjected to torque and force loads at its free end; bolted joints; and adhesive joints. Factors considered in the analysis of each design include strengths, displacements, portions of loads borne by the matrices and fibers of various subcomponent plies under various loading conditions, shear buckling, and safety factors. In the case of bolted joints, there is additional focus on modes of failure and distributions of stresses. Loads include both static and cyclic components. Hygrothermal effects and residual stresses in laminates are taken into account.

This work was done by P. L. N. Murthy and C. C. Chamis of **Lewis Research Center**. *Further information may be found in NASA TM-103113 [N90-24384], "Simplified Design Procedures for Fiber Composite Structural Components/Joints."*

Copies may be purchased [prepayment required] from the National Technical Information Service, Springfield, Virginia 22161, Telephone No. (703) 487-4650. Rush orders may be placed for an extra fee by calling (800) 336-4700.
LEW-15191

Origin and Behavior of Asymmetric Vortices

Features of flow about an ogive/cylinder are analyzed

A report presents a theoretical study of the vortices shed by an ogive/cylinder body of revolution that faces an oncoming flow at various angles of attack. This study focuses attention on two phenomena that have been observed in prior computer numerical simulations of such flows: (1) mean flow that is asymmetrical, at a moderate to high angle of attack, about the plane that contains the angle of attack and (2) fluctuations at higher angles of attack.

A major part of this study is directed toward providing a theoretical basis for a hypothesis, advanced in a previous study, that these phenomena are explained by instabilities of two kinds: absolute and convective. According to this hypothesis, where an absolute instability is indicated, those fluctuations of a flow that are triggered by a brief excitation persist and continue to grow to an equilibrium fluctuating state, even after the excitation is removed. If a convective instability is indicated, then those initially growing fluctuations that are triggered by a brief excitation are washed downstream, and, in the absence of further excitation, the flow returns to its original unperturbed state.

The result of prior numerical simulations and related experiments are analyzed from the perspective of applicable theories concerning mechanisms and mathematical models of instabilities and are found to confirm the hypothesis. The analysis leads to the following principal conclusions:

- At moderate angles of attack at which the nose influences flow over the entire body, the observed asymmetric mean flow is the result of a convective instability of a flow that would be symmetric if it were not for a permanent asymmetric disturbance applied at the tip (e.g., a pin or a speck of dust sticking out to the right or left). At higher angles of attack at which the flow over the aft part of the body escapes the influence of the nose, the otherwise original nominally steady, symmetric flow is also absolutely unstable in the presence of a temporary asymmetrical disturbance (e.g., a pin stuck out momentarily to the right or left, then retracted). Once the absolute instability has been triggered, the shedding of both parallel and oblique vortices occurs. The fluctuations involved in the shedding of these vortices may occur about a symmetric mean flow in the absence of a fixed asymmetrically disposed disturbance, or about the asymmetric mean flow that results from the convective instability triggered by a fixed disturbance at the tip.
- The experimentally confirmed existence of bistable states, in which variation of the side force with the angle of roll about the axis of nominal symmetry of the body approaches a square-wave distribution, is attributable to the dominant influence of a pair of vortices that trail from the ogival forebody. The formation of these vortices and the virtual freedom of these vortices from the influence of the shape of the nose is made possible by the appearance, beyond a critical value of the angle of attack, of foci of separation in the skin-friction-line pattern.
- At low to moderate angles of incidence, the experimentally demonstrated extreme sensitivity of the orientation of the asymmetric flow to the shape of the nose is attributable, in theory, to an indeterminate phase in the family of possible solutions for the equations of a system of the three-dimensional waves.

This work was done by Murray Tobak and Gregory G. Zilliz of **Ames Research Center** *and David Degani of Technion-Israel Institute of Technology. To obtain a copy of the report, "Analytical Study of the Origin and Behavior of Asymmetric Vortices," Circle 33 on the TSP Request Card. ARC-12818*

Propagation of Sound in Curved Ducts

Knowledge accumulated from 1878 through 1989 is reviewed and systematized.

A monograph presents a concise, comprehensive summary of the knowledge of propagation of acoustic waves in ducts and pipes that include bends. It pulls together information from Lord Rayleigh's book *Theory of Sound*, published in 1878, and from 33 papers scattered throughout various scientific journals published between 1945 and 1989. The monograph should prove useful to scientists and engineers interested in such diverse topics as musical instruments, air-conditioning ducts, and jet engines. This material is not available in current texts.

The significant contributions of each paper are reported in a form as close as possible to that of the original, and the comments and findings of its author(s) are cited carefully. Such details as mathematical derivations and experimental procedures are omitted, and readers are referred to the original works for such information.

The main part of the text begins with the basic differential equations of motion. It is easy to solve these equations on ducts with straight boundaries but difficult where boundaries are curved: consequently, a significant portion of the monograph discusses various approaches to analytical solutions with curved boundaries, with special attention to finding angular wave numbers for hard-wall and acoustically lined bends. (Angular wave numbers are eigenvalues of characteristic equations and orders of Bessel functions that appear in the solutions.)

There are chapters devoted to phase velocity, velocities of particles and distributions of pressures on hard-wall and acoustically lined bends, reflection and transmission, impedances and resonances, attenuation, and flow of acoustic energy. One chapter discusses bends equipped with turning vanes; this is an important topic because bends with long turning vanes along centerlines are effective as mufflers over large ranges of frequencies.

Although most of the monograph focuses on propagation in ducts of rectangular cross section, one chapter addresses propagation at bends in round pipes. There is a short chapter on propagation at a rounded corner, a chapter that summarizes the main acoustical characteristics of bends, and a brief chapter of concluding remarks.

This work was done by Wojciech Rostafinski of **Lewis Research Center**. *Further information may be found in NASA RP-1248 [N91-15848], "Monograph on Propagation of Sound Waves in Curved Ducts."*

Copies may be purchased [prepayment required] from the National Technical Information Service, Springfield, Virginia 22161, Telephone No. (703) 487-4650. Rush orders may be placed for an extra fee by calling (800) 336-4700. LEW-15396

Predicting Fractures in Fiber/Matrix Composites

Guidelines for qualification, inspection intervals, and retirement of components can be devised.

A NASA technical memorandum discusses the status of an emerging methodology of computational simulation of fractures in fiber/matrix composite structural components. Part of the methodology consists of step-by-step procedures to simulate fractures in individual and mixed modes in a variety of generic composite-material components. Another part of the methodology is embodied in the computer program CODSTRAN (Composite Durability Structural Analysis), which incorporates mathematical models of the mechanical properties of composites and of fracture mechanics. The authors assert that the methodology is ready for widespread application.

The document presents example problems and results as evidence for the contention that with careful selection of the mathematical models that pertain to the physical regimes at the various steps of a multistep simulation, one can simulate the entire history of a fracture process that, heretofore, could be learned only through experiment. In the first set of examples, a beam is notched at one end, simple edge supports are provided at both ends, and a concentrated force is applied at or near the middle. The simulation procedures and results are described for three different combinations of failure modes that occur under different loading conditions and configurations of composites.

The second set of examples involves laminated components in which initially small delaminations of various types grow under in-plane loading. The numerical results are interpreted as showing that local small delaminations have negligible effects on buckling loads. In the third set of examples, flaws in plate and shell structures grow under various loading conditions.

Following the examples, the document presents general remarks about the status of the methodology and the matters to be addressed in future research. Included in this presentation is a generalized step-by-step simulation procedure, which is paraphrased as follows:

1. Develop a global structural and stress-analysis mathematical model.
2. Apply specified loading conditions.
3. Identify concentrations of loads that occur under these loading conditions.
4. Introduce flaws at the points of concentration.

5. With specified loads on the global model, propagate flaws.
6. Monitor degradation in the performance of the structure (displacement, buckling loads, frequencies) versus propagation of the flaws.
7. Identify the sizes of flaws at which the degradation in performance becomes unacceptable.
8. Set criteria for initial qualification of the structure, inspection intervals, and retirement for cause on the basis of the degradation of performance as predicted via the simulated propagation of flaws.

This work was done by C. C. Chamis and P. L. N. Murthy of **Lewis Research Center**. *Further information may be found in NASA TM-102505 [N90-21821], "Computational Simulation of Structural Fracture in Fiber Composites."*

Copies may be purchased [prepayment required] from the National Technical Information Service, Springfield, Virginia 22161, Telephone No. (703) 487-4650. Rush orders may be placed for an extra fee by calling (800) 336-4700. LEW-15384

Stresses in a Cylinder Welded With Mismatch

Stresses are computed by use of finite-element and conventional theoretical methods.

A NASA technical memorandum presents a parametric study of the additional stresses that are introduced into a cylindrical pressure vessel that is round except for a radial mismatch in a longitudinal butt weld in the sidewall. The study was prompted by concern over fatigue caused by cyclic stresses in the longitudinally welded cylindrical titanium inlet of the high-pressure turbopump in the main engine of the Space Shuttle. However, the results appear to be applicable to any round cylindrical pressure vessel that can be characterized by the parameters, and that conform to the simplifying assumptions, used in the analysis.

The simplifying assumptions are the following: the cylinder is long, the radius is much greater than the thickness of the wall, and the weld bead is flush with the wall and has a radial thickness equal to that of the wall. Under these assumptions, the stresses in the vicinity of the mismatch can be approximated by the stresses in two flat plates welded similarly with a mismatch and loaded in tension along the axis perpendicular to the weld in the plane of the plates.

The parametric study is performed on this plate model and consists of two independent analyses. One is a finite-element analysis by means of the ANSYS computer program. The other is a theoretical analysis in which the weld bead is approximated as a rigid body attached to the two plates, and the stresses and strains in each plate are computed by use of the conventional equations for a simple cantilever beam/column that is (1) loaded in tension along its length and (2) loaded at its weld end by a torque that is approximately proportional to the tension and the degree of mismatch.

The contribution of the weld mismatch to the maximum total stress, σ_T, is expressed in terms of an offset stress-concentration factor, $K_{off} = \sigma_T/\sigma_0$, where σ_0 is the tensile stress in the absence of mismatch. Values of K_{off} are computed for various mismatches up to 0.6× the thickness of the wall and for various widths of the weld up to 4× the thickness. Values of K_{off} were also computed for Poisson's ratios of 0 and 0.3 and for a few cases in which the Young's modulus of the weld bead differed from that of the wall.

This work was done by J. B. Min, K. L. Spanyer, and R. M. Brunair of **Marshall Space Flight Center**. *Further information may be found in NASA TM-103534 [N91-23502], "Parametric Study in Weld Mismatch of Longitudinally Welded SSME HPFTP Inlet."*

Copies may be purchased [prepayment required] from the National Technical Information Service, Springfield, Virginia 22161, Telephone No. (703) 487-4650. Rush orders may be placed for an extra fee by calling (800) 336-4700.
MFS-27268

Roller Locking Brake

This electomagnetically releasable brake provides high locking torque.

Goddard Space Flight Center, Greenbelt, Maryland

The roller locking brake illustrated in the figure is a normally braking rotary mechanism that allows free rotation when an electromagnet in the mechanism is energized. The roller locking brake is well suited to robots and other machinery in which automatic braking upon removal of electrical power may be required. In comparison with prior normally braking mechanisms that sustain equal holding torque, the roller locking brake is more compact and reliable. In addition, it requires little electrical power to maintain free rotation and therefore exhibits minimal buildup of heat.

The rotation to be allowed or resisted is that of a shaft (not shown in the figure), which is attached via bolt holes to a drive disk in the brake mechanism. The drive disk rotates in a stationary housing, suspended in the housing by ball bearings. A ring in the housing called the roller-locking and -lifting ring ("locking ring" for short) is restrained against most rotation by six outwardly-projecting torque-reacting segments that engage bolts in the housing. (However, the locking ring is allowed to undergo small rotation against the stiffness of O-rings between it and the bolts, as part of an arrangement to prevent loads other than torques about the nominal axis of rotation from giving rise to braking action and to ensure that the brake will release on command.)

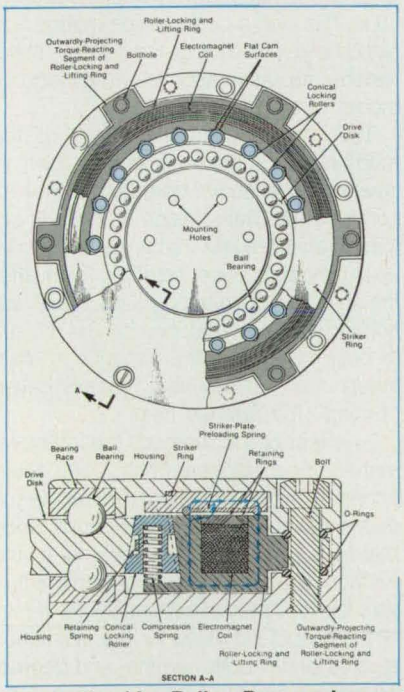

Conical Locking Rollers Become Jammed between the drive disk and the flat cam surfaces of the roller-locking and -lifting ring when any attempt is made to turn the drive disk, unless the electromagnet is energized.

Conical locking rollers are preloaded upward by compression springs against the conical outer rim of the drive disk and against angled flat cam surfaces in the locking ring. A retaining spring in slots in the rollers provides some additional radially outward preload against the flat cam surfaces. When the drive disk starts to rotate in either direction, each conical roller starts to roll up one of its flat cam surfaces and immediately becomes jammed between the cam surface and the outer rim of the drive ring. The angles of the cam surfaces are chosen so that the frictional torque attributable to the jamming force builds up more rapidly than the turning torque does. Thus, any further microrotation only jams the rollers more tightly, tending to stretch the locking ring, compress the drive disk, and flatten the conical locking rollers.

A striker ring above the locking ring is normally spring-loaded upward and plays no role during braking. The electromagnet coil lies in an annular groove in the locking ring, and it, too, plays no role during braking. When this coil is energized, it pulls the striker ring downward against the slightly protruding upper ends of the conical locking rollers, thereby pushing the rollers downward, out of engagement with the locking ring and drive disk. This action eliminates jamming, and the drive disk is then free to rotate.

Because the downward pull on the striker ring is not sufficient to overcome the frictional upward force from jamming when the brake is locked at high torque, a motor (not shown) is energized briefly to counteract the load torque and eliminate jamming immediately prior to release. Once the brake is released, the striker ring rests on top of the locking ring, so that the magnetic-flux path includes essentially zero air gap; consequently, little electromagnet current is required thereafter to maintain the unlocked mode.

This work was done by John M. Vranish of **Goddard Space Flight Center**. *For further information, Circle 58 on the TSP Request Card.*

This invention is owned by NASA, and a patent application has been filed. Inquiries concerning nonexclusive or exclusive license for its commercial development should be addressed to the Patent Counsel, Goddard Space Flight Center [see page 20]. Refer to GSC-13376.

Kalman-Filter Estimation of Unmeasured Output Variables

Systematic deviations of these variables are represented as bias state vectors.

Ames Research Center, Moffett Field, California

A Kalman-filter "observer" algorithm has been proposed for use in estimating unmeasured output variables (e.g., rates of flow) of a turbofan engine. The unmeasured output variables are needed along with the measured output variables as feedback data to characterize the state of the aircraft-and-engine system for control purposes. A subsystem or processor that implemented the proposed Kalman-filter algorithm would be incorporated into an adaptive digital control system, called a "performance-seeking" control system, that is being developed to compute engine-control settings to optimize the performance of the aircraft under given pseudo-steady-state cruise conditions (see figure). The basic concept of the algorithm is not restricted to the aircraft-engine application and could probably be extended to internal-combustion engines in land vehicles, for example.

The nominal state of the aircraft-and-engine system, as computed by the dynamical model used in the control computations, is represented by the vector **x**. Systematic deviations from the nominal state, caused by errors and uncertainties in the model and by degradation of the engine over time, are represented by the bias vector, **b**. A new augmented state vector, **z**, is defined by adjoining **b** to **x**.

Then the Kalman-filter estimate of the state of the system is governed by

$$\dot{\hat{\mathbf{z}}} = A_1\hat{\mathbf{z}} + B_1\mathbf{u} + PC_1^T R^{-1}[\mathbf{y} - C_1\hat{\mathbf{z}} - D\mathbf{u}]$$

where $\hat{\mathbf{z}}$ denotes the estimate of **z**; A_1, B_1, C_1, and D are system matrices in state-variable representation that are derived from corresponding matrices of the Kalman-filter equations of the dynamical model of the system; P is the matrix that represents the steady-state solution of an equation that involves the above-mentioned matrices, the state-noise-covariance matrix, and the measurement-noise-covariance matrix; **u** is the control input vector; and **y** is the output vector.

The auxiliary set of unmeasured output variables is represented by the vector $\mathbf{y}_{aux}$. Once **z** has been estimated by use of the Kalman filter, one can compute the estimate, $\mathbf{y}_{aux}$ of this vector from

$$\hat{\mathbf{y}}_{aux} = H\mathbf{z} + F\mathbf{u}$$

where H is a matrix that reflects the effects of estimated biases and of perturbations, F is also a perturbation matrix, and both H and F are computed from the state-variable representation of the dynamical model of the system.

The mathematical formalism of the Kalman filter is not sufficient, by itself, to develop an effective operational filter algorithm. The main design problem is obtaining an adequate mathematical model upon which to base the filter. Even after the selection of an appropriate model, the noise-covariance matrices can be difficult to determine. The determination is often made in a trial-and-error process called "tuning" the Kalman filter.

In a test of the method, the measurement-noise-covariance matrix was determined by analysis of flight data, while the elements of the state-noise-covariance matrix were determined by the tuning method. The resulting proposed algorithm was found to predict accurately the values of the output variables for the simulation studies under both nominal and degraded engine conditions.

This work was done by Glenn B. Gilyard of Dryden Flight Research Facility and Gurbux S. Alag of PRC System Service for **Ames Research Center**. *Further informa-*

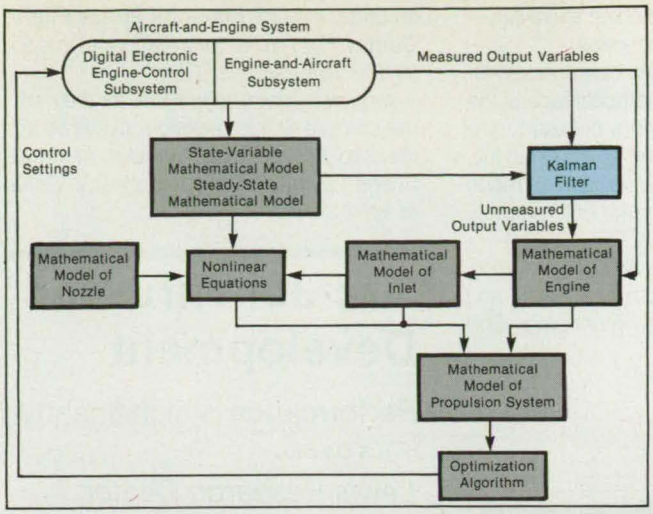

The **Proposed Kalman Filter** would estimate unmeasured output variables for use in computing control settings.

tion may be found in NASA TM-4234 [N91-19099], "A Proposed Kalman Filter Algorithm for Estimation of Unmeasured Output Variables of an F100 Turbofan Engine."

Copies may be purchased [prepayment required] from the National Technical Information Service, Springfield, Virginia 22161, Telephone No. (703) 487-4650. Rush orders may be placed for an extra fee by calling (800) 336-4700. ARC-12913

Linear Motor With Air Slide

The air cushion reduces friction and unwanted vibrations.

Marshall Space Flight Center, Alabama

An improved linear actuator comprises an air slide and a linear electric motor. In comparison with typical prior electromagnetic linear actuators, the improved unit exhibits low friction, low backlash, and more nearly even acceleration. Actuators like this one could be used in machinery in which positions, velocities, and accelerations must be carefully controlled and/or vibrations must be suppressed.

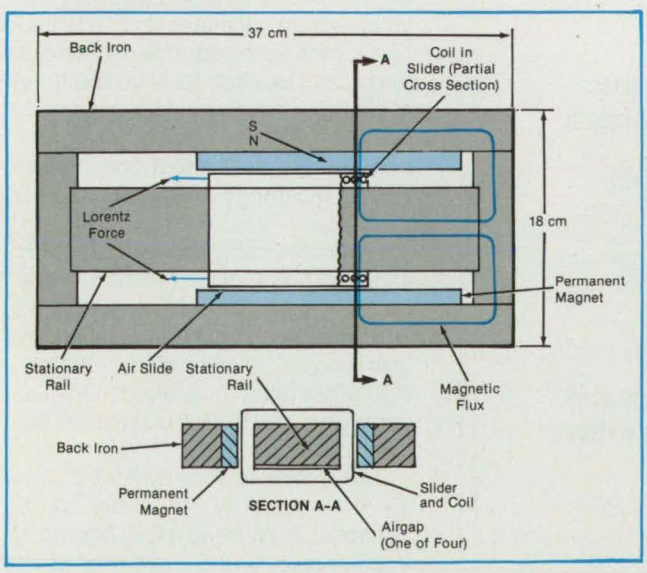

Current in the Coil on the Slider interacts with the flux from the permanent magnets to produce a Lorentz force. The force propels the slider on the rail while a film of compressed air separates the slider form the rail.

The actuator includes a stationary rail flanked by permanent magnets (see figure). The air slide, which rides the rail on a cushion of compressed air, contains an electromagnet coil. The electrical current in the coil interacts with the permanent magnetic field to generate a force that propels the slide along the rail. The current is adjusted to provide the requisite force.

Besides guiding the slider, the rail serves as part of the path for the magnetic flux. Four pieces of back iron complete the magnetic circuit by providing a low-reluctance return path for the flux.

The hose that supplies compressed air to the slider and the electrical leads to the coil on the slider are springy but exert minimal sliding friction. If even this minimal friction is objectionable, the coil can be made stationary, and the permanent magnets and back iron movable.

This work was done by Bruce G. Johnson, Michael J. Gerver, Timothy J. Hawkey, and Ralph C. Fenn of SatCon Technology Corporation, Inc., for **Marshall Space Flight Center**. *For further information, Circle 97 on the TSP Request Card.*

Inquiries concerning rights for the commercial use of this invention should be addressed to the Patent Counsel, Marshall Space Flight Center [see page 20]. Refer to MFS-26169.

Arc-Jet Thrustor Development

Performance is significantly improved.

Lewis Research Center, Cleveland, Ohio

Low-power (1–2 kW) arcjet systems provide average propellant-utilization efficiencies 1.5 to 2 times higher than those obtained with state-of-art chemical and resistojet systems. Use of arcjet systems for such functions as north–south stationkeeping of geosynchronous communications satellites can reduce propellant requirements by several hundred kilograms. This savings can, in turn, be used to reduce total launch mass, increase on-orbit lifetime, and/or increase payload.

Two flight-type 1.4-kW hydrazine arcjet systems were developed and tested under a Lewis program. Each of these systems consist of a thrustor, gas generator, and power-processing unit. In operation, liquid hydrazine is broken down to its decomposition products in the gas generator,and this gas mixture (H_2, N_2, and NH_3) is heated by an electrical arc that originates from a cathode tip near the upstream side of the nozzle throat and extends through the throat of attach in the diverging section of the nozzle. The exhaust is partially ionized and exits the nozzle at average velocities in the range of 4,500 to 5,500 km/s.

Environmental qualification, performance, and endurance tests have been performed on the flight-type systems, and an arcjet system integration test was successfully completed. Arcjet technology has been transferred to the user community, and the first commercial flight is anticipated in 1993.

This work was done by F. M. Curran, J. A. Hamley, R. P. Gruber, J. M. Sankovic, T. W. Haag, W. E. Marren, C. J. Sarmiento, and L. Carney of **Lewis Research Center**. *For further information, Circle 5 on the TSP Request Card.*

LEW-15284

Stirling Converters for Solar Power

Two designs are expected to meet long-term goals for performance and cost.

Lewis Research Center, Cleveland, Ohio

Two conceptual designs have been proposed for advanced systems to convert solar thermal power to electrical power. Each such system, designed to operate with an 11-m-diameter paraboloidal reflector, would include a solar-energy receiver, a liquid-metal heat-transport subsystem, a free-piston Stirling engine, a cooling subsystem, an alternator or generator coupled directly or indirectly to a commercial electric-power system, and control and power-conditioning circuitry. The system would convert the ~75 kW of input solar thermal power falling on the collector to about 25 kW of output electrical power at a cost of less than $450/kW (1984 prices).

In each design, the reflector would focus the solar power through an aperture of 203-mm diameter in the face of the receiver. In the system illustrated in Figure 1, the surface of the evaporator would be covered with a powdered-metal wick integrated with circumferential and radial arteries. Sodium was chosen as the liquid

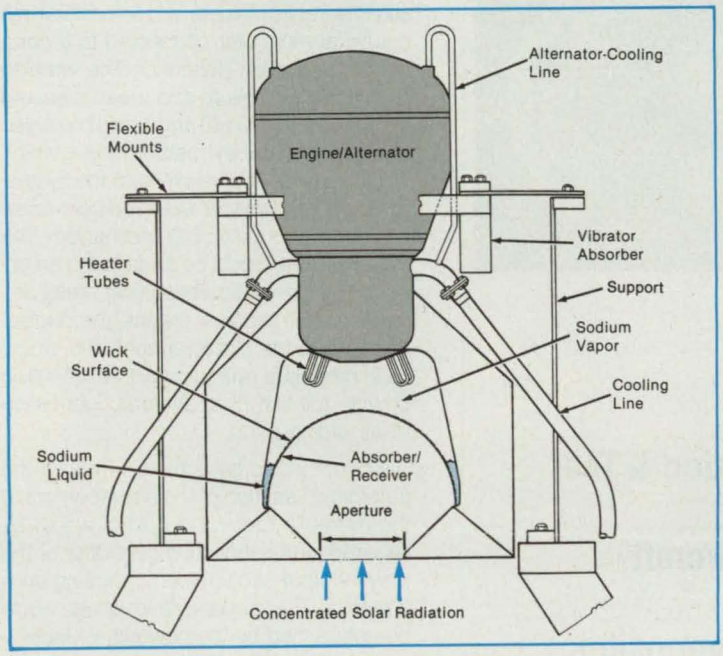

Figure 1. This **Solar-to-Electric Power-Conversion System** would include a heat-pipe solar receiver integrated with a free-piston Stirling engine connected to a linear alternator.

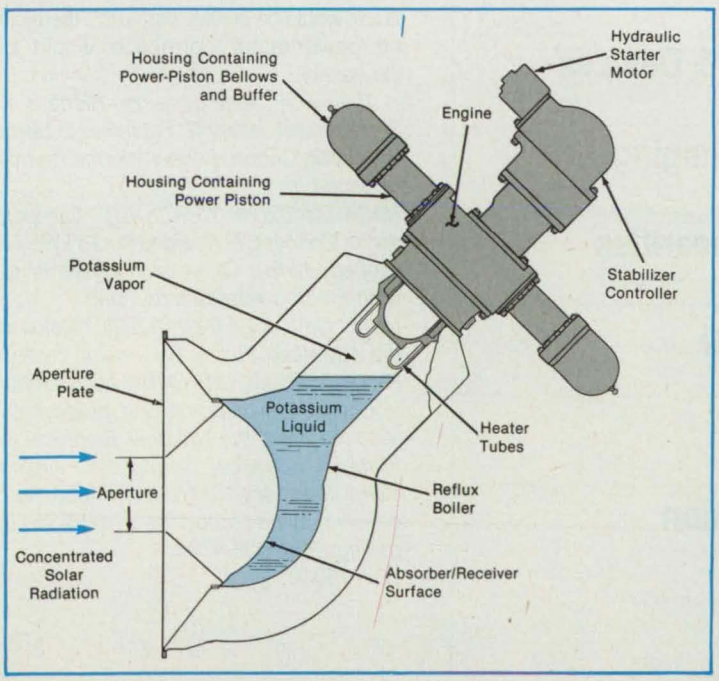

Figure 2. This **Solar-to-Electric Power-Conversion System** would include a reflux-boiler receiver integrated with a Stirling-engine hydraulic system that would drive a rotary induction generator.

metal. A heat-pipe cavity behind the absorber/evaporator surface is designed so that the condensed liquid would drain by gravity to the arteries at the base of the evaporator shell. The heat pipe should minimize local hotspots, thereby providing longer life for the Stirling heater-head tubes.

The single-cylinder Stirling engine would be integrated with a permanent-magnet linear alternator to convert the solar thermal energy to electricity directly. There would be only two moving parts: a displacer and a power piston. The heater head is designed to operate at a temperature of 700°C. The working fluid would be helium at a mean pressure of 10.5 MPa (1,520 psi).

The regenerator and cooler would have an annular configuration. Hydrodynamic gas bearings would allow the use of close-tolerance, noncontacting seals to eliminate wear. A spin motor would drive the power piston and displacer to create the hydrodynamic effect. The engine and the alternator would be contained in a hermetically sealed vessel.

The alternator would be connected to a series tuning capacitor and to the powerline through an autotransformer. The frequency and the output voltage of the autotransformer would be essentially constant and established by the powerline. The voltage at the alternator terminals would be adjusted to match the changes in power while keeping the temperature of the heater head at its design point.

In the system illustrated in Figure 2, the solar receiver would be a reflux boiler containing liquid and vapor potassium, which would be evaporated in a manner similar to that of a double boiler to provide uniform temperature at the Stirling heater-head tubes. The system would be configured so that the heater-head tubes would never be submerged in the potassium pool, regardless of the elevation angle of the reflector.

The free-piston Stirling/hydraulic engine would be hermetically sealed with metal bellows. The engine would deliver high-pressure hydraulic fluid to a commercial hydraulic pump/motor connected to a commercial induction generator. The working fluid would be helium at a mean pressure of 17.9 MPa (2,630 psi) and would be sealed into the displacer by metal bellows, which would separate the helium from the hydraulic fluid. The displacer would be connected hydraulically to a stabilizer mechanism. The power pistons would be arranged in an opposed-piston configuration with metal bellows seals. The power pistons, the displacer rod, and the stabilizer/controller would be immersed in hydraulic fluid, which would provide full film hydrodynamic lubrication of all sliding parts.

Control would be achieved through the automatic variation of the displacement of the hydraulic motor. No control would be required for the induction generator or the power-output circuit when operating on a powerline. The frequency and voltage would be established by the powerline. Under a majority of loading conditions, the power factor would be greater than 0.85; therefore, no power-factor correction would be necessary.

This work was done by Richard K. Shaltens and Jeffrey G. Schreiber of **Lewis Research Center**. *Further information may be found in:*

NASA TM-102085 [N89-26781], "Comparison of Conceptual Designs for 25 kWe Advanced Stirling Conversion Systems for Dish Electric Applications," and

NASA TM-104528 [N91-31023], "Status of the Advanced Stirling Conversion System Project for 25 kW Dish Stirling Applications."

Copies may be purchased [prepayment required] from the National Technical Information Service, Springfield, Virginia 22161, Telephone No. (703) 487-4650. Rush orders may be placed for an extra fee by calling (800) 336-4700.

LEW-15009

Books and Reports

These reports, studies, handbooks are available from NASA as Technical Support Packages (TSP's) when a Request Card number is cited; otherwise they are available from the National Technical Information Service.

Creating a Data Base for Design of an Impeller

An application of the Taguchi method of parametric design is described.

A report describes the use of the Taguchi method of parametric design to create a data base that facilitates optimization of the design of the impeller in a centrifugal pump. This data base enables a systematic design analysis that covers all significant design parameters. In comparison with other data bases that might be used, this one reduces the time and, thereby, the cost of parametric optimization of design: for the particular impeller considered, one can cover 4,374 designs by computational simulations of performance for only 18 cases.

In general, a data base of the type in question is intended to speed the design-optimization process by giving the designer information on the effects of changes in the input (independent) design parameters on the objective parameters (output or dependent design parameters, including characteristics of performance). The Taguchi method was chosen for this purpose because it reduces simulation time and eases the processing of the data after the simulations.

Eight input design parameters (e.g., the number of blades and the impeller-tip diameter) were chosen for the design-optimization data base. Two levels of one parameter (the number of blades) and three levels of each of the other parameters were chosen to lie within ranges shown by experience yet not to constrain the parameter space available for simulations. Having chosen the input design parameters, an L_{18} orthogonal array was chosen because such an array enables the completion of the data base in only 18 simulations and is designed for one two-level input parameter and seven three-level input parameters.

Eighteen objective parameters were identified as significant to the design and to optimization of the design. These include, for example, ratios between various components of velocities, the inlet blade angle, and stage efficiency. Because of the large number of objective parameters, design and analysis computer codes were modified and developed to ease the simulations and the postprocessing of data generated in the simulations.

The results of the simulation are presented in graphs — each a plot of one of the output parameters as a function of one of the design parameters. By use of these graphs, a design engineer can quickly optimize the design; the trades among the various objective parameters for each input design parameter can be identified readily, and each design parameter can be chosen to optimize each objective parameter without compromising the other objective parameters.

This work was done by George H. Prueger and Wei-Chung Chen of Rockwell International Corp. for **Marshall Space Flight Center**. *To obtain a copy of the report, "Impeller Design and Optimization Database," Circle 88 on the TSP Request Card.*

Inquiries concerning rights for the commercial use of this invention should be addressed to the Patent Counsel, Marshall Space Flight Center [see page 20]. Refer to MFS-29847.

Fabrication Technology

Cam-Action Scribing Tool

This tool scribes a constant-depth line in an out-of-round workpiece.

Marshall Space Flight Center, Alabama

A cam-action scribe designed for use on a lathe produces a continuous, constant-depth circumferential line on a nominally cylindrical workpiece, even when the workpiece is somewhat out of round. Conventionally, a circumferential line is scribed manually by use of a Johansson-block setup, or else machined on the lathe by use of a thin parting tool. Neither of these conventional techniques provides accurate control of the depth of the scribed line, and, in the lathe technique, the line on an out-of-round workpiece may not be continuous.

The cam-action scribe is mounted on the lathe in the same manner as that of a depth-of-cut indicator (see figure). The scribing point is set to the desired scribe-line depth below the wheel. The position of the tool along the axis of the lathe and the cylindrical workpiece is adjusted so that the scribing point lies at the desired axial position of the line to be scribed. The radial position of the tool is adjusted so that the wheel is spring-loaded against the workpiece. The lathe is then turned on, and, as the workpiece rotates, the wheel follows its circumference like a cam, allowing the scribing point to push against the surface until it extends its full preset depth into the workpiece.

This work was done by R. Michael Malinzak and Gary N. Booth of Rockwell International Corp. for **Marshall Space Flight Center**. *No further documentation is available.*
MFS-29851

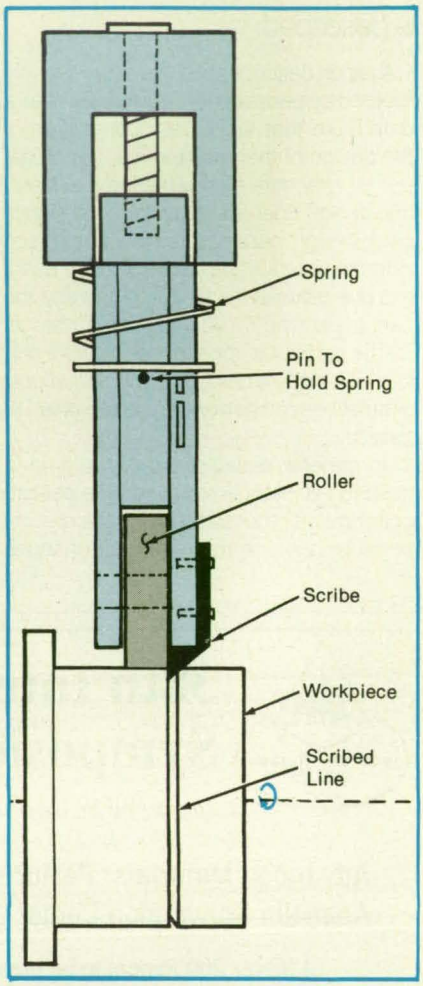

The **Wheel Rides on the Workpiece,** limiting the depth of penetration of the scribe to the preset value as the workpiece turns in a lathe.

Tool for Installation of Seal in Tube Fitting

A plierslike tool helps to secure a repair seal in a fitting.

Lyndon B. Johnson Space Center, Houston, Texas

A plierslike tool helps to install a cylindrical repair seal (Seal-Saver™ or equivalent) in a leaking (Dynatube™, Dual-Seal™, or equivalent) fitting. Previously, it was necessary to insert a repair seal by hand and to rely on a slight interference fit to hold it in place. Often, however, the repair seal fell from the tube fitting during further assembly operations because normal variations in dimensions prevented a tight fit. The tool crimps the repair seal into the tube fitting, ensuring a tight fit every time.

The tool (see figure) is a modified pair of snapring pliers, to which knife-edge jaws have been added. A spring is added between the handles. The tool also includes

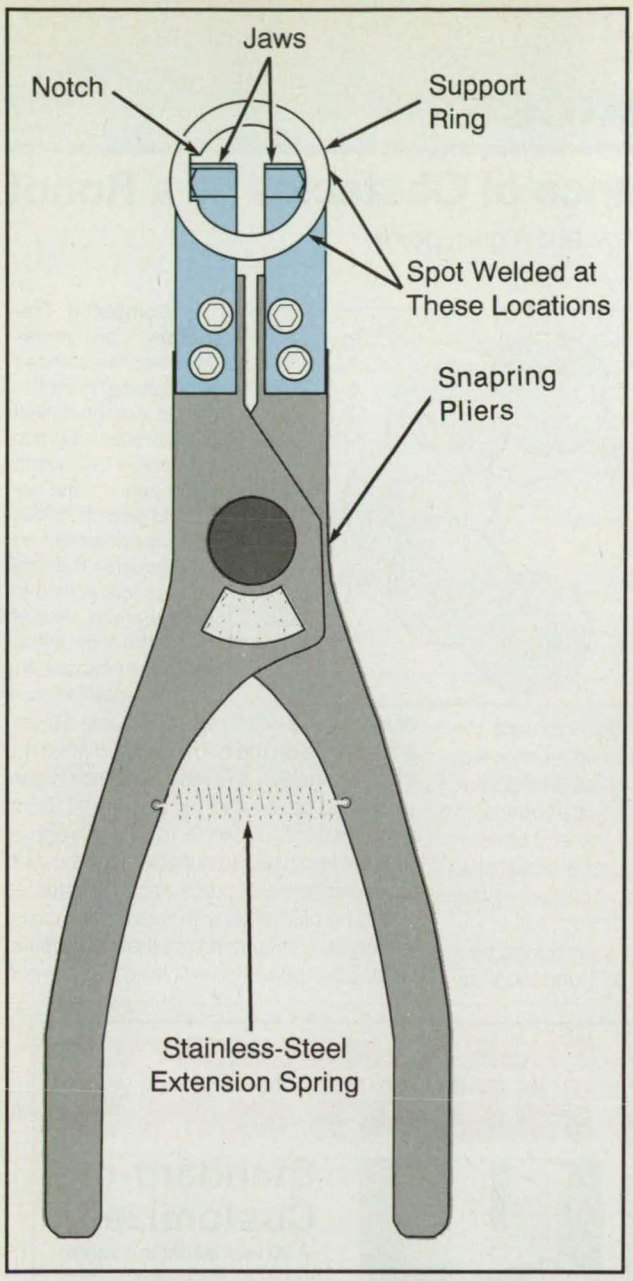

The **Pliers like Tool** includes crimping jaws. Prior to crimping, the jaws hold the support ring and a repair seal (not shown) that is placed on the support ring.

a separate, accompanying support ring.

The handles are first spread to move the jaws together; then the repair seal is placed over the knife edges and onto the support ring. The user then releases the handles, allowing the spring to pull them together and thereby push the jaws outward so that their knife edges make contact with the inside of the repair seal. In this configuration, the jaws hold the repair seal on the support ring by spring pressure.

The user maneuvers the tool to place the repair seal in the male half of the tube fitting. The user then squeezes the handles together until the left jaw bottoms in the notch on the support ring. In this movement, the knife edges crimp the repair seal by a preset amount at two diametrically opposed positions, thus securing the repair seal in the fitting. Thereafter, the repair seal will not fall out, regardless of the orientation of the fitting. Because the movement of the jaws is limited by the inner diameter of the support ring and the depth of the notch, the knife edges do not damage the repair seal or the fitting.

This work was done by Joseph R. Trevathan of **Johnson Space Center.** *For further information, Circle 38 on the TSP Request Card. MSC-21956*

Potential-Field Scheme for Avoidance of Obstacles by a Robot

The end effector would be guided around obstacles, toward a goal point.

John F. Kennedy Space Center, Florida

Developmental software for the guidance of a robot intended to operate in a plant-growth chamber provides for the end effector of the robot to avoid obstacles (e.g., parts of plants) that are at known positions. The software includes algorithms that implement the potential-field method for guidance away from the obstacles and toward a goal point, where an object to be manipulated by the end effector may be located.

The potential-field method was introduced in 1979, and aspects of it have been discussed previously in *NASA Tech Briefs*. The essence of the method is to compute the trajectory of the affected part of the robot (in this case, the end effector) as though it were moving in a repulsive potential field that surrounds the obstacles and in an attractive potential field that surrounds the goal point. At each location along the trajectory, the next increment of movement of the end effector is computed as a small vector along the direction of the local net force of the field.

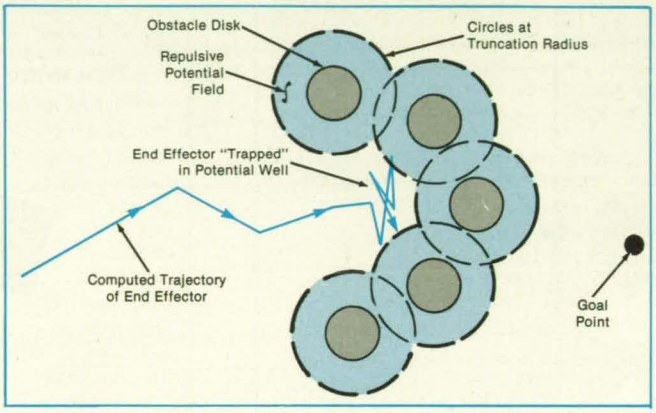

In the present state of development, the guidance scheme is based on a simplified, two-dimensional model of the workspace. In this model, the obstacles are represented as circular disks, and the end effector is represented as a point or a small disk. The robot arms are not included in this simplified representation.

Each obstacle disk is surrounded by a larger circle, defined by a "truncation" radius, beyond which it is considered to exert no force on the end effector. Within the truncation radius, the repulsive force is considered to be inversely proportional to the square of the distance from the edge of the disk and directed outward from the disk.

Under some circumstances, obstacles could be clustered with overlapping truncation radii in such a way that they define a concave potential well in which the end

The **Computed Trajectory** can sometimes be characterized by "trapping" in the fictitious potential well that surrounds a group of obstacles. The software detects the repeated short bounces within the potential well and modifies the fictitious potential field to push the end effector out of the trap, allowing it to proceed toward the goal point.

effector could be "trapped" on its way to the goal point (see figure). The software signals that such "trapping" has occurred when the computed trajectory fails to emerge from within a region of specified small size after a specified number of steps of the computation. The direction of the attractive force exerted by the goal is then modified temporarily to drive the end effector out of the potential well. After the trajectory is recomputed to guide the end effector around the potential well, the trajectory is "cleaned up" by eliminating the points within the potential well.

The obstacle-avoidance software is written in Microsoft C and has been made modular so that different algorithms can be used. This technique was demonstrated in a prototype system containing a PUMA robot, a Perceptics version system, and a Macintosh supervisory computer. The software is designed to be interactive and easy to use. The operator chooses the starting and goal points on a digitized image of an obstacle-strewn environment by use of a computer mouse, and can interactively change variables in the control equations to optimize the computed trajectory.

At present, the operator must place the disks over the obstacles. This is easily accomplished by using the mouse to identify the center and the radius of each disk. All of the software is menu-driven and is designed so that a novice can easily identify obstacles and obtain excellent results.

This work was done by Dan Wegerif, Roy Tharpe, and Mike Sklar of McDonnell Douglas Space Systems Co. for **Kennedy Space Center**. *Further information, Circle 1 on the TSP Request Card.*
KSC-11491

Transforming Vectors Measured by Noncoaligned Instruments

The complete transformation can be obtained from two nonparallel vectors.

Langley Research Center, Hampton, Virginia

In a novel method for computing the relationships between the coordinate axes of two vector-measuring instruments that are not aligned with each other, it is not necessary to perform calibrating measurements in advance. Instead, one need only measure two nonparallel vectors **u** and **v** simultaneously in both coordinate systems: these measurements provide all the data needed to compute the transformation of any vector from one coordinate system to

the other. The method should be particularly useful in computing alignments and transformations between accelerometers, gyroscopes, and other instruments mounted on platforms that are subject to vibrations, thermal strains, and other distortions that may cause alignments to vary unpredictably with time.

Let the subscripts 1 and 2 denote the representations of a given vector in the first and second coordinate system, respectively. It can be shown that the transformation between the two coordinate systems can be expressed in terms of a single rotation of the first coordinate system about an axis ω, such that if both representations of both vectors were displayed simultaneously, $\mathbf{u}_1$ and $\mathbf{v}_1$ would appear to rotate simultaneously into $\mathbf{u}_2$ and $\mathbf{v}_2$, respectively (see Figure 1). The unit vector in the ω direction is given by the vector product where the circumflexes denote unit- length versions of the noted vectors.

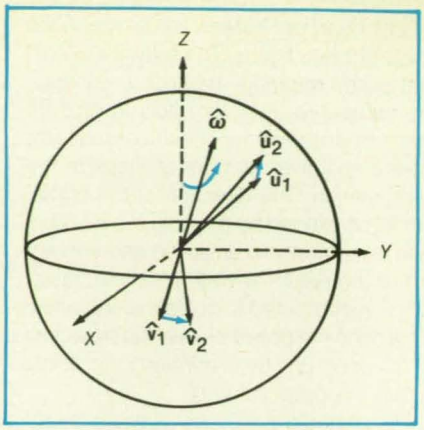

Figure 1. A **Single Rotation of The First Coordinate System** (which contains $\hat{u}_1$ and $\hat{v}_1$) about the $\hat{\omega}$ axis simultaneously transforms $\hat{u}_1$ into $\hat{u}_2$ and $\hat{v}_1$ into $\hat{v}_2$.

The method is based on an Euler-angle representation of the foregoing transformation in a global X,Y,Z coordinate system. First, the global coordinate system is rotated sequentially about two axes with ω. Then it is rotated through the required angles about ω. Next, it is rotated in a reverse sequence about two axes. The final position of the global system with respect to the original position of the global system is equivalent to the required Euler-angle representation (see Figure 2). The transformation matrix, from which the Euler angles can be extracted, can be constructed by multiplying the matrices of the rotations in the sequence.

This work was done by James R. Ritter and Eric L. Dahlstrom of Lockheed Engineering & Sciences Co. for **Langley Research Center.** *For further information, Circle 7 on the TSP Request Card. LAR-14619*

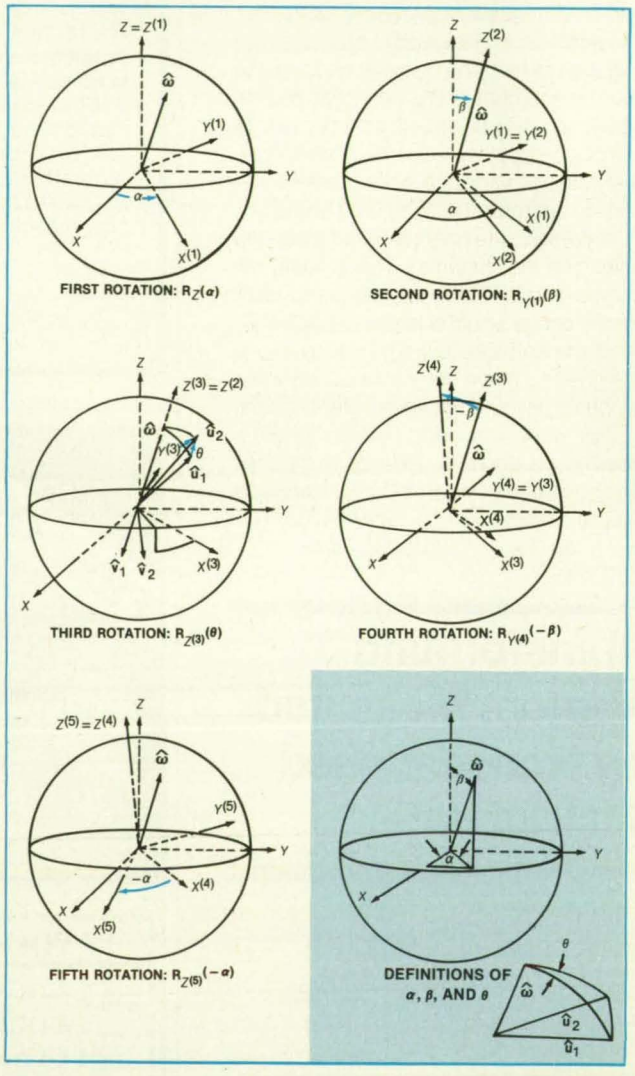

Figure 2. **A Sequence of Rotations** of the *X,Y,Z* coordinate system yields the desired Euler-angle representation. In each case, the subscript on *R* denotes the axis about which the rotation occurs, and the angle of rotation is indicated in the larger parentheses.

Bag for Formulating and Dispensing Intravenous Solution

Sterile solution can be prepared and dispensed in a nonsterile environment without other special equipment.

Lyndon B. Johnson Space Center, Houston, Texas

The figure illustrates a large-volume parenteral (LVP) bag in which a predetermined amount of sterile solution is formulated by combining a premeasured, prepackaged amount of sterile solute (in either powder or concentrate form) with a predetermined amount of water. The bag is designed to hold a predetermined amount — typically 1 L — of sterile solution. Sterility of the solution is maintained during mixing by passing the water into the bag through a sterilizing filter. This system could be used in field or other hospitals that do not have proper sterile facilities, and in field research.

The bag is equipped with a number of ports: a port for the injection of water into the bag, a port for the injection of medication or solute into the bag, a port for administration of solution to the patient, and a redundant port. The sterilizing filter is sealed into the edge seal of the bag, downstream of the water-injection port. The bag/port/filter assembly and the solute are presterilized during fabrication. Sterile protective covers are used to ensure the sterility of the ports.

The fittings on the ports are also chosen with a view toward maintaining sterility: the ports can be equipped with such standard sterile fittings as the standard Luer or Luer-lok (or equivalent) or other fittings of appropriate design to ensure that only sterile surfaces are in contact with solute or solution. The ports also incorporate one-way check valves to ensure that the solutions used flow in the proper direction and do not come in contact with any nonsterile surfaces. The valves can be standard "off-the-shelf" valves or can be designed specifically for this purpose.

As the bag is filled with water, medication can be injected into the bag, and the solution can be mixed by squeezing the outside of the bag or by shaking the bag. Metering and/or flow devices (not shown) ensure that the proper amount of water is introduced into the bag.

The bag includes an internal seal that defines both the volume in which the solute is stored and a path for the flow of solution, along which path water and solute are mixed. The shape of the septum has been determined experimentally to create turbulence, which aids the mixing of the water and the solute. The shape also accelerates mixing as the water and solute flow into the main volume of the bag. In addition, this shape has been shown experimentally to help contain the solute in the designated storage volume; this reduces the surface area of the solute, reducing the potential amount of water vapor that can be transmitted through the walls of the bag and into the solute during storage.

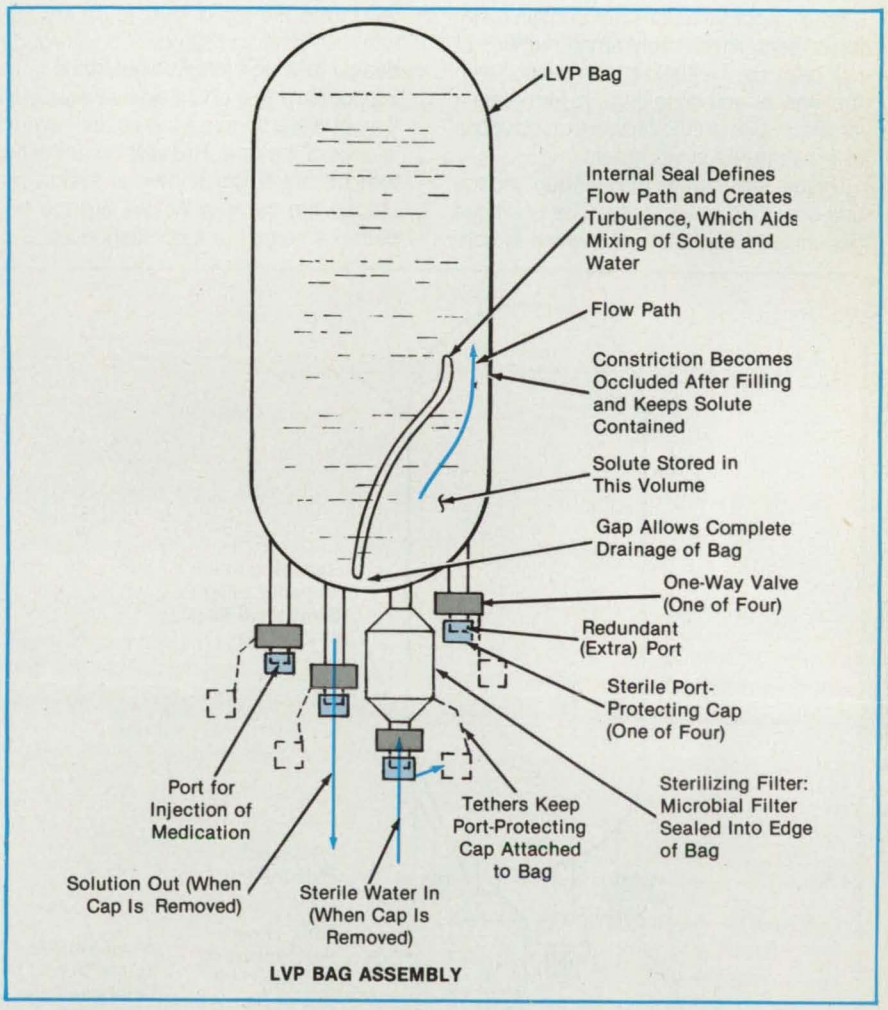

This **Large-Volume Parenteral Bag** can be used to formulate and dispense a sterile intravenous solution in a nonsterile environment.

This work was done by Jim Kipp, Jim Owens, Mike Scharf, Mike Finley, Tom Dudar, Joe Veillon, and Jim Ogle of Baxter International Inc. for **Johnson Space Center**. *No further documentation is available.*

Title to this invention has been waived under the provisions of the National Aeronautics and Space Act [42 U.S.C. 2457(f)], to Baxter International Inc. Inquiries concerning licenses for its commercial development should be addressed to

Baxter International Inc.
One Baxter Parkway
Deerfield, IL 60015

Refer to MSC-21835, volume and number of this NASA Tech Briefs *issue, and the page number.*

Unit-Dose Bags for Formulating Intravenous Solutions

These flowthrough bags can be used to formulate sterile solutions in nonsterile environments.

Lyndon B. Johnson Space Center, Houston, Texas

Smaller unit-dose flowthrough bags have been devised for use with large-volume parenteral (LVP) bags in preparing sterile intravenous solutions. A premeasured amount of solute stored in such a unit-dose bag is flushed by a predetermined amount of water into the LVP bag, which is similar to the bag described in the preceding article, except that it does not contain an internal seal. A relatively small number of LVP bags can be used in conjunction with the smaller unit-dose bags to formulate a large number of LVP intravenous solutions in a nonsterile environment.

Figure 1 illustrates the LVP-bag and the unit-dose-bag assemblies. The unit-dose bag includes an inlet port, which is connected to the source of sterile water, and an outlet port, which is connected to the inlet of the sterile filter on the LVP bag.

Figure 2 illustrates two examples of unit-dose bags. The principal design feature of these bags is that they are configured to ensure that the water flowing through them flushes all the solute into the LVP bag. The version at the top of this figure shows a relatively long and slender "flowthrough" design in which longitudinal seals in the interior form flow channels that enable the flow of water to force the solute from the interior of the bag. The version at the bottom of this figure shows a design that utilizes the same principle, but the flow path is shaped like a horseshoe, allowing for a more-compact container.

Both versions are equipped with one-way inlet and outlet valves. These valves are used to seal the ends of each unit-dose bag and to ensure that water can flow through the interior of the bag only after it has been properly connected to both a source of water and an LVP bag.

This work was done by Mike Finley, Jim Kipp, Mike Scharf, Jeff Packard, and Jim Owens of Baxter International Inc. for **Johnson Space Center**. *For further information, Circle 18 on the TSP Request Card.*

Title to this invention has been waived under the provisions of the National Aeronautics and Space Act [42 U.S.C. 2457(f)], to Baxter International Inc. Inquiries concerning licenses for its commercial development should be addressed to

Baxter International Inc.
One Baxter Parkway
Deerfield, IL 60015

Refer to MSC-21836, volume and number of this NASA Tech Briefs *issue, and the page number.*

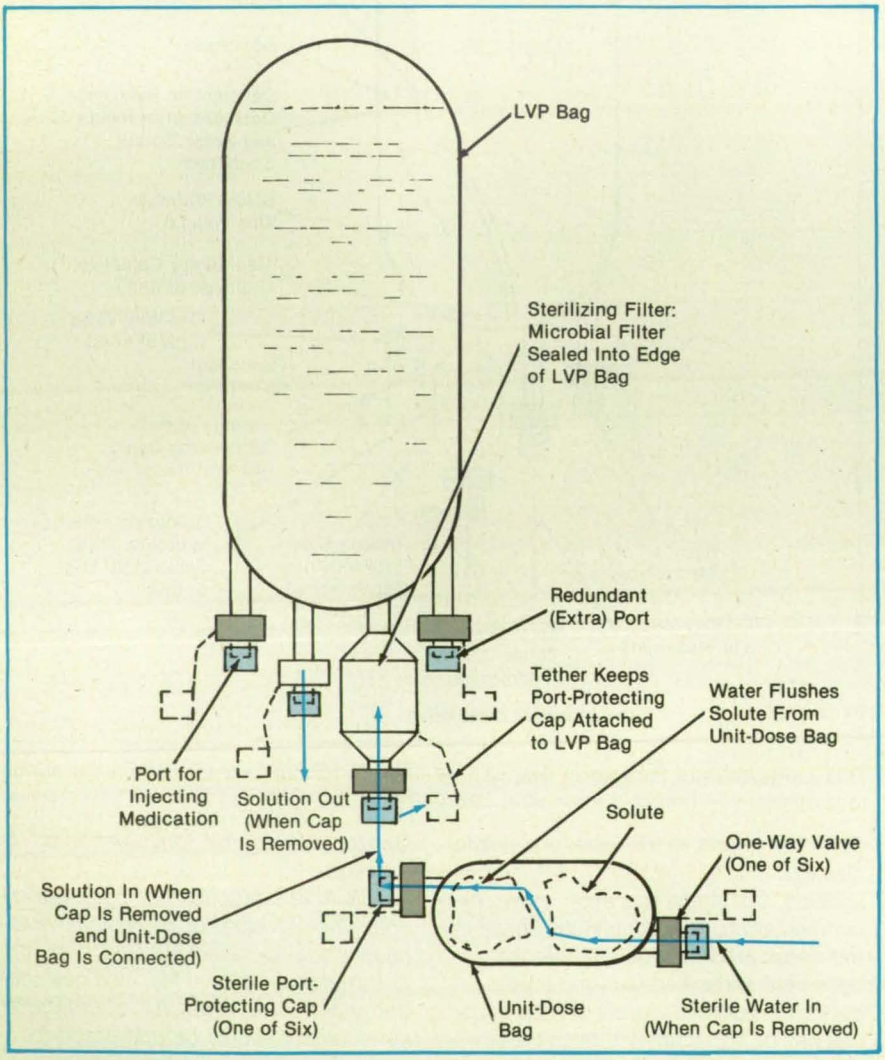

Figure 1. **Sterile Intravenous Solution** is prepared by flushing the sterile content of a unit-dose container into a large-volume parenteral (LVP) bag, using a predetermined volume of sterile water.

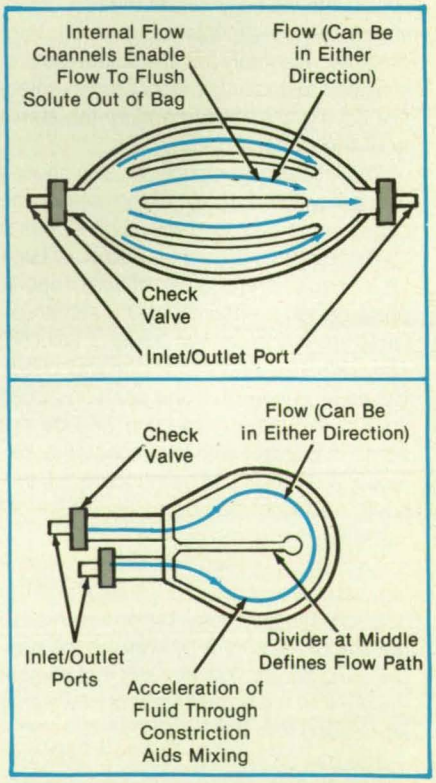

Figure 2. The **Unit-Dose Bags** are designed to optimize the dissolution of the solute and the flushing of the resulting sterile solution into the LVP bag.

Multiple Pages Intentionally Left Blank

Solute-Filled Syringe for Formulating Intravenous Solution

The syringe delivers the solute to form a sterile solution in a nonsterile environment.

Lyndon B. Johnson Space Center, Houston, Texas

A prefilled syringe that contains a premeasured amount of solute in powder or concentrate form can be used to deliver the solute to the sterile interior of a large-volume parenteral (LVP) bag. A predetermined amount of sterile water is also added to the LVP bag through a sterilizing filter, and is mixed with the contents of the syringe, to yield a sterile intravenous solution of the specified concentration.

The figure illustrates the version in which the syringe has been prefilled with a powdered solute. The syringe is used in conjunction with an LVP bag that is similar to the one described in "Bag for Formulating and Dispensing Intravenous Solution" (MSC-21835) on the preceding pages, except that (1) it does not contain an internal seal and (2) instead of a redundant port, a specially designed docking port is sealed into the edge of the bag. The docking port and syringe are designed such that the syringe snap-fits and seals into the docking port prior to injection of the solute powder.

The snap fit between the docking port and the syringe is designed to be a "one-way" fit. Once the syringe is snapped into the docking port, it cannot be removed without destroying the bag assembly.

The sterility of the docking port prior to use is ensured by two seals. One of the seals is an exterior cap that prevents contamination of the port by touch. This cap is removed prior to use. The other seal is a plug seal or frangible septum on the inside. The syringe also includes two similarly configured seals: an outer cap to prevent contamination by touch and an inner plug seal or frangible septum.

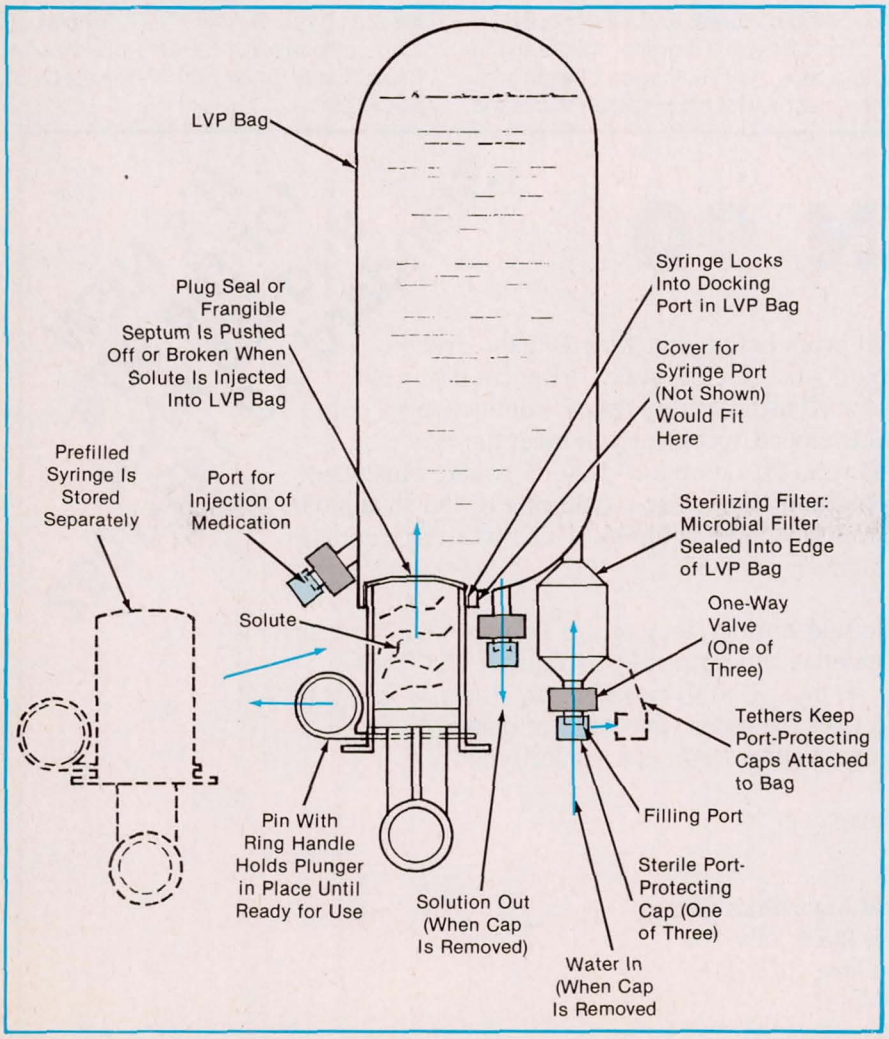

A **Syringe Prefilled With Powdered Solute** is used to prepare a sterile intravenous solution in a large-volume parenteral bag.

Solute is injected into the LVP bag according to the following procedure: First, the outer caps are removed from both the syringe and bag. Sterility of the system and retention of the water in the bag are maintained at this stage by the inner seals in the bag and syringe. The syringe is then snapped into the docking port; this can be done at any time during the filling process. A pin that holds the plunger in place in the syringe is removed, and the plunger is depressed, breaking the inner seals and forcing the solute into the bag.

In the version (not shown) in which the syringe is prefilled with solute in concentrate form, such standard syringe fittings as Luer or Luer-lok (or equivalent) can be used. The procedure for injecting concentrate into the bag is the same as that for powdered solute. In both versions, the syringe can be equipped with a detachable plunger, which provides for smaller storage volume. In addition, the plunger can be tethered to the syringe barrel, or it can be detached for use with a number of syringes and bags.

This work was done by Jim Owens, Al Bindokas, Tom Dudar, Mike Finley, and Mike Scharf of Baxter International Inc. for **Johnson Space Center**. *For further information, Circle 19 on the TSP Request Card.*

Title to this invention has been waived under the provisions of the National Aeronautics and Space Act [42 U.S.C. 2457(f)], to Baxter International Inc. Inquiries concerning licenses for its commercial development should be addressed to

Baxter International Inc.
One Baxter Parkway
Deerfield, IL 60015

Refer to MSC-21837, volume and number of this NASA Tech Briefs *issue, and the page number.*

Books and Reports

These reports, studies, handbooks are available from NASA as Technical Support Packages (TSP's) when a Request Card number is cited; otherwise they are available from the National Technical Information Service.

Chemicals Reduce Need To Mow Grass

Herbicides are used to retard the growth of Argentine bahia grass.

A brief report discusses the use of the herbicides Roundup®, Campaign®, and Oust® to retard the growth of Argentine bahia grass growing adjacent to the runway at the Space Shuttle landing facility at Kennedy Space Center. Here the temperature, humidity, and rich soil provide the grass with a good environment for growth; this results in the need for frequent mowing. Mechanical mowing exposes numerous insects and seeds, attracting many hungry birds, which are a potential source of damage to aircraft in that they can be ingested by jet engines.

The report specifies rates of application for the herbicides, which are applied in the form of aqueous solutions to which a blue dye has been added to provide a visual guide to aid even application. The herbicide is applied by use of a spraying apparatus pulled by a tractor. The operators must wear respirators, long-sleeve coveralls, rubber gloves, and rubber boots.

This "chemical mowing" can keep the grass at a "freshly mowed" height with less mechanical mowing than is needed for untreated grass. However, the "chemical mowing" technique causes browning and/or yellowing of the grass. The effectiveness of the herbicide and yellowing of the grass depend on the pH of the soil, which can vary significantly within a distance of 20 ft (about 6 m).

It is suggested that this technique might be applied to the grass on the shoulders of roads to reduce the time spent on mowing. Reduction of mechanical mowing would also reduce the dangers that arise when mowers throw debris into roadway traffic.

This work was done by Brooks Humphrys and Max Farley of **Kennedy Space Center** *and Larry J. Gast of EG&G. To obtain a copy of the report, "Growth Retardant for Grass," Circle 54 on the TSP Request Card.*
KSC-11466

NASA Tech Briefs LITERATURE SPOTLIGHT

Free catalogs and literature for NASA Tech Briefs' readers. To order, circle the corresponding number on the Reader Action Request Form (page 85).

DESIGN OPTIMIZATION SOFTWARE WITH FEA ENGINEERING BUILT-IN.

Free catalog. See why Algor is a world leader in engineering design optimization in which FEA analysis is tightly integrated. Includes solid and surface modeling. Enables engineers to finalize designs before the CAD documentation phase. All popular FEA analyses, including nonlinear. For DOS and UNIX. Adds value to all CAD, CAM, and CAE setups. Tel: 412-967-2700, Fax: 412-967-2781.

ALGOR, INC.

For More Information Circle No. 301

THE SCRAMNET NETWORK

is a real-time shared-memory network designed to connect dissimilar computers (those with different backplanes). SCRAMNet avoids the limitations of physical shared-memory architectures and message passing LANs to deliver true and real-time speed, deterministic performance, and positive system control with no software overhead. Features include data filtering, programmable byte swapping, and a sophisticated interrupt structure. Tel: 513-252-5601 or 1-800-252-5601.

SYSTRAN Corp.

For More Information Circle No. 302

LOW-COST DIGITAL VIBRATION CONTROLLERS

Easy to use Expansion Card & Software from VTS convert your 386 or 486 personal computer to a powerful Digital Sine or Random Vibration Controller. Frequency ranges—Random 500, 1000, or 2000 Hz, Sine 5 to 6250 Hz. Many other unique features. Free demo disk available (learn to operate Controller in less than one hour).

Vibration Test Systems

For More Information Circle No. 303

HIGH RESOLUTION VIDEO CCD CAMERA

Brochure from Tietz Video & Image Processing Systems GmbH describes compact CCD-1000 1250-line camera with RS-232 programmable gain/exposure control. 25 fps interfaced. Analog/digital ports transmit 60 dB dynamic range images to monitor or BSS-1000 frame grabber. Complete image processing solutions for medical, industrial, and surveillance applications. Fax USA: 602-622-7866.

For More Information Circle No. 304

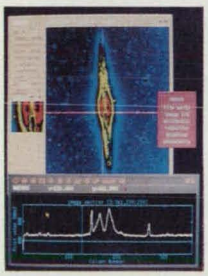

MS-DOS®IMAGE ANALYSIS SOFTWARE

New! Axiom Research Inc. MIRA (Microcomputer Image Reduction & Analysis) software: fast, full-featured, low-cost image display, reduction, and analysis for MS-DOS 5.0 input 3/16 bit integer, 32-bit real 1D/2D data, including CCD images to 2K x 2K with user-defined formats. Over 100 operations coded in assembly language for workstation graphical/numerical performance. Multi-window graphical interface.

For More Information Circle No. 305

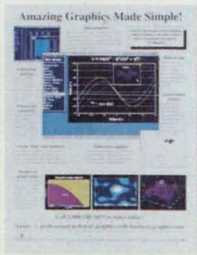

NEW TECHNICAL GRAPHICS SOFTWARE

FREE brochure on new Axum 3.0 technical graphics and data analysis software for PCs. Create publication-quality 2D, contour, and 3D technical graphs. Interactively edit and customize. Export graphs to WordPerfect/Word. Import Lotus, dBase or ASCII. Do statistics, curve fitting, and data smoothing. Tel: 1-800-548-5653, Ext. 251.

TriMetrix, Inc.

For More Information Circle No. 306

FIBER OPTIC VIDEO TRANSMISSION SYSTEMS FOR C³I & BROADCAST

Data sheets detail systems design specs for DYNAIR's video, audio, data, and high resolution RGB graphics transmission systems. Maximum distance 15 km with multimode fiber. Tel: 800-854-2831 or 619-263-7711.

DYNAIR Electronics, Inc.

For More Information Circle No. 307

WALL-SIZED DISPLAY FOR COMMAND & CONTROL

Media Wall ™ transforms an array of monitors or projectors into a giant computer screen for "wall-sized" displays of text, graphics, animation and scanned photographs. A direct digital interface to a computer produces images of startling clarity, making Media Wall the ideal system for command and control applications and photo analysis.

RGB Spectrum®

For More Information Circle No. 308

RECIRCULATING CHILLERS

72-page catalog features a complete line of recirculating chillers for cooling water-cooled equipment. These chillers offer steady cooling with heat load removal up to 75 kW, spanning temperature ranges of -5°C to +35°C. Chillers feature LED display, operating status gauges, and easy access to internal components. Also available are Constant Temperature Bath/Circulators and Benchtop Personal Freezers. Call toll-free at 1-800-258-0830.

NESLAB Instruments, Inc.

For More Information Circle No. 309

STANDARD REFERENCE MATERIALS CATALOG

The National Institute of Standards and Technology's Standard Reference Data Program has been providing evaluated, high-quality data compilations to the world's scientists and engineers for thirty years. Our databases are designed to meet your needs. Contact us at 301-975-2208 to receive a free catalog.

National Institute of Standards and Technology

For More Information Circle No. 310

DIAMONEX® DIAMOND PRODUCTS

Diamonex's new brochure describes their Polycrystalline and Amorphous Diamond-coated products for manufacturers using advanced technology. Polycrystalline Diamond enhances the performance of high-power FET heat spreaders, hybrid multichips, and laser diodes. Amorphous Diamond coatings for medical implantables, surgical implements, medical packaging, thermal printheads, hard disks and magnetic tapeheads enhance the lifetime and wear of products.

Diamonex, Inc.

For More Information Circle No. 311

GPS-SYNCHRONIZED TIMING PRODUCTS

TrueTime's Precision Timing Products catalog features GPS-Synchronized Clocks in rackmount, portable, and board-level configurations. Includes illustrations and product specifications for our complete line of Synchronized Clocks, Time Code products, and remote displays to fit a variety of time and frequency applications.

TrueTime, Inc.

For More Information Circle No. 312

NEW TEST & MEASUREMENT CATALOG

Keithley's new 1993-1994 catalog features 240 pages of electronic test and measurement instruments, including DMMs, electrometers, sources, picoammeters, source-measure units, switch systems, LCZ meters, and much more. This valuable reference guide includes product specifications, selector guides, and comprehensive technical data. Tel: 800-552-1115, Fax: 216-248-6168.

Keithley Instruments, Inc.

For More Information Circle No. 313

CATALOG DESCRIBES DATA ACQUISITION SYSTEMS

General and specialized data acquisition systems are described in this new catalog from Hi-Techniques. Modular in design, these products contain all the software for acquisition of signal data, calculation of data parameters, and output of finished documentation for research and routine test applications. Tel: 608-221-7500.

Hi-Techniques, Inc.

For More Information Circle No. 314

CATALOG COMBINES ESQ AND EMCOR I ENCLOSURE LINES

Emcor Products describes its ESQ and Emcor I modular enclosure systems in this free, color catalog. This inclusive, 72-page catalog summarizes new options, features metric conversions, dimensional diagrams, and contains an easy ordering guide.

Emcor Products

For More Information Circle No. 315

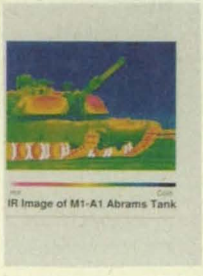

SEE THE HOT SPOTS?

An M1-A1 tank may not be attacking you now, but a hot spot probably is. Industrial and research infrared cameras are available to get or keep you out of the hot seat. For more information, call 513-573-6275, or fax 513-573-6290. Address is 7500 Innovation Way, Mason, OH 45040.

Cincinnati Electronics, Detector Labs

For More Information Circle No. 316

B92 CATALOG RELEASE

The latest catalog from W.M. Berg Inc. coincides with Berg's silver anniversary. Founded in 1967, Berg has grown to become a recognized industrial leader of miniature precision mechanical components. A significant number of new items are added as well as expanding previous product lines. Featuring 50,000 standard components, 80% of which we are able to ship from stock within 24 hours. Available in metric version too: M92.

W.M. Berg, Inc.

For More Information Circle No. 317

ELECTRONIC HARDWARE CATALOG

Broadest selection of hardware for electronic assemblies. 300-page free catalog includes a full range of standoffs, captive screws and nuts, chassis fasteners, handles, ferrules, spacers and washers. Special sections—new, unusual products, metric information and Mil-plating specifications. Full inventory, fast turnaround, samples. Tel: 1-800-237-0013, Fax: 201-661-3408.

Accurate Screw Machine Co.

For More Information Circle No. 318

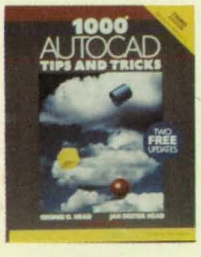

THE BEST WAY TO STAY AHEAD OF AUTOCAD!

Ventana Press offers seven best-selling books and companion disks on working in 3D, never before published shortcuts and tips, an overview of commands and features, using AutoCAD's Advanced Modeling Extension for solid modeling, and using AutoLISP to solve simple drawing problems. ALL BOOKS UPDATED FOR RELEASE 12. Contact Ventana Press, P.O. Box 2468, Chapel Hill, NC 27515. For orders, call 800-743-5369. Other inquiries: 919-942-0220, Fax: 919-942-1140.

For More Information Circle No. 319

FREE 1993 TODD OEM POWER SUPPLY CATALOG

The TODD catalog contains information and specifications on more than 130 highly reliable, technologically advanced, standard, modified, and custom OEM switching power supplies from 150 to 1500 watts. TODD is ISO 9002 registered. Call: 800-223-8633 or 516-231-3366; or Fax: 516-231-3473.

TODD POWER SUPPLIES

For More Information Circle No. 320

OPTICS FOR METEOROLOGY

This 106-page catalog gives information, including prices, on X-Y tables, microfinishing equipment, toolmakers' microscopes, alignment and monocular zoom microscopes, borescopes and miniborescopes, and fiber optic and miniature illumination systems. Also described are centering microscopes, optical cutting tool geometry analyzers, and more.

Titan Tool

For More Information Circle No. 321

LIFT/SUPPORT MECHANISMS, APPLICATIONS

A booklet illustrates Suspa's engineering know-how for gas spring and fluid-drive lift systems for height adjustment, counter-balancing and damping of seats, doors, lids, hatches, racks, work surfaces, benches, platforms, etc. Tel: 616-241-4200, Fax: 616-531-3310. Address: 3970 Roger Chaffee SE, Grand Rapids, MI 49548-3497.

Suspa, Inc.

For More Information Circle No. 322

POWER CONVECTION® VACUUM FURNACES

Surface®Combustion offers a two-page "sell sheet" featuring its standard line of Power Convection, Single Chamber Vacuum Furnaces, designed for performing high quality heat treating processes including annealing, hardening, sintering, brazing, and other special vacuum processes. Specifications and performance data are listed. Tel: 419-891-7150, Fax: 419-891-7151.

Surface Combustion, Inc.

For More Information Circle No. 323

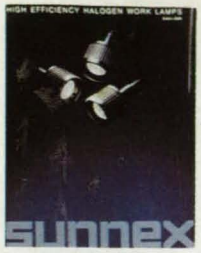

HALOGEN TASK LAMPS

High efficiency halogen task lamps provide "natural" white light, excellent color rendition. Long-life halogen bulbs assure high intensity illumination with minimal energy consumption. Compact housing provides an unobstructed view. Aplanatic, dual lens magnifier/lamp combinations allow distortion-free viewing over entire work surface.

Sunnex, Inc.

For More Information Circle No. 324

SPECIALTY GAS AND EQUIPMENT CATALOG

Free! The 1993 rare and specialty gas and equipment catalog from Spectra Gases of Irvington, NJ, contains specifications on rare gases, excimer laser gas mixtures, halogen gas pre-mixtures, helium-3 and isotopic gases, research gases and mixtures, gas safety cabinets, automatic and manual gas-handling systems, and related equipment. Krypton and argon ion-laser tube remanufacturing, halogen scrubbers, and "oil free" vacuum pumps are among the products and services highlighted.

For More Information Circle No. 325

PRECISION MASS FLOW CONTROLLERS

SIDE-TRAK monitors and controls the mass flow of air and process gases in ranges from 0-10 SCCM to 0-200 SCFM. The instrument delivers 1% FS accuracy, .15% repeatability and one second time response to set point changes. Patented access ports at both ends of the sensor tube reduce maintenance downtime.

Sierra Instruments, Inc.

For More Information Circle No. 326

TOOLING COMPONENTS & EQUIPMENT

New 400-page reference catalog offers a full range of tooling components and equipment. Items include handwheels, handles, knobs, spring & ball plungers, leveling pads, clamps, locating devices, cutting tools, rivets, thread inserts, hard-to-find tools, and metric items. Contains complete specifications and pricing. All items are stocked for same day shipment. Tel: 1-800-253-0421; Fax: 800-438-1145.

Reid Tool Supply Company

For More Information Circle No. 327

SELF CLINCHING PANEL FASTENER ASSEMBLIES

This PEM®panel fastener bulletin includes specifications on pre-assembled, spring loaded assemblies, flush mounted panel screw components and plunger assemblies. The entire line of panel fasteners and plungers is easily installed by squeezing them into properly sized punched or drilled holes. For a complete PEM catalog call **1-800-237-4736.** Penn Engineering & Manufacturing Corp., P.O. Box 1000, Danboro, PA 18916-1000.

For More Information Circle No. 328

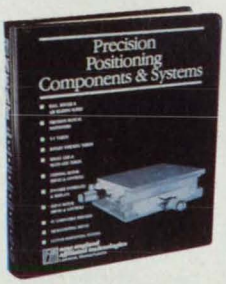

PRECISION POSITIONING AND MOTION CONTROLS

NEAT's 1993 catalog includes the latest additions to its family of precision positioning components and systems. Featured are single-axis, multi-axis, rotary, high-vacuum, and air bearing stages; plus a complementary line of stepping, servo, and linear motor drives and controls. Stage travels range to 30+ in. with repeatability of 1 micron, speeds to 80 in/sec, and resolutions to 5 nm. Our engineers use CAD/CAM machining facility to provide custom turnkey solutions for a wide spectrum of applications. Tel: 800-227-1066.

For More Information Circle No. 329

DOS SOFTWARE FOR INSTRUMENTATION SYSTEMS

The free eight-page LabWindows®2.0 brochure describes the dramatically enhanced instrumentation software used by QuickBASIC and C programmers for test and measurement, data acquisition, and instrument control application programs. LabWindows 2.0 features an Instrument Library of drivers for more than 150 GPIB, VXI, and RS-232 instruments. A free demo disk is available. Tel: 512-794-0100 or 800-433-3488, Fax: 512-794-8411.

National Instruments

For More Information Circle No. 330

MERLIN PRECISION MEDICAL IMAGING

Merlin Engineering brings its vast experience in professional broadcast video processing, from the first video tape recorder to HDTV, to the critical medical and industrial imaging fields with a family of digital image processors and scan converters. 36 individual units provide image enhancement, solid state video storage, or conversion from/to non-standard video in both laboratory and airborne environments.

For More Information Circle No. 331

MEMBRANE SWITCH CATALOG

Memtron's full line of switches and graphic products can be found in this catalog. We specialize in tactile/non-tactile, PC board backed, and Elastomer switches. Also available, a full line of services including custom engineering, CAD design, and creative art capabilities.

Memtron Technologies, Inc.

For More Information Circle No. 332

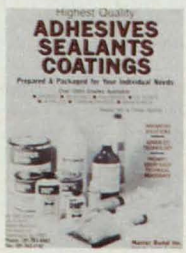

ADHESIVES/ SEALANTS/ COATINGS

Master Bond Inc. manufactures over 3000 grades of adhesives, sealants and coatings. Line consists of epoxies, anaerobics, cyanoacrylates, silicones, and acrylics. Both one- and two-part systems. Systems are designed to meet specific requirements. One-on-one assistance available with our highly knowledgeable technical staff. Tel: 201-343-8983, Fax: 201-343-2132.

MASTER BOND, INC.

For More Information Circle No. 333

NEW FUME HOOD CATALOG AND BLOWER BOOKLET

Labconco's new Protector® Laboratory Fume Hoods and Accessories Catalog provides details on protector fiberglass, specialty and walk-in hoods as well as safety accessories such as the Guardian™ Air Monitor. The back pocket contains a 16-page blower booklet.

Labconco Corp.

For More Information Circle No. 334

Request Information on the . . . Protector Controlled Atmosphere Glove Box.

The 32-page, full-color Protector Glove Boxes Catalog describes Labconco's line of controlled atmosphere and multi-hazard glove boxes featuring one-piece or stainless steel liners.

Labconco Corp.

For More Information Circle No. 335

1993 PUBLICATIONS AND INFORMATION SERVICES CATALOG

For the first time INSPEC and the IEE combine their catalog—INSPEC Publications and Services, abstracts journals, online database, tape services, CD-ROM, IEEE/IEE Periodicals Ondisc (IPO) are featured along with the books, conference proceedings, professional journals and distance learning (Video and CBT) materials of The Institution of Electrical Engineers (IEE). Tel: 908-562-5553, Fax: 908-981-0027.

For More Information Circle No. 336

FLEXIBLE CIRCUITRY

This new brochure from Hughes Interconnect Systems details the flexible circuit capabilities available to build smaller, faster, and lighter products. It details Hughes' technologies including fine line, multilayer, and low cost compression interconnects, outlines complete process and test regimens available, and discusses valued-added assembly and design services that will get your products to market faster. For more information, contact: Hughes Interconnect Systems; 17150 Von Karman Avenue, Irvine, CA 92714, Tel: 714-660-5772.

For More Information Circle No. 337

'5-IN-1' AIR SYSTEMS

The Graham-White 5-in-1 air systems extend a money back performance guarantee for dry, oil-free, clean compressed air. The water, oil varnish, and particle contaminants are removed from the compressed air without the hassle of refrigeration and CFC emissions. Tel: 703-387-5600, Fax: 703-387-5639.

GRAHAM-WHITE MANUFACTURING COMPANY

For More Information Circle No. 338

ATE POWER PRODUCTS

Elgar's free catalog includes programmable AC power sources, DC power systems and loads, VXP power systems, plug-in oscillators, global and on-line UPS's. Application needs are cross-referenced with Elgar products in several easy-to-use tables throughout the catalog.

ELGAR

For More Information Circle No. 339

MEASUREMENT SERVICES BROCHURE

UV-VIS-NIR and NIR-MIR Reflectance and Transmittance Measurement Services. A new 4-page brochure describes Labsphere's service capabilities for NIST traceable measurements of reflectance and transmittance in the UV-VIS-NIR and NIR-MIR wavelength ranges. Three standard data format options are offered as well as custom calibrations. The brochure describes the spectroscopic instruments used in Labsphere's Reflectance Spectroscopy Laboratory.

Labsphere, Inc.

For More Information Circle No. 340

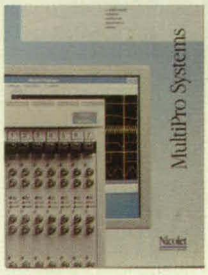

MULTI-CHANNEL TRANSIENT ANALYZERS

The Nicolet MultiPro Transient Analyzer gives you all the inputs you need to handle two or 200 channel applications. These complete turnkey systems, which are up and running in minutes, are powerful and flexible, and use an easy-to-follow Microsoft® Windows™ environment.

Nicolet Measurement Instruments

For More Information Circle No. 341

WORKSTATIONS, LAB FURNITURE

20-page illustrated guide covers the Techlab line of technical work stations and laboratory systems furniture. Included are stations of different lengths, combined with a choice of cabinets, shelves, parts drawers, partitions, and other accessories. Catalog has dimensions, shows arrangements, describes work surfaces, and has a color selection guide. Tel: 800-832-5227, Fax: 616-372-6116. Address: Box 1165, Kalamazoo, MI 49005.

For More Information Circle No. 342

MASS FLOW CALIBRATOR

Brochure provides complete technical information on the new molbloc fundamental mass flow element and molbox mass flow calibrators. These are compact, highly accurate, and easy-to-use new tools for the laboratory or in-situ verification and calibration of mass flow meters and controllers. DH Instruments, Inc., Tempe, AZ; Tel: 602-967-1555.

DH Instruments, Inc.

For More Information Circle No. 343

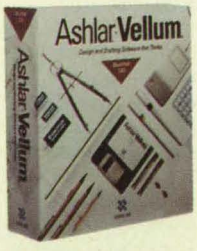

REDUCE YOUR DESIGN TIME IN NO TIME

Ashlar Vellum 3D is a 2D and 3D design package for every engineer and designer. By reducing your design time, Vellum will make you more productive and your company more competitive and profitable. Call for our free, eight-page color brochure, it's loaded with valuable information. Tel: 800-344-2571. Dept. A193.

Ashlar Inc.

For More Information Circle No. 344

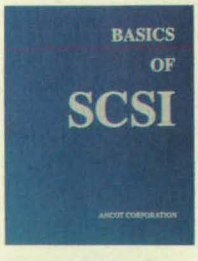

BASICS OF SCSI...FREE

A 50-page gentle introduction to the most popular peripheral bus in the industry today! Learn about SCSI 1&2: the terms, buzzwords, and practical aspects, free from ANCOT, the leader in SCSI tools of engineering development, production testing, and field service applications.

ANCOT Corporation

For More Information Circle No. 345

CUSTOMIZED CAMERA SYSTEMS

SARNOFF can address your complex packaging, image processing, cooling, and image quality needs. We specialize in the manufacturing, design, research and development of state of the art UV, visible, and infrared imagers and camera systems. Tel: 609-734-2553, Fax: 609-734-2443.

SARNOFF

For More Information Circle No. 346

A complete guide

on API's family of large area avalanche photodetectors, including single- and multi-anode configurations as well as detector modules that incorporate large area avalanche photodiodes, high voltage power supply, and integrated amplifier electronics.

Advanced Photonix, Inc.

For More Information Circle No. 347

ADVANCED COMPOSITE WORKSHOPS

The brochure describes ten different "hands-on" workshops in advanced composite materials technology. They cover fabrication, repair, tooling, blueprint reading, adhesive bonding, engineering design for specialized repairs, and ultrasonic inspection of composites. Emphasis is on prepreg carbon and aramid fiber material and processes, utilizing vacuum bagging and high-temperature curing methods. Tel: 800-638-8441, Fax: 702-827-6599.

ABARIS TRAINING RESOURCES

For More Information Circle No. 348

STATIC CONTROL PRODUCTS

This catalog is ideal for individuals in the electronics, business products, medical, and other markets where electrostatic discharge is a concern. The catalog introduces several new products including Zinc-Free Floor Finish and new Heel Grounder with D-Ring fastening system. For your copy call: 508-485-7390, or fax: 508-480-0257.

Plastic Systems, Inc.

For More Information Circle No. 349

MEASURING MASS FLOW

ABB K-Flow® Coriolis meters measure mass flow at 0.25% accuracy; plus they also measure density, temperature, multi-phase constituency (%solids/liquids/mass), specific gravity, net flow, and concentration. For flows from a few cc's to 2500 lbs/min, for hundreds of fluids, ABB K-Flow meters are economical and unmatched in capability. Engineering data package available.

ABB K-Flow, Inc.

For More Information Circle No. 350

COMPACT CONTROLLERS FOR MACHINE/PROCESS CONTROL

ANAFAZE CLS™ are versatile, inexpensive, 4, 8, and 16 multi-loop PID controllers to run small processes, experiments, machines. Key features: Autotune (Instant Setup); accepts most sensor input types (even Infrared); 50 Digital I/O for alarms, events, triggers; computer I/O/Network features. New brochure free! Tel: 408-479-0415, FAX: 408-479-0526.

For More Information Circle No. 351

LIGHT DETECTORS FOR SPECTROSCOPY AND IMAGING

Our colorful four-page brochure describes our latest Optical Multichannel Analyzer OMA® 4 System, based on the highest quality CCD detectors and signal processing instrumentation available. The brochure provides illustrations of our application-specific software developed for spectroscopy and imaging.Tel: 609-530-1000; Fax: 609-883-7259.

EG&G Instruments Princeton Applied Research

For More Information Circle No. 352

OXYGEN ANALYZERS

A full-color brochure introduces a complete line of oxygen analyzers for the laboratory or process line. They are ideally suited for monitoring the oxygen levels in all types of gas streams. Trace oxygen levels from ppb to 100% are accurately determined by these ruggedly constructed instruments. No periodic maintenance or special operator skills are required. Intrinsically-safe and battery-operated models are also available.

Illinois Instruments Inc.

For More Information Circle No. 353

GPS TIMING FOR PC AND VMEBUS

This information folder from Bancomm describes new PCbus and VMEbus board-level Global Positioning System (GPS) Satellite Receivers. These products provide world-wide precision time (100 nanosecond) and frequency (1 Part in 10E7) references inside the host computer.

Bancomm

For More Information Circle No. 354

MOTION CONTROL HANDBOOK

Four-color 44-page book sets forth the basic DSP fundamentals; motion controller, servo filters, background PLC, circular interpolation moves, blended moves, cubic spline moves. Includes 10 programming examples, summarizes PMAC commands and variables with G-code section. Details PMAC's options and accessories, as well as hardware and software.

Delta Tau Data Systems, Inc.

For More Information Circle No. 355

SRS CATALOG

Stanford Research System's 1992-93 Catalog contains full information on its scientific and engineering instruments, featuring the latest function generator, current preamplifier and digital lock-in amplifier products. The 160 page catalog contains complete specifications, technical discussions and application notes on SRS's products, and is a useful reference for a wide range of test and measurement applications. Phone: 408-744-9040. Address: 1290 D Reamwood Ave., Sunnyvale, CA 94089.

Stanford Research System

For More Information Circle No. 356

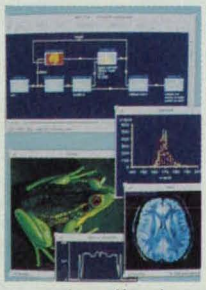

IMAGE ANALYSIS WITH WIT

WIT image processing development software offers an advanced visual programming environment allowing a user to interactively design algorithms by forming arbitrarily complex graphs using icons and links. WIT provides a large set of commonly used imaging operators, supports Datacube hardware, and runs on either Sun, HP, or SGI workstations. For free demo disk call 604-435-2587 or Fax: 604-435-8840.

Logical Vision, LTD.

For More Information Circle No. 357

New on the Market

Roland Digital Group, Irvine, CA, has unveiled the CAMM-3 Model 2500 **desktop modeler**, which produces highly precise working prototypes from wax, wood, and nonferrous metals. It features a cutting speed of 1.18 inches per second and an extended spindle speed range of 3000-12000 rpm. The model 2500 is sold with CAD/CAM tutorial software and a G-Code Driver to bring complex manufacturing capabilities directly to the workstation.

For More Information Circle No. 794

Soft Warehouse Inc., Honolulu, HI, has released DERIVE XM (eXtended Memory), **software** designed for large symbolic math problems and heavy number crunching. Like the regular memory DERIVE, the enhanced program solves symbolic and number problems in algebra, trigonometry, calculus, and matrix algebra. In addition, DERIVE XM can use up to four gigabytes of memory to solve much larger problems.

For More Information Circle No. 800

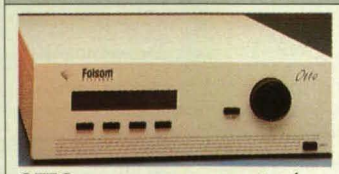

OTTO, a new **scan converter** from Folsom Research Inc., Folsom, CA, automatically configures itself to virtually any input video. It accepts interlaced and noninterlaced video inputs up to 100 kHz horizontal, including HDTV. OTTO supports all standard video outputs, including NTSC, PAL, SVHS, RS-170A, and CCIR RGB, and can output both NTSC and PAL from the same unit.

For More Information Circle No. 784

Silicon Graphics Inc., Mountain View, CA, has announced a **computer line** that puts the power of up to 18 Cray Y-MP™ class supercomputers in a single RISC-based system. The Power Challenge™ shared-memory symmetric multiprocessing systems, based on the new 64-bit MIPS® TFP streaming super-scalar RISC process, deliver up to 5.4 GFLOPS of peak performance. Prices start under $120,000.

For More Information Circle No. 782

Hawkeye, a miniature cordless **pointing device** based on infrared optical technology, is available from Pointer Systems Inc., Burlington, VT. This "mouse without a tail" works like a penlight remote unit and features a resolution of up to 12 bits for use with high-resolution monitors. It employs infrared technology to detect hand motions, permitting the user to move about freely up to four meters in front of the computer.

For More Information Circle No. 792

Applied Laser Systems, Grants Pass, OR, has incorporated protective and troubleshooting circuitry into its lines of **visible laser modules** (VLM™s) for greatly improved reliability. The circuitry was successfully tested to Mil-Std-883C, Method 3015.2, Category B (greater than 2200v). The VLMs—which contain the pointing lens, diode laser, circuitry, protective housing, green LED on/off indicator, and leads—operate at 3-6 VDC and draw only 55 mA.

For More Information Circle No. 798

Researchers at Conductus Inc., Sunnyvale, CA, have successfully demonstrated a **high-temperature superconductive digital electronic circuit** running at 120 GHz. Developed in collaboration with Sandia National Laboratories and AT&T Bell Laboratories, the 32-bit shift register chip is based on yttrium-barium-copper-oxide technology and operates at liquid nitrogen temperature (-196° C). It contains 64 Josephson junctions in the form of "nanobridges" and uses a single flux quantum logic architecture.

For More Information Circle No. 788

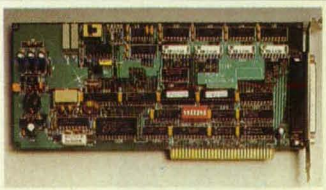

The new DAS-TEMP **board** from OMEGA Engineering Inc., Stamford, CT, offers high-precision measurement of 32 temperature inputs. It can read AD592 current source sensors directly to a resolution of 0.1° C. Capable of measuring up to 200 samples per second, the board is suitable for applications in the -25° to 105° C range.

For More Information Circle No. 786

It has twice the resolution of any printer in its class.

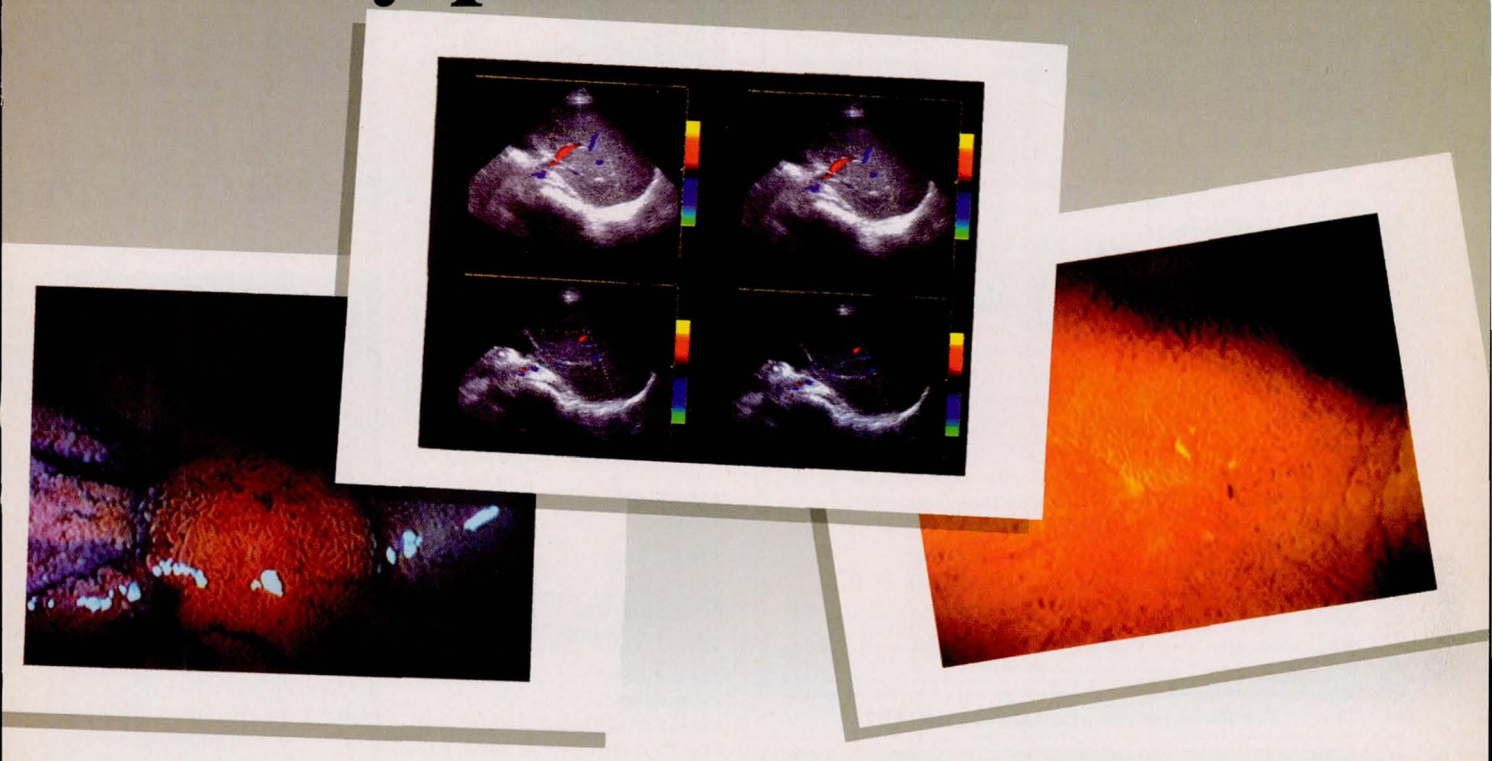

No one makes it clearer.

Toshiba's new HC-1600A Image Master Video Printer gives you brilliant, striking color images. Even when screen images are composed of many intermediate colors, this third-generation dye sublimation thermal printer reproduces them with every shade – finely gradated and lifelike.

With a remarkable resolution of 8 dots /mm (1280 dots horizontal x 1024 dots vertical) and a thermal head which can display 256 gradations of color for each 8-bit dot (yielding a palette of more than 16.7 million total colors), the Image Master gives you extremely high realism with any medical imaging system.

Because the Image Master has more input/output capabilities than any other printer in its class (and more than some costing quite a bit more), you can choose from almost any video input. You can even download the screen memory directly to your laptop's hard drive and transmit it anywhere in the world, via modem. And for all its capabilities, the Image Master presents you with only four buttons to operate; the technician keys in all other information.

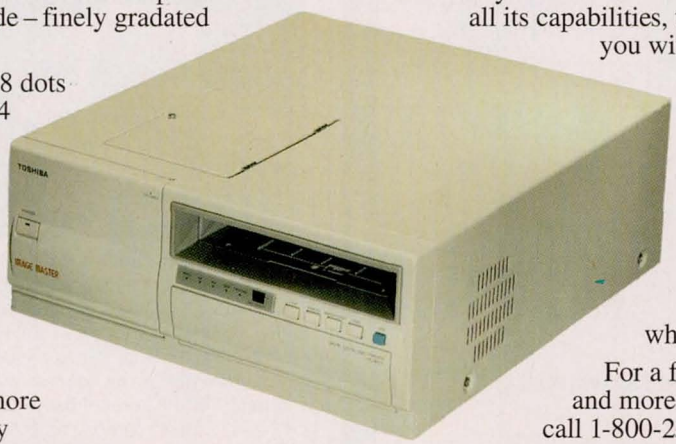

You could pay three times as much for a printer which parallels, but does not surpass, the Image Master's resolution and I/O capabilities. But one thing's not clear: why would you?

For a free brochure and more technical detail, call 1-800-253-5429, then press 6131.

In Touch with Tomorrow

TOSHIBA

TOSHIBA AMERICA C.P., INC. Information and Imaging Technologies Group 1010 Johnson Drive Buffalo Grove, Illinois 60089-6900

For More Information Circle No. 482

CALL FOR PAPERS

TECHNOLOGY 2003

December 7-9, 1993, Anaheim, CA Convention Center

Technology 2003, the fourth national technology transfer conference and exposition, offers a unique forum to present new inventions and innovations to America's top technology managers. Over 8000 research directors, project leaders, senior design engineers, and technology acquisition managers from industry and government are expected to attend the three-day event, to discover technology advances they can use in developing products, solving engineering problems, or improving their manufacturing processes.

Who Should Present Papers Researchers from federal agencies/laboratories and their contractors who have produced important new technologies that are available for commercial use.

Paper Categories Papers should describe innovations developed by or for a government agency/laboratory in one of the following categories:

Advanced Manufacturing
Biotechnology
Computer Software
Environmental Technology
Materials Science
Optics/Lasers
Simulation/Video/Imaging
Robotics
Artificial Intelligence
Computer Hardware
Electronics
Life Sciences
Medical Technology
Power & Energy
Test & Measurement

Deadline For Submissions Paper abstracts must be submitted to the Program Chairman no later than May 1, 1993. They should be 1 to 1-1/2 pages long and must describe the technology's importance and commercial potential (see abstract format below). Abstracts submitted by government contractors should include the name of the agency/laboratory for which the work was done and the contract number. An independent industry panel will judge the abstracts on the basis of technical merit and potential commercial or industrial applications. All submittors will be notified by June 30, 1993. Mail or fax abstracts to:

Leonard A. Ault
Program Chairman,
Technology 2003
Code CU
NASA Headquarters
300 E Street SW
Washington, DC 20546
FAX: (202) 358-3938

Please follow this format:

Technology 2003
Paper Abstract

Name:
Position/Title:
Affiliation:
Address:
Phone Number:
Fax Number:
Govt. Agency/Lab The Subject
Technology Was Developed By/For:
(if contractor-developed, please include contract #)

Category:
Paper Title:
Description:

Questions? Call Leonard Ault at (202) 358-0721 or Wendy Janiel at (212) 490-3999.

New Literature

Scientific Technologies Inc., Hayward, CA, has released a 224-page **optical products** catalog describing its optical sensors, safety light curtains, safety mats, profiling scanners, photoelectric fiber optic sensors, power monitors, temperature controls, and wireless data communications equipment. New products featured include the FlexSafe™ multi-segmented light curtain for machine guarding, the long-range MiniSafe® miniature light curtain designs, an enhanced Opto-Safe® light curtain with 100-foot range, the Optofence™ perimeter guard, and the OptoMat™ safety mat line.
For More Information Circle No. 702

Krautkramer Branson, Lewistown, PA, has introduced a catalog of its AEROTECH™ **ultrasonic transducers**. The 27-page booklet highlights a wide range of contact, angle beam, dual element, immersion, and thickness gauging transducers, as well as cables, adaptors, search tubes, test blocks, and couplants. Certification data, an acoustic impedance and velocity table, and a focal length chart are provided.
For More Information Circle No. 708

A **polyurethane** technical guide from Mearthane Products Corp., Cranston, RI, provides an overview of the material's electrical properties and its resistance to tension, shear, vibration, flexing, compression, temperature, abrasion, and friction. The booklet includes a chart comparing Mearthane® polyurethane to natural and synthetic rubbers, a chemical resistance table, and a glossary.
For More Information Circle No. 704

Information Gatekeepers Inc., Boston, MA, has published the *1993 International Fiber Optic Yellow Pages*, a directory of worldwide **fiber manufacturers, suppliers, service providers, consultants, and publishers**. It includes a listing of more than 2500 companies; product and country directories; a glossary; listings of information sources and fiber optics standards organizations worldwide; and a 1993 calendar of optics-related events.
For More Information Circle No. 710

Literature from CalComp Inc., Anaheim, CA, profiles the DrawingMaster series of **wide-format image plotters**. Included are sections on the DrawingMaster Plus family, which offers a standard resolution of 200 dpi; the high-end DrawingMaster Professional series, with plot nesting and 406-dpi resolution; and RasterMaster, a 200-dpi plotter that uses CalComp's Versatec VPI (Greensheet) raster format.
For More Information Circle No. 712

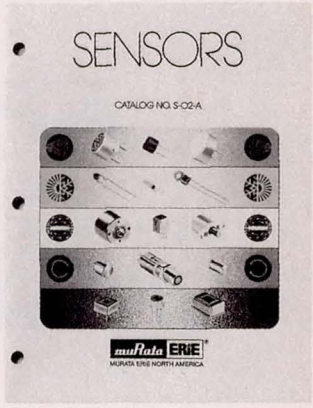

A 40-page catalog of **electronic sensors** has been announced by Murata Erie North America, Smyrna, GA. The publication spotlights various sensor types, including pyroelectric infrared, magnetic angle, ultrasonic, magnetoresistive, and rotation. Temperature sensors and PTC and NTC thermistors also are available.
For More Information Circle No. 706

An **environmental design guide** published by the Healthcare Division of the Society of the Plastics Industry Inc. (SPI), Washington, DC, is intended to help designers of plastic medical products and packaging to address life cycle environmental concerns. Applicable to a wide range of industries, the 30-page booklet uses flow charts and step-by-step instructions to illustrate ways to incorporate environmental goals into product development and packaging design.
For More Information Circle No. 714

POSITIONS WANTED

Seeking ME position in design/development and analysis. MSME, BS in mechanical engineering, seven years experience in design, three years in finite element analysis, four years experience in CAD and CAE. Experience in thermal design and refrigeration.
Box number 10A

Successful and working technical trainer. Strong background in curriculum development, aircraft navigation and control systems, automated material handling systems, and computer electronics. Experienced in development of expert system technology used for trouble shooting automated systems. Seeks challenging training or R&D position in the West or Southwest.
Box number 11A

Mechanical design or R&D position - MSME, 10+ years hands-on research, design and some manufacturing experience with projects of precision gyroscope based electro-mechanical systems from initiative to commercial introduction. Mathematical simulation, dynamics, kinematics, vibration, stress, FEA; excellent analytical, problem solving, drawing and computer (MS/DOS, VM/SP; AutoCAD, FORTRAN, C, LISP) skills.
Box number 12A

Ph.D in artificial intelligence and software engineering with 12 years of experience seeks a research or consulting permitting part-time teaching. Excellent writing skills, having written numerous proposals, magazine articles, and journal publications. Strong math and communication skills. DOD clearance. Will travel or relocate.
Box number 13A

Ph.D in mechanical engineering (thermofluids and aerosol science). Broad academic and industrial research experience in aerosol/particle measurement in gases, vacuums, liquids & surfaces; aerosol beams; filtration; CFD and numerical methods; thin-film and vacuum technology. Excellent publication/patent record. Seeks industry or academic position in relevant area.
Box number 14A

Dynamic and energetic manager with 14 years of progressive experience seeking professionally challenging career opportunity with a growth-oriented electronics manufacturing company. Experience includes manufacturing management, ME, QE, and TE. Emphasis on SMT, ATE, JIT, training, employee employment, personnel development, CE, and TQM. Strengths are vision, values, and technical leadership.
Box number 15A

Mechanical engineer with experience in design, construction, and operation of nuclear and fossil fired power plant systems and equipment. Additional skills in safety analysis reports, safety system classification, safety system functional inspection, design bases documents, vendor document review. BE (mechanical), ME (mechanical), licensed professional mechanical engineer, and certified lead QA auditor.
Box number 16A

MSMH/BSME, experienced in management, QC, ME design/manufacturing. Marketing/sales: strong interest in stress/fracture analysis, composite material studies, and product compatibility study. Seeking engineering-related management or aerospace-related mechanical analysis work.
Box number 17A

Ph.D physical chemist/physicist with strong product and process development background seeks contract assignments; periodic or long term, any location. 30 years experience in semiconductor materials and e-o detector arrays. Crystal growth by CVD, vapor transport & melt (Czochralski & float zone). Slice polishing, device fabrication and packaging. Microgravity processing. Silicone rubber and plastic properties.
Box number 18A

Manager process/product engineering, technical sales, quality, manufacturing. Strong mathematics, statistics, logic, PC programming skills. Capabilities in presentations and technical/non-technical writing. 30 years experience, primarily with structural and controlled porosity powder metal components. BS in engineering. Willing to travel. William Mossner, 145 Forest Park, Janesville, WI 53545-4103, Tel. 608-752-0246.
Box number 19A

Rocket scientist. BS in engineering physics. Six years experience in orbital mechanics, launch vehicle flight performance analysis, and simulation code writing. Seeking position with launch vehicle manufacturer/operator in trajectory/orbital operations department. Tel. 602-326-9350.
Box number 20A

Recent analytical chemist graduate (BSCM) seeks work involving the design and fabrication of analytical instruments. Interests include methods development, computer optimization, microprocessor circuit design, design and analysis of experiments, analytical separations, and general problem solving. Very outgoing and quick learner of computer languages and theory of instrument operations.
Box number 21A

Seeking management and/or marketing position. Proven ability to manage multi-faceted complex programs within schedule and budget. Eight years in management and five in engineering. Successful company start-up, writing business plans, solicitation and acquisition of operating funds, negotiations, developed marketing and sales system. Extensive experience in administration, engineering, training and development, purchasing and contracts management. Strong technical and business skills with excellent communication abilities. Randall Smith, 305 Buttercup Trail, Buda, TX 78610, Tel. 512-295-2427.
Box number 22A

Mechanical/project engineer. Large and small aerospace and manufacturing project experience. 20 years development experience carrying projects through production. Machine design/development, automation, mechanisms. Aerospace structures. 3D CAD, CAE, solids modeling, finite element modeling (structural, thermal, vibration), and kinematics. Digital control systems designing and integration. Consulting or full-time. Call 310-600-3557.
Box number 23A

Applied mathematician (Ph.D) experienced in academia, government, industry and independent consulting. Excellent communication skills. Writing (books, papers), editorial, publishing, and training experience. Extremely computer literate. Proven problem solver. Experienced in sonar, radar, communications, computers, optics, more! Desire technical consulting or management of R&D group in engineering, sciences, or computers.
Box number 24A

Electronic engineer/manager/pilot. Analog and digital design, instrumentation, computers and circuits to systems capability. 23 years in R&D with industrial and academic experience. Broad background in aeromechanics, computers, radar, transportation, and machinery. Available for assignments anywhere in the solar system.
Box number 26A

Quality manager/mechanical engineer seeks challenging position in a high-tech environment. Experience in manufacturing, space propulsion, ordnance, and composites. Strong quality engineering and program management background. Trained in SPC, Continuous Improvement, ISO 9000, Mil-Q-9858, and NHB 5300.4. DOD clearance, MBA.
Box number 27A

Drafting electro/mechanical, AutoCAD 10 and 11. Commercial and aerospace 20+ years experience. STDS, DOD and DOS. Cable and harness design. Recent hospital equipment design. Schematics, logic diagrams. Orange County, California job site preferred but willing to relocate.
Box number 25

Electro-mechanical packaging engineer/designer and/or engineering consultant. Experiences in product planning, design and development; background also includes client/vendor liaison, supervision, training, budgets, and personnel. State of the art design/packaging of products/systems in the fields of electronics, electro-mechanical, mechanical, and mechanisms. Seeking direct or contract position; relocation is optional. Call Jerry at 510-651-8360.
Box number 28A

Coordinated ISO 9000 certification and accelerated stress screening for Malcolm Baldridge National Quality Award winner. Quality manager handling: Dr. Deming's 14 points, TQM, SPC, JIT, DOE, benchmarking. MSEE with 16 years experience in electronics, strong hardware, computer, mechanical skills, very efficient and energetic. Seeking challenging quality director/quality manager position.
Box number 29A

Ph.D electrical/electronics engineer with 15 years experience in lasers (FEL, CO_2, YAG), pulsepower, plasma physics, cogeneration, power distribution, computers (Unix, DOS, C), machine shop, CAD/CAM, and manufacturing. Private consultant, manager, budgets, team leader. I make things happen. Looking for interesting, challenging assignments anywhere, anytime.
Box number 30A

To submit an ad for inclusion in this column, send a copy of your resume and a 50-word summary to: *NASA Tech Briefs*, 41 East 42nd St., New York, NY 10017, ATTN: Gregg McQueen.

To Request Resumes:

To obtain resumes corresponding to the above **Positions Wanted Ads**, fill out this form and mail to: *NASA Tech Briefs*, 41 East 42nd St., New York, NY 10017. ATTN: Gregg McQueen, or call 1-800-944-NASA and ask for Gregg McQueen.

Send resumes for the following box numbers (limit 5):

Box_____ Box_____ Box_____

Box_____ Box_____

Name: _____

Company Name: _____

Street Address: _____

City/State/Zip: _____

MARKETPLACE To Advertise—Call (212) 490-3999

ADVERTISERS INDEX

* RAC stands for Reader Action Card. For further information on these advertisers, please cirle the RAC number on the Reader Actin Card in this issue. This index has been compiled as a service to our readers and advertisers. Every precaution is taken to insure its accuracy, but the publisher assumes no liability for errors or omissions.

NASA Tech Briefs, ISSN 0145-319X, USPS 750-070, copyright © 1993 in U.S., is published monthly by Associated Business Publications Co., Ltd., 41 E. 42nd St., New York, NY 10017-5391. The copyrighted information does not include the (U. S. rights to) individual tech briefs which are supplied by NASA. Editorial, sales, production and circulation offices at 41 East 42nd Street, New York, NY 10017-5391. Subscription for non-qualified subscribers in the U.S., Panama Canal Zone, and Puerto Rico, $75.00 for 1 year; $125.00 for 2 years; $200.00 for 3 years. Single copies $10.00. Foreign subscriptions one-year U.S. Funds $150.00. Remit by check, draft, postal, express orders or VISA, MasterCard, and American Express. Other remittances at sender's risk. Address all communications for subscriptions or circulation to NASA Tech Briefs, 41 East 42nd Street, New York, NY 10017-5391. Second-class postage paid at New York, NY and additional mailing offices.

POSTMASTER: please send address changes to NASA Tech Briefs, 41 E. 42nd Street, Suite 921, New York, NY 10017-5391.

THE TECHNOLOGY CONNECTION

THE FASTEST WAY TO PUT 25 GB ON A SINGLE TAPE.

The CY-8500 can store up to 25 GB on a single tape, at speeds of up to 90 MB per minute, completely unattended.

How? With hardware data compression that can boost capacity by up to five times.

No other 8mm tape drive can match the capacity, speed, and price-performance of this best-selling drive.

ADVANCED. You'll never be left in the dark. A bright, backlit status display gives you the command under execution, transfer rate, compression ratio, amount of tape remaining and more.

Our *data compression* option is the fastest available. And it's switch selectable, so you can still read and write standard tapes. Locate and restore files quickly and easily with our *accelerated file access* option. Add *data encryption* to control backup and restore operations through the use of encoded card keys.

FLEXIBLE. The CY-8500 is plug compatible with virtually every computer system. Rack mounting options, dual drive configurations and a variety of cable lengths ensure a seamless fit into your computing environment. And as storage needs grow, you can upgrade to our ten tape library, capable of managing between 25 GB and 250 GB–all without manual intervention.

RELIABLE. A sophisticated Error Correction Code yields a bit error rate of less than one in 10^{17}–the best in the industry. A MTBF rate of 60,000 hours ensures reliability.

Each turnkey subsystem features a 12-month warranty that includes technical support from our experienced in-house engineering groups.

Everything you want in a backup subsystem is available right now.

Call today for information at

(804)873-9000

TRUE PLUG COMPATIBILITY

Alliant	McDonnell Douglas
Alpha Micro	Motorola
Altos	NCR
Apollo	NeXT
Arix	Novell
AT&T	OS/2
Basic-4	PS/2
Concurrent	Parallel Port
Convergent	PC 386/ix
DataGeneral	PC MS-DOS
DEC 3100/5000	PC Xenix/Unix
DEC BI-Bus	Pertec
DEC DSSI	Plexus
DEC HSC	Prime
DEC Q-Bus	Pyramid
DEC TU/TA81	Sequent
DEC Unibus	Silicon Graphics
Gould/Encore	STC
HP	Stratus
IBM AS/400	Sun
IBM Mainframe	Texas Instruments
IBM RISC/6000	Unisys
IBM RT	Wang
IBM S/38	*and more*
ICL	
Intergraph	
Macintosh	

CONTEMPORARY
CYBERNETICS

Rock Landing Corporate Center • 11846 Rock Landing
Newport News, Virginia 23606 • Fax (804)873-8836

For More Information Circle No. 522

Have Design Secrets to Unlock? Try our New Block...

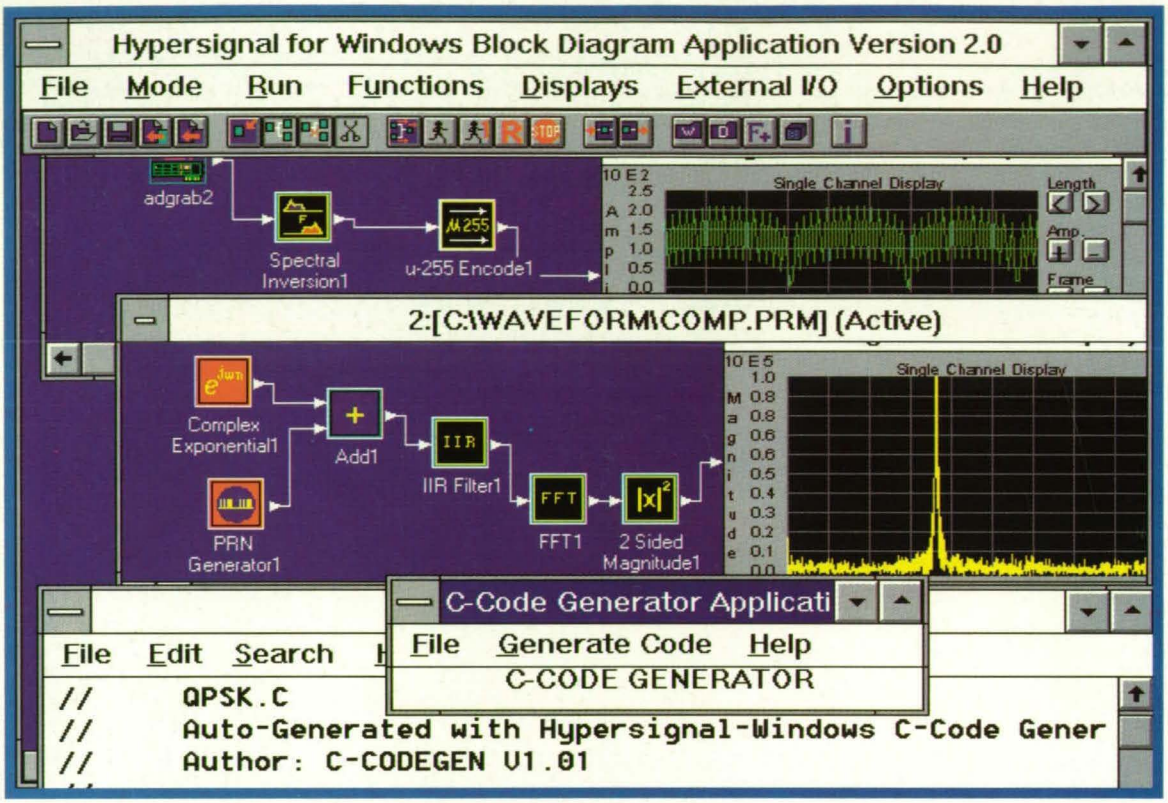

Hypersignal® for Windows Block Diagram V2.0

Advanced Object-Oriented Simulation Software under the Microsoft® Windows™ Operating System

- **Visually Programmed** Simulation Environment for algorithm simulation and development
- Optional **C Code Generator** available for outputting 'C' source code
- **Open Software Architecture** with Presentation Quality Graphics
- **Real-Time support** of DSP/Acquisition Boards
- New Blocks may be created using standard C compilers
- New Block Generator utility for automating the creation of user-defined blocks
- Software architecture allows for many digital signal processing (DSP) applications including multi-dimensional algorithms
- **Hierarchical Capability** simplifies project design
- Improved conditional programming blocks
- **Flexible interface** to allow virtually every algorithm application from classical telecom applications to Digital Image Processing

Hyperception

For More Information Circle No. 551

For more information, including Free Catalog and Demo, contact: Hyperception, Inc.

9550 Skillman LB 125 • Dallas, Texas 75243
phone (214) 343-8525 • fax (214) 343-2457

International Distributors:

AUSTRALIA - Electro Optics PTY, LTD.: phone +61-2-654-1873; FAX +61-2-654-1539, • **DENMARK** - Assentoft Electronics; phone +45-86-16-29-26; FAX +45-86-16-20-12, • **FINLAND** - ITT: phone +358-90-739100; FAX +358-90-701-5683, • **ISRAEL** - IES, LTD.: phone +972-3-7526333; FAX +972-3-7510927, • **KOREA** - Seoil Enterprise Co.: phone +82-2-237-0872; FAX +82-2-237-0874, • **SINGAPORE** - Bliss Services PTE LTD.: phone +65-3381300; FAX +65-3381900, • **TAIWAN, ROC** - Exartech International Corporation: phone +886-2-977-6828; FAX +886-2-977-6829, • **UK, IRELAND** - Loughborough Sound Images, LTD.; phone (0509) 231843, TLX 341409 LUFBRA G. FAX: (0509) 262433.